



Master's thesis  
Geoinformatics

QUIET PATHS FOR PEOPLE:  
DEVELOPING ROUTING ANALYSIS AND WEB GIS APPLICATION

Joose Helle  
2020

Supervisors:  
Tuuli Toivonen

University of Helsinki  
Faculty of Science  
Department of Geosciences and Geography  
PL 64 (Gustaf Hällströmin katu 2)  
00014 University of Helsinki



Tiedekunta/Osasto – Fakultet/Sektion – Faculty <b>Faculty of science</b>	Laitos/Institution – Department <b>Department of Geosciences and Geography</b>
Tekijä/Författare – Author <b>Joose Helle</b>	
Työn nimi / Arbetets titel – Title <b>Quiet paths for people: developing routing analysis and Web GIS application</b>	
Oppainaine /Läroämne – Subject <b>Geoinformatics</b>	
Työn laji/Arbetets art – Level <b>Master's thesis</b>	Aika/Datum – Month and year <b>May 2020</b>
Tiivistelmä/Referat – Abstract <p>It is likely that journey-time exposure to pollutants may limit the positive health effects of active transport modes (e.g. walking and cycling). One of the pollutants caused by vehicular traffic is traffic noise, which is likely to cause various negative health effects such as increased stress levels and blood pressure. In prior studies, individuals' exposure to community noise has usually been assessed only with respect to home location, as required by national and international policies. However, these static exposure assessments most likely ignore a substantial share of individuals' total daily noise exposure that occurs while they are on the move. Hence, new methods are needed for both assessing and reducing journey-time exposure to traffic noise as well as to other pollutants.</p> <p>In this study, I developed a multifunctional routing application for 1) finding shortest paths, 2) assessing dynamic exposure to noise on the paths and 3) finding alternative, quieter paths for walking. The application uses street network data from OpenStreetMap and modeled traffic noise data of typical daytime traffic noise levels. The underlying least cost path (LCP) analysis employs a custom-designed environmental impedance function for noise and a set of (various) noise sensitivity coefficients. I defined a set of indices for quantifying and comparing dynamic (i.e. journey-time) exposure to high noise levels. I applied the developed routing application in a case study of pedestrians' dynamic exposure to noise on commuting related walks in Helsinki. The walks were projected by carrying out an extensive public transport itinerary planning on census based commuting flow data. In addition, I assessed achievable reductions in exposure to traffic noise by taking quieter paths with statistical means by a subset of 12180 commuting related walks (OD pairs).</p> <p>The results show significant spatial variation in average dynamic noise exposure between neighborhoods but also significant achievable reductions in noise exposure by quieter paths; depending on the situation, quieter paths provide 12–57 % mean reduction in exposure to noise levels higher than 65 dB and 1.6–9.6 dB mean reduction in mean dB (compared to the shortest paths). At least three factors seem to affect the achievable reduction in noise exposure on alternative paths: 1) exposure to noise on the shortest path, 2) length of the shortest path and 3) length of the quiet path compared to the shortest path. I have published the quiet path routing application as a web-based quiet path routing API (application programming interface) and developed an accompanying quiet path route planner as a mobile-friendly web map application. The online quiet path route planner demonstrates the applicability of the quiet path routing method in real-life situations and can thus help pedestrians to choose quieter paths. Since the quiet path routing API is open, anyone can query short and quiet paths equipped with attributes on journey-time exposure to noise. All methods and source codes developed in the study are openly available via GitHub.</p> <p>Individuals' and urban planners' awareness of dynamic exposure to noise and other pollutants should be further increased with advanced exposure assessments and routing applications. Web-based exposure-aware route planner applications have the potential to help individuals to choose alternative, healthier paths. When developing exposure-based routing analysis further, attempts should be made to enable simultaneously considering multiple environmental exposures in order to find overall healthier paths.</p>	
Avainsanat – Nyckelord – Keywords <b>Dynamic exposure, traffic noise, environmental impedance, least-cost path analysis, Web GIS</b>	
Säilytyspaikka – Förvaringsställe – Where deposited	
Muita tietoja – Övriga uppgifter – Additional information	



Tiedekunta/Osasto – Fakultet/Sektion – Faculty <b>Matemaattis-luonnontieteellinen tiedekunta</b>	Laitos/Institution – Department <b>Geotieteiden ja maantieteen laitos</b>
Tekijä/Författare – Author <b>Joose Helle</b>	
Työn nimi / Arbetets titel – Title <b>Reititysanalyysin ja Web GIS sovelluksen kehittäminen hiljaisempien kävelyreittien etsintään</b>	
Oppaine /Läroämne – Subject <b>Geoinformatiikka</b>	
Työn laji/Arbetets art – Level <b>Pro gradu -tutkielma</b>	Aika/Datum – Month and year <b>Toukokuu 2020</b>
Tiivistelmä/Referat – Abstract <p>Altistuminen saasteille saattaa vähentää merkittävästi aktiivisten liikkumismuotojen, kuten kävelyn ja pyöräilyn terveyshyötyjä. Yksi liikenteestä johtuvista saasteista on melu, joka voi aiheuttaa terveyshaittoja, kuten kohonnutta verenpainetta ja stressitasoja. Aikaisemmissa tutkimuksissa ja selvityksissä melulle altistumista on arvioutu yleensä kotipaikan suhteen ja liikkumisen aikana tapahtuva altistus on jänyt vähemmälle huomiolle. Koska liikkumisen aikainen (dynaaminen) melualtoitus saattaa muodostaa merkittävän oan kaupunkilaisten kokonaismelualtoistuksesta, tarvitaan kehittyneempiä menetelmiä dynaamisen melualtoituksen arvioimiseen ja vähentämiseen.</p>	
<p>Tässä tutkielmassa kehitin kävelyn reititysmenetelmän ja sovelluksen, jolla voi 1) etsiä lyhimmän reitin, 2) mallintaa kävelyn aikaisen melualtoituksen ja 3) löytää vaihtoehtoisia, hiljaisempia reittejä. Sovellus hyödyntää OpenStreetMap-tieverkostoaineistoa ja mallinnettua aineistoa tieliikenteen tyypillisistä päiväajan melutasoista. Reitinetsintä perustuu kehittämääni melukustannusfunktioon ja alhaisimman kustannuksen reititysanalyysiin. Melukustannukset lasketaan sovelluksessa lukuisilla eri meluherkkyykskertoimilla, minkä ansiosta sovellus löytää useita vaihtoehtoisia (hiljaisempia) reittejä. Jotta eri reittien meluisuutta (melualtoitsuksia) voidaan vertailla, kehitin sarjan melualtoitusindeksejä. Tapaustutkimussa tutkin Helsingistä tehtävien työmatkojen aikaisia melualtooksia; selvitin rekistereihin perustuvien työmatkojen mukaiset joukkoliikennereitit ja tutkin reittien kävelyosuuksien aikaisia melualtooksia reitittämällä kävelyreitit uudestaan kehittämälläni reitityssovelluksella. Lisäksi tutkin hiljaisempien reittivaihtoehtojen mahdollistamia vähennyksiä melualtooksissa työmatkoihin liittyvillä kävelyreiteillä joukkoliikenteen pysäkeille.</p>	
<p>Tapaustutkimuksen tulokset indikoivat, että tyypilliset dynaamiset melualtoukset vaihtelevat huomattavasti eri asuinpaikkojen välillä. Toisaalta merkittävä osa melulle altistumisesta on mahdollista välttää hiljaisemmillä reittivaihtoehdolla; tilanteesta riippuen, hiljaisemmat reitit tarjoavat keskimäärin 12–57 % vähennyksen altistuksessa yli 65 dB melutasoille ja 1.6–9.6 dB keskimääräisen vähennyksen reittien keskimääräisessä melutasossa. Altistuksen mahdolliseen vähennykseen näyttäisivät vaikuttavan ainakin 1) melualtouksen suuruus lyhimmällä (ts. verrokki) reitillä, 2) lyhimmän reitin pituus, eli etäisyys lähtö- ja kohdepisteen välillä reititysgraafissa ja 3) hiljaiseman reitin pituus lyhimpään reittiin verrattuna. Julkaisin hiljaisten kävelyreittien reitityssovelluksen avoimena web-rajalintapalveluna (API - Application Programming Interface) ja kehitin hiljaisten kävelyreittien reittioppaan mobiiliomitoituna web-karttasovelluksena. Kaikki tutkielmassa kehitetyt menetelmät ja lähdekoodit ovat avoimesti saatavilla GitHub palvelussa.</p>	
<p>Yksilöiden ja kaupunkisuunnittelijoiden tietoutta dynaamisesta altistuksesta melulle (ja muille saasteille) tulisi lisätä kehittämällä altistusten arvointiin ja vähentämiseen kehittyneempiä analyyseja ja sovelluksia. Tässä tutkielmassa kehitetty web-karttasovellus havainnollistaa hiljaisten reittien reititysmenetelmän toimivuutta tosielämän tilanteissa ja voi siten auttaa jalankulkijoita löytämään hiljaisempia, ja siten terveellisempiä, reittivaihtoehtoja. Kun ympäristöllisiin altistuksiin perustuvaa reitinetsintää kehitetään pidemmälle, tulisi pyrkiä huomioimaan useampia erillisiä altistuksia samanaikaisesti ja siten reitittämään yleisesti ottaen terveellisempiä reittejä.</p>	
Avainsanat – Nyckelord – Keywords <b>Dynaaminen altistus, liikennemelu, alhaisimman kustannuksen reitinetsintä, Web GIS</b>	
Säilytyspaikka – Förvaringsställe – Where deposited	
Muita tietoja – Övriga uppgifter – Additional information	

## TABLE OF CONTENTS

I.	INTRODUCTION .....	1
II.	BACKGROUND .....	4
2.1	Defining noise .....	4
2.2	Traffic noise and health.....	4
2.3	Traffic noise modeling .....	6
2.4	Active modes of transport in cities .....	7
2.5	Concepts and approaches in assessing dynamic exposure.....	8
2.6	Graph theory and least cost path analysis .....	10
2.7	Exposure-based impedances in routing.....	12
2.8	Web GIS concepts and developments.....	14
III.	DATA & METHODS .....	19
3.1	Overview of the methods .....	19
3.2	Study area.....	19
3.3	Data .....	20
3.3.1	Modelled traffic noise data .....	21
3.3.2	OpenStreetMap data.....	25
3.3.3	Register based origin-destination (OD) commuting data .....	26
3.3.4	Online routing service of the local public transport authority .....	26
3.4	Technical framework and architecture.....	27
3.5	Quiet path routing method .....	28
3.5.1	Network acquisition and manipulation .....	29
3.5.2	Environmental impedance function .....	31
3.5.3	Quiet path routing application .....	33
3.5.4	Noise exposure assessment of short and quiet paths .....	37
3.6	Web-based quiet path route planner.....	39
3.7	Case study: pedestrians' exposure to traffic noise in Helsinki .....	41
3.7.1	Overview of the analysis.....	41
3.7.2	Estimating local walking routes by PT commutes.....	44
3.7.3	Least cost path calculations: short and quiet paths .....	49

3.7.4 Assessment of dynamic exposure to traffic noise.....	50
3.8 Assessment of achievable reductions in exposure to traffic noise .....	51
IV.    RESULTS .....	53
4.1 Quiet path routing API.....	53
4.2 Quiet path route planner.....	55
4.3 Case study: Pedestrians' exposure to traffic noise in Helsinki .....	60
4.3.1 Pedestrians' exposure to traffic noise .....	60
4.3.2 Spatial patterns in pedestrians' exposures to traffic noise .....	62
4.4 Achievable reductions in exposure to traffic noise.....	68
4.5 Sharing of the methods and results .....	73
V.    DISCUSSION AND CONCLUSIONS .....	75
5.1 Significant but varying reductions in traffic noise exposure can be achieved by routing quiet paths .....	75
5.2 Publishing a green path routing application online can facilitate citizens to choose healthier paths .....	76
5.3 Alternative quiet paths need to be calculated to suit different situations and personal preferences .....	77
5.4 Advanced routing features and higher performance may require revised technical implementation.....	78
5.5 Usability of the quiet path routing application depends also on the quality of the shortest paths .....	80
5.6 Indirect assessment of pedestrians' dynamic exposures to traffic noise can reveal unequal distribution of exposures to high noise levels.....	83
5.7 The presence of alternative paths limits the accuracy of the indirect dynamic exposure assessment.....	84
5.8 Uncertainties in exposure-response relationships challenge the environmental impedance function .....	85
5.9 Exposure-based routing should be developed as a concept to simultaneously consider multiple exposures.....	87
VI.    REFERENCES.....	90
ACKNOWLEDGEMENTS .....	98
APPENDICES .....	99

## LIST OF FIGURES

Figure 1. Equal loudness contours as in ISO 226 ( <i>Acoustics – normal equal-loudness contours. International Standard ISO 226</i> ). ....	4
Figure 2. Composed scatterplot between $L_{den}$ and percentage of highly annoyed (HA%) for several studies on road traffic noise and annoyance by Guski et al. (2017). ....	6
Figure 3. Dynamic exposure to traffic noise level on a path as distances (left) and durations (right) of different traffic noise levels.....	9
Figure 4. An illustration of the sequence of steps in finding least cost paths with Dijkstra's algorithm by Jasika et al. (2012).....	11
Figure 5. A figure by Veenendaal et al. (2017): "Interacting web services feeding into apps within application workflows." .....	16
Figure 6. Illustration by Veenendaal et al. (2017): "Focus and trends in increasing web mapping functionality".	18
Figure 7. Illustration of the internal dependencies of the methods and results of the study.....	19
Figure 8. The study area and its key transportation networks.....	20
Figure 9. Modelled daytime traffic noise levels (dB(A)) in Helsinki.....	23
Figure 10. Modelled daytime traffic noise levels (dB(A)) in Viikki. ....	24
Figure 11. Modelled daytime traffic noise levels (dB(A)) in Kallio and Vallila (in Helsinki).....	25
Figure 12. Technical framework of the study: internal (blue) and external (grey) technical dependencies (* = Python library). The several external dependencies of the used Python libraries are not included in the graph.....	28
Figure 13. Workflow of street network graph acquisition and construction.....	30
Figure 14. Workflow of extracting exposures to traffic noise (contaminated distances) to the edges of the graph. ....	30
Figure 15. Noise cost coefficients for dB range 45–75 dB calculated with both equations presented in this chapter (Table 3).....	33
Figure 16. Workflow of calculating and adding noise sensitivity specific edge costs as new edge attributes. ....	35
Figure 17. The sequence of high-level actions included in solving a common pathfinding problem with quiet path routing application. ....	37
Figure 18. Technical architecture of the quiet path route planner web application. ....	40
Figure 19. Workflow of the analysis for modelling origin – PT stop (or commuting destination) walking routes and estimating their utilization rates based on commuter flows (as in 3.7.2). I analyzed census based commuting flow data and extracted the first walks of planned public transport itineraries to commuting destinations. These first walks are referred to as <i>local walking routes</i> in the study.....	43
Figure 20. Workflow of the analysis for 1) calculating short and quiet paths for local walking routes (3.7.3), 2) assessing exposures to traffic noise on the paths (3.7.4) and 3) assessing achievable reductions in traffic noise exposure by taking quiet paths (3.8).....	44
Figure 21. Extent of the itinerary planning analysis by commuting flow data. In the Helsinki case study, I assessed exposure to noise during commutes originating within the municipality (marked with red). In the analysis, public transport itineraries were planned for all commutes and first walks of the travel chains were extracted for noise exposure assessment. The point symbols represent “central workplace location” of each city district. ....	45

Figure 22. An example of projected walking routes and their utilization rates from one origin to public transport stops and workplaces. The walking routes are extracted from planned public transport itineraries (travel chains) to all commuting destinations from the origin as per census based commuting flow data. ....	47
Figure 23. Inclusion (%) of commutes per origin in the itinerary planning analysis for finding local walking routes to PT stops and commuting destinations. Only commuting destinations located in Helsinki Metropolitan Area, or max. 3 km from origins, were included in the analysis. Consequently, for some origins, significant shares of commutes were excluded in the analysis (shown with grey and black squares on the map). For these origins, the accuracy of the assessment was thus limited. Yet for majority of the origins, more than 70 % of all commutes were included in the analysis (green squares). ....	48
Figure 24. Number of commutes vs. commutes included in the itinerary planning analysis (%) per origin.....	49
Figure 25. All shortest paths visualized with feature blending method: overlapping paths show darker on the map. I routed shortest- and quiet paths for all local walking routes to PT stops modelled in the previous phases of the assessment.....	50
Figure 26. A typical sequence of actions included in solving one pathfinding problem from the perspective of the route planner application (grey) and user (blue).....	58
Figure 27. The user interface of the quiet path route planner when showing two alternative paths (one shortest path and one quiet path).....	59
Figure 28. The user interface of the quiet path route planner when showing several alternative paths (one shortest path and six quiet paths). In the third picture, longest paths are filtered out by a user-defined length threshold. ....	59
Figure 29. "Add to home screen" -functionality of the web application; the quiet path route planner can be "installed" on user's phone to work similarly as installed apps (without web browser and address bar).....	60
Figure 30. Mean walking distances from homes to public transport (PT) stops. The averages are weighted with the estimated utilization rates of the walks based on the total flow of commutes using each origin – PT stop pair.63	
Figure 31. Mean traffic noise level (dB(A)) on walks from homes to PT stops. The averages are weighted with the estimated utilization rates of the walks based on the total flow of commutes using each origin – PT stop pair.64	
Figure 32. Mean exposures to +65 dB(A) traffic noise levels (m) on walks from homes to public transport (PT) stops. The averages are weighted with the estimated utilization rates of the walks based on the total flow of commutes using each origin – PT stop pair.....	65
Figure 33. Mean exposures to +70 dB traffic noise levels (m) on walks from homes to public transport (PT) stops. The averages are weighted with the estimated utilization rates of the walks based on the total flow of commutes using each origin – PT stop pair. ....	66
Figure 34. Mean exposure to +65 dB(A) traffic noise levels (%) on walks from homes to public transport (PT) stops. The averages are weighted with the estimated utilization rates of the walks based on the total flow of commutes using each origin – PT stop pair. ....	67
Figure 35. Mean exposure to +70 dB(A) traffic noise levels (%) on walks from homes to public transport (PT) stops. The averages are weighted with the estimated utilization rates of the walks based on the total flow of commutes using each origin – PT stop pair. ....	68

Figure 36. Regression analysis between the reductions in traffic noise exposures on quiet paths and the initial traffic noise indices. The analysis covers shortest paths in the length range of 300 to 600 m and the respective quiet paths. The red lines represent the regression lines of the regression analysis and the green lines show the theoretical maximum reductions in the noise exposure indices. ....	70
Figure 37. Regression analysis between the reductions in traffic noise exposures on quiet paths and the initial traffic noise indices. The analysis covers shortest paths in the length range of 700 to 1300 m and the respective quiet paths. The red lines represent the regression lines of the regression analysis and the green lines show the theoretical maximum reductions in the noise exposure indices. ....	71
Figure 38. Side-by-side comparison of the street network graphs of the quiet path route planner (A) and OpenTripPlanner (B) in Koskela, Helsinki. Most street segments tagged as private in OpenStreetMap are used in OpenTripPlanner but missing from the quiet path route planner. However, private streets are only usable at the beginning or end of a route in OpenTripPlanner. Map data by © OpenStreetMap contributors. ....	82
Figure 39. Side-by-side comparison of the street network graphs of the quiet path route planner (A) and OpenTripPlanner (B) in Kumpula campus, Helsinki. Additional ("virtual") edges are created in OpenTripPlanner to allow traversing through walkable areas in pathfinding. Map data by © OpenStreetMap contributors. ....	83

## LIST OF TABLES

Table 1. Data that were used in the study. ....	21
Table 2. Query strings for street network data downloads to be used with Overpass API and OSMnx python library. ....	26
Table 3. Noise cost coefficients for dB range from 45 dB to 75 dB calculated with both equations presented in this chapter (3 & 4).....	<b>Error! Bookmark not defined.</b>
Table 4. The noise exposure indices that were defined for measuring dynamic traffic noise exposure and reduction in noise exposure on quiet paths. ....	39
Table 5. Parameters used in public transport itinerary planning with Digitransit routing API. ....	46
Table 6. Descriptive statistics of the length of the shortest paths to PT stops and commuting destinations, both separately and combined (n=31291).....	49
Table 7. Descriptions of the path properties returned by the quiet path routing API. ....	53
Table 8. A FeatureCollection of two paths returned from the quiet path routing API. ....	55
Table 9. Minor features and functionalities of the route planner UI that aim to improve the overall user experience of the application. ....	56
Table 10. Descriptive statistics of exposure to traffic noise on the first walks of public transport itineraries to workplaces and on direct walks to nearby workplaces (n=30160). ....	61
Table 11. Descriptive statistics of exposure to traffic noise on the first walks of public transport itineraries to workplaces (direct walks to nearby workplaces are filtered out, n=17891). ....	61

Table 12. Descriptive statistics of the achievable reductions in noise exposure index $ER_{+65dB}$ on different subsets of the paths. The subsets were defined by 1) the length of the shortest path, 2) the length difference of the quiet path and 3) the initial $ER_{+65dB}$ ( $n_{300-600m} = 4338$ , $n_{700-1300m} = 7842$ ). ....	72
Table 13. Descriptive statistics of the achievable reductions in noise exposure index $dB_{mean}$ on different subsets of the paths. The subsets were defined by 1) the length of the shortest path, 2) the length difference of the quiet path and 3) the initial $dB_{mean}$ ( $n_{300-600m} = 4103$ , $n_{700-1300m} = 6925$ ). ....	73
Table 14. Differences in path length between shortest paths and reference paths (n=31228).....	80
Table 15. Statistics of offsets (i.e. distances) between the origin and destination points of the paths and the origin and destination points of the reference paths.....	82

## ABBREVIATIONS

API	Application Programming Interface
A-weighting	A method for modeling perceived loudness of sounds of different frequencies
CNOSSOS-EU	Common Noise Assessment Methods in Europe (framework)
dB(A)	A-weighted sound pressure level in decibels
EIF	Environmental Impedance Function
ERR	Exposure-response Relationship
GeoJSON	A geospatial adaptation of the JSON format
GIS	Geographic Information System
GPS	Global Positioning System
HOPE	Healthy Outdoor Premises for Everyone (EU project)
HRT	Helsinki Region Transport (HSL)
HTML	Hypertext Markup Language
JS	JavaScript (programming language)
JSON	JavaScript Object Notation format
$L_{Aeq}$	A-weighted Equivalent Continuous Sound Pressure Level
LCP	Least Cost Path
$L_{den}$	Day Evening Night Sound Level
OD	Origin-Destination
OSM	OpenStreetMap
PT	Public Transport
PWA	Progressive Web Application
REST	Representational State Transfer
RESTful API	See REST & API
SPA	Single-page (web) Application
SPL	Sound Pressure Level
UI	User Interface
WGS84	World Geodetic System

## I. INTRODUCTION

Active transport modes are getting increasing attention among policy makers and urban planners. The term active transport usually refers to walking and cycling but also to other active transport modes such as e-scooters and even city rowboats that are emerging in urban context. Undoubtedly, walking has remained the most popular mode of active transport since it doesn't require any accessories and it is essential part of all itineraries made by public transport.

Significant health, societal and environmental benefits have been anticipated and identified from shift to active transport modes from using private cars (Pucher & Buehler, 2010; Rabl & de Nazelle, 2012); increasing popularity of active transport modes can reduce traffic related pollution and support better health for individuals due to the physical activity. Thus, cities often have a strong willingness to facilitate and promote active transport modes for urban mobility. In encouraging people to choose active transport modes, it is essential for the cities to provide sufficient infrastructure and suitable environments to make walking and cycling practical and pleasant.

Multiple factors affect the ease with which active transport is applicable in different urban environments. While infrastructure for cycling is predominantly defined by the more or less exclusive network of cycleways and bike lanes, the one for walking (footpaths, sidewalks etc.), on the other hand, is denser and more evenly distributed. However, not only the physical properties of street networks define their applicability and desirability for active transport modes (i.e. walkability or bikeability), but also multiple more ambiguous factors need to be considered (Maghelal & Capp, 2011). These include variables such as safety, presence and types buildings, openness of spaces, proximity to opportunities, quietness, air quality and green spaces – all perceived differently by different individuals.

Many of the factors limiting walkability, or the convenience of active transport modes in general, are caused by other, “non-human” users of the urban space. Evidently, one of the most significant of these is vehicular traffic and the related infrastructures. Vehicular traffic affects walkability and bikeability by establishing large and typically unpleasant built structures to urban spaces. These structures often act as barriers fragmenting the networks that support active transport modes and thus reduce the opportunities for walking and cycling.

Moreover, vehicular traffic consumes the opportunities for active transport with at least two “invisible” ways. Firstly, since most of it is powered by gasoline engines, it has a negative impact on air quality due to the exhaust gases. According to many studies, individuals’ exposure to the urban

air pollutions can cause or worsen many lung diseases such as asthma or even cancer (WHO Europe, 2018a) and result in pre-mature death (EEA 2019; WHO 2013). Secondly, varying levels of community noise are caused by both the engines and the wheels of the vehicles. According to several studies, individuals' exposure to traffic noise is likely to cause adverse health effects such as increased stress levels and problems related to blood circulation (Babisch et al., 2005; Ising et al., 1980; Passchier-Vermeer & Passchier, 2000). The list of potential health effects of traffic noise is longer but lacking explicit scientific evidence. The influences of continuous urbanization, namely the increase of daily commuters and increased traffic flows, are likely to amplify the adverse health effects of traffic noise on public health (Passchier-Vermeer & Passchier, 2000).

Since the adverse health effects of traffic noise stem from individuals' *exposure* to it, several approaches have been developed for assessing these exposures. Population-level assessments of individuals' exposure to traffic noise have been driven by national and international policies and enabled by advanced noise modeling. In these assessments, use of geographic information systems (GIS) have been efficient in managing and analyzing spatio-temporal (or at least spatial) data of community noise and population distributions. Majority of the exposure assessments have been carried out on residential basis, i.e. with respect to home location. However, it seems that significant share of individuals' exposure to pollutants can occur while on the move (Beckx et al., 2009). Acknowledging this observation has accelerated development of advanced exposure assessments that better consider individuals' dynamic, i.e. journey-time, exposures to pollutants.

Furthermore, emerging conceptual and technical developments in routing analysis and Web GIS have been applied for increasing individuals' awareness on dynamic environmental exposures. These applications have been fueled by the proliferation of openly available data of urban pollutants and street networks. Several studies have already demonstrated how dynamic exposure to pollutants can be incorporated in routing algorithms and applications in order to find alternative, and potentially healthier paths (e.g. Alam et al., 2018; Hasenfratz et al., 2015; Hertel et al., 2008; Sharker et al., 2012; Su et al., 2010).

From the perspective of walkability, this study can be seen as an attempt to address a narrow but important component of it - assessing dynamic exposure to environmental pollutants has the potential to offer relevant spatial information of routes and areas of low utility for active transport modes. The proposed approach can also be applied in studying potential spatial (in)equalities in health risks associated with active transport modes. Methodologically, this study aims to develop a conceptual and technical framework for assessing and reducing dynamic (i.e. journey-time) exposure to

environmental pollutants, using traffic noise as an example. The feasibility of the developed methods is demonstrated through a case study of Helsinki.

In the light of this context, the key objectives or research questions of the study are defined as follows:

- 1) Develop a routing method that can both assess dynamic (i.e. journey-time) exposure to traffic noise and find alternative, quieter paths;
- 2) Develop a mobile-friendly web-based route planner application that employs the “quiet path routing method”;
- 3) Discover spatial patterns and possible (in)equalities in pedestrians’ dynamic exposure to traffic noise in Helsinki;
- 4) Assess achievable reductions in dynamic exposure to traffic noise by using the quiet path routing method in Helsinki.

The ideal outcomes of the study are to 1) facilitate development of also other exposure-based routing tools, 2) help individuals to find healthier (quieter) walking routes and 3) facilitate city planners to discover areas of problematic walking conditions with respect to traffic noise. The first and second outcome can be seen as a short-term and the third as a long-term solution in mitigating the negative effects of dynamic noise exposure on individuals’ health.

## II. BACKGROUND

### 2.1 Defining noise

Noise can be defined simply as an unpleasant sound. Also other defining expressions such as unwanted, loud and disruptive reflect the subjective nature of the concept of noise. The lack of explicit definition derives from *noise* being indistinguishable from *sound* by its physical properties; both are fundamentally just vibrations in the air (or other transmission medium). Regardless of this ambiguity, the concept of noise is critical in assessing health effects from exposure to high or unpleasant sounds.

A common measure of noise has been sound pressure level (SPL) which is measured in decibels. The decibel (dB) is a logarithmic unit and works well in measuring audible differences in sound levels. However, since human ear is unequally sensitive to sounds of different frequencies, SPL does not reflect the perceived loudness well as such. Thus, so-called A-weighting is often used to balance out these unequal (perceived) responses to different frequencies. A-weighting method utilizes standardized equal loudness contours, where loudness-SPL (phon-dB) relationships are modeled for a range of frequencies starting at different SPLs (Figure 1).

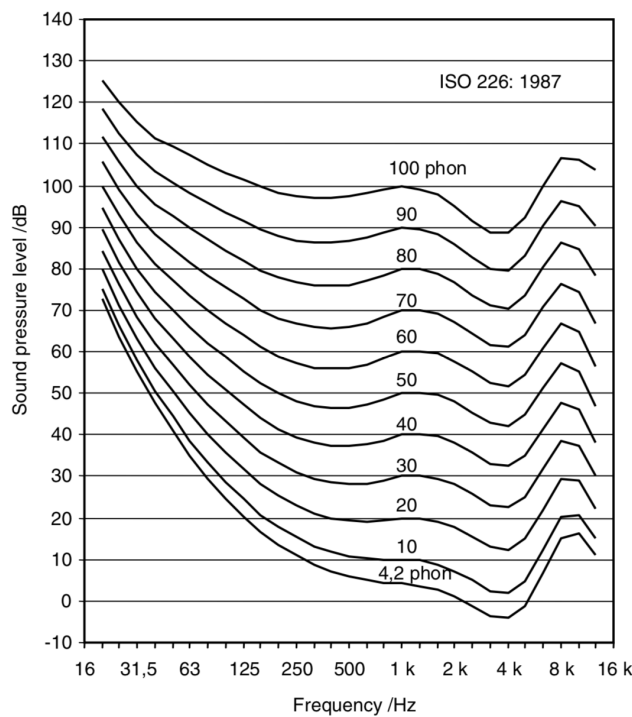


**Figure 1.** Equal loudness contours as in ISO 226 (*Acoustics – normal equal-loudness contours. International Standard ISO 226*).

### 2.2 Traffic noise and health

In urban areas, vehicular traffic is usually one of the major sources of community noise. The level of noise is affected by at least the flow and speed of traffic and the type of vehicles and road surface. Increased but varying traffic noise levels are typical to highways and other major roads.

A variety of metrics has been developed to measure the level of traffic noise. The metrics aim to reflect the perceived loudness but given the time-varying nature of traffic noise, this gets rather challenging. Different vehicles and road surfaces cause noise of different frequencies and tones, resulting in differences in perceived loudness due to human ears' varying sensitivity to different frequencies. A widely used approach to measure and compare traffic noise levels is to use the A-weighted sound pressure level averaged at certain time frames of the day. According to Torija & Flindell (2015), A-weighting may be particularly suitable for modeling the loudness of traffic noise due to the appropriate weighting of the low-frequency sounds. The environmental noise guidelines by WHO Europe (2018b) as well as scientific traffic noise research commonly utilize metrics that are based on averaged "equivalent continuous sound pressure levels" for different times of the day (e.g.  $L_{day}$ ,  $L_{evening}$  and  $L_{night}$ ). One of the standard metrics for community noise levels considers day, evening and night-time noise levels together ( $L_{den}$ ), and features additional weightings for evening and night-time noise levels (WHO Europe, 2018b). These metrics are heavily compressed, and thus lose information about the fluctuations of SPL in time. Nevertheless, uniform metrics are needed in order to efficiently compare different noise environments in space and time.

Several studies have aimed to evaluate the relationship between noise level and annoyance by statistical means (e.g. Babisch et al., 2009; Brown et al., 2015). A common approach has been assessing and comparing the percentages of highly annoyed people (HA%) to average noise level (e.g.  $L_{den}$  or  $L_{Aeq}$ ). An important feature of these assessments is that they consider exposures to noise only with respect to home locations. Guski et al. (2017) reviewed many of the studies and plotted the found HA% values against SPL ( $L_{den}$ ) (Figure 2). Both somewhat linear and non-linear relationships can be seen in the scatterplot, indicating an unclear and case-specific statistical relationship between static noise exposure and annoyance.

According to two literature reviews on traffic noise and annoyance (Brown & Van Kamp, 2017; Guski et al., 2017) and a report on those reviews by WHO Europe (WHO Europe, 2018b), prolonged exposure to noise levels above 53 dB can cause negative health effects and should therefore be avoided. Accurate assessment of different health effects from traffic noise exposure has been challenging due to different temporal realizations of the effects and overlapping exposure-response - relationships of multiple pollutants (Passchier-Vermeer & Passchier, 2000); it is likely that some of

the health effects are developed over years or decades of cumulative exposure while some are perceived and realized in the present time. Accordingly, the potential longer-term effects from exposure to traffic noise include e.g. respiratory infections and cardiovascular disease whereas the short-term effects can be e.g. annoyance or stress (Recio et al., 2016; Van Kempen et al., 2018; WHO, 2011). Moreover, the net health effect from and perception of noise is affected by various “nonacoustic factors” such as gender, age, education and subjective noise sensitivity (WHO Europe, 2018b: 14).

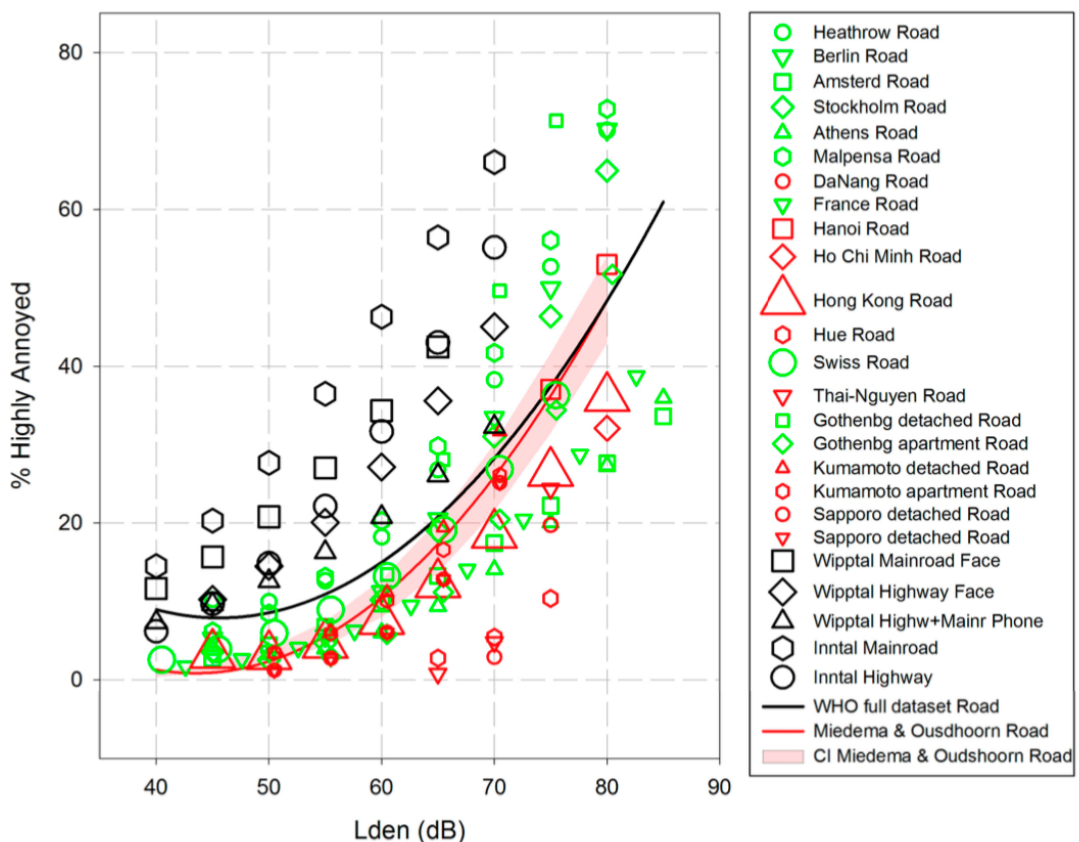


**Figure 2.** A figure by Guski et al. (2017) on relationships between  $L_{den}$  and the percentage of highly annoyed people (HA%) by several studies on road traffic noise and annoyance.

### 2.3 Traffic noise modeling

While air pollution is often challenging to quantify, measure and model, due to its heavy fluctuations and composite nature, then traffic noise can be measured and modeled in a more straightforward manner. Despite varying in space and time, fewer number and more immutable factors affect the occurrence of traffic noise and also it can be measured with more uniform units (e.g. sound pressure level). Vehicular traffic noise levels have been spatially modeled in many European

cities with fairly high spatial resolution – not only since enabled by advanced and spatially explicit technical methods, but also as required by national legislation and the environmental policies of the EU (e.g. Directive 2002/49/EC, 2002).

Advanced software is nowadays available to perform ever more complex noise modeling. Noise models are usually based on methodological frameworks established by the national or international policies. The EU has recently established a noise modeling framework “Common noise assessment methods in Europe” (CNOSSOS-EU) that is being employed in member countries’ policies and assessments (Kephhalopoulos et al., 2012). In the Nordics, a commonly used noise model has been Nord2000 (Jonasson & Storeheier, 2001), which is now being used in parallel or already replaced with the models of CNOSSOS-EU.

Many environmental features can be included in the noise models in calculating modeled noise surfaces. Typically, two kinds of input data are needed to run the models: 1) spatial data of the noise sources and 2) spatial data on features that affect the pathways and absorption of noise. Noise sources usually cover measured or modeled data on vehicular traffic flow, rail traffic and air traffic whereas the latter category includes features such as 3D surface model of the landscape, buildings, noise barriers and weather conditions.

## **2.4 Active modes of transport in cities**

In the last decades, city planners and policy makers have acknowledged the need to promote environmentally, socially and economically more sustainable travel modes (Anciaes & Jones, 2020, Pucher & Dijkstra 2003). Consequently, opportunities for active transport modes have improved and are improving in many cities. Due to the improved opportunities and public support, particularly walking and cycling have become increasingly popular. In the case of Helsinki, for example, the popularity of walking and cycling have increased for several consecutive years and reached the shares of 29 % and 9 % (respectively) of all trips (Brandt et al., 2018).

Walking and cycling are widely promoted as healthy and sustainable alternatives to private cars, as indicated by relevant research (e.g. Litman 2010, Pucher & Buehler, 2010; Rabl & de Nazelle, 2012). While the positive health effects arise from the physical activity, then adverse environmental exposure during the activity may limit the net health effect. Vehicular traffic consumes the opportunities for active transport modes in several ways, including increasing risk for accidents and via air and noise pollution (Jacobsen et al., 2009). Therefore, where the modal shift from car to active transport modes is arguably beneficial in societal level (i.e. socially and economically more

sustainable), individuals may experience also adverse health effects from the increased exposure to pollutants (Hartog et al., 2010; Jacobsen et al., 2009). As per De Hartog et al. (2010), the net health effect of walking and cycling is challenging to assess since it tends to vary in different situations and environments. Nevertheless, based on their extensive literature review, Hartog et al. (2010) concluded that “...the estimated health benefits of cycling were substantially larger than the risks relative to car driving for individuals shifting their mode of transport”. This finding strongly suggests that the modal shift to active transport modes is likely to provide net health benefits already on an individual level, even if many desired societal effects develop only after a substantial share of citizens have adopted the shift.

## 2.5 Concepts and approaches in assessing dynamic exposure

In this chapter, literature on dynamic exposure either to either air pollution or traffic noise is reviewed, since only a few studies have focused solely on noise exposure, and the concepts and spatial analysis methods for assessing dynamic exposures to different pollutants have been more or less analogous.

Due to the suggested mixed health effects of active transport modes (chapter 2.4; Rabl & de Nazelle, 2012; Reynolds et al., 2010; Tainio et al., 2016), means for assessing pedestrians’ exposure to pollutants have been developed in order to enable estimating the net health effect. The concept *journey-time exposure* has been used in a few studies (e.g. Davies & Whyatt, 2009, 2014; Mölter & Lindley, 2015), emphasizing the relative importance of dynamic exposure as a component in individual’s total daily exposure. Journey-time exposure occurs in space and time, where both location of the individual and environmental conditions are dynamic. These considerations introduce a conceptual and technical challenge in implementing assessments for journey-time exposure: the used data needs to have both high spatial and temporal resolution. In the later parts of the thesis, the concept *dynamic exposure* is used interchangeably with the concept *journey-time exposure*.

Exposure to a pollutant is commonly measured simply as either duration or distance of exposure to certain concentrations or levels of the pollutant (e.g. Figure 3). A commonly used index of exposure to a pollutant can be calculated simply by multiplying a set of travel times by the respective levels or concentrations of the chosen pollutant (e.g. Hasenfratz et al., 2015). Specific to studies on exposure to air pollution, one of the metrics has been (estimated) total inhaled doses of different pollutants. Depending on the study setting, dynamic exposures can finally be aggregated by predefined thresholds for concentration (or level) or spatially by using a set of area, street or trajectory features.

In the studies where pedestrians' exposure to pollutants is assessed on modeled trajectories, distance and duration of exposure are often considered proportional and hence used interchangeably (Gulliver & Briggs, 2005). Another type of spatial approximation of dynamic exposures to noise is demonstrated by Sheng & Tang (2011); instead of assessing dynamic exposure by measured or modeled trajectories, they analyze relative significances and lengths of sidewalks and respective traffic noise levels.

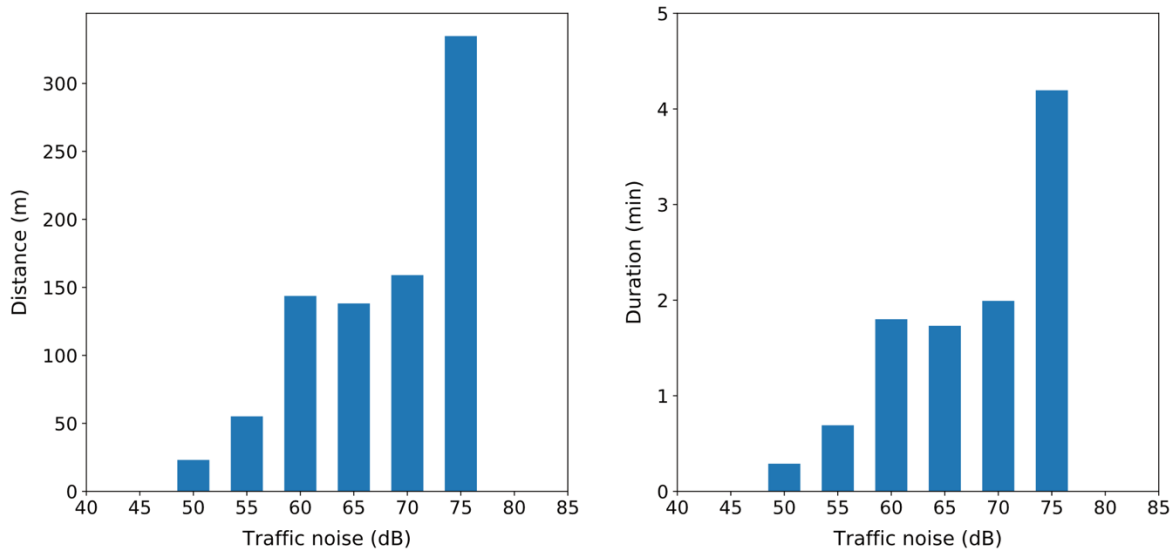


**Figure 3.** An example of quantification of dynamic exposure to traffic noise (on an arbitrary path) as distances (left) and durations (right) of different traffic noise levels.

Based on the previous literature, at least three common approaches for assessing pedestrians' or cyclists' dynamic exposure to pollution exist:

- 1) Direct approach: using measurement instruments (e.g. air quality or volume sensor) attached to members of a study group and tracking them temporally and spatially with GPS or other sensors (e.g. Apparicio et al., 2016; Cole-Hunter et al., 2012).
- 2) Semi-direct approach: using measured and modeled pollutant surfaces and spatial analysis to assess exposure to pollution on realized mobility (again captured with GPS or other sensors) (Whyatt et al., 2007).
- 3) Indirect approach: using measured and modeled pollutant surfaces and spatial analysis to assess exposure to pollution by either simulated or modeled mobility (using e.g. travel surveys or census-based OD data).

However, due to varying urban contexts and availability of technology and data in different studies, the methodologies and study questions have been rather case specific. Hence, along with the three

approaches listed above, other alternative or mixed methodologies have been used to assessing dynamic exposure. Different approaches are suitable for different spatial and temporal scales. While the entirely direct approach (1) can provide accurate data on dynamic exposure for a small subset of the population, then spatial exposure analysis by modeled routes and pollutant surfaces (3) can reveal broader patterns in individuals' exposures. The latter approach is more appropriate in studying population or district level health effects from exposure to pollutants but relies on the knowledge of composition of individual's dynamic exposure gained via direct measurements (1).

GIS, as a technical framework, has been widely utilized in processing and analyzing data in indirect dynamic exposure analysis. Its advantage is clearly the ability to spatially and temporally compare data on both pollutants and individuals' movements. A common step for many dynamic exposure assessments has been the spatial join between pollutant surfaces and GPS-trajectories or modeled routes of people. It is a critical step in determining the dynamic exposure as durations or distances of different concentrations (or levels) of pollutants. Technicalities of the spatial join vary depending on the schema and type (e.g. raster or vector) of the pollutant data, route data, used software and possibly programming environment.

Furthermore, methods for dynamic exposure assessments can empower exposure-based routing. In the following two chapters, approaches and methods for minimizing dynamic exposures through routing analysis are reviewed.

## 2.6 Graph theory and least cost path analysis

Graph is a data structure that can model connected phenomena or a set of objects such as social network, decision tree (abstract phenomena) and transport network (physical phenomena). Essentially, graphs consist of nodes and edges that represent connections and features in the modeled network. Edges are connections between nodes and thus allow "traveling" from one point (node) to another, given that the required connections between the two nodes exist in the graph. Depending on the type of the graph, between any two nodes, one or more edges can exist, and the edges may or may not be traversable to both directions.

One of the widely adapted applications of graphs is modeling and analyzing street networks. In the typical abstraction, intersections are modeled as nodes and streets as edges. Both features can have arbitrary number of attributes describing their physical properties. Numerical edge attributes enable routing analysis within the modeled street network. A common application of graph theory is the least cost path (LCP) analysis, which aims to find the path of least total cost by a given edge attribute

between any two (connected) nodes in a graph. If the length of edges is used as the cost attribute (i.e. weight), least cost path becomes the same as the shortest path. However, as any numerical non-negative edge attribute can be used as the cost, a variety of routing problems can be addressed by solving adapted LCP problems.

Several algorithms exist for least cost path routing, one of the most well-known being Dijkstra's algorithm, accordingly originally developed by Edsger W. Dijkstra (1959). Dijkstra's algorithm finds the very least cost paths between two nodes in a graph by first finding the least cost paths from an origin node to all other nodes of the graph, as illustrated by Jasika et al. (2012) in Figure 4. If the shortest path is needed for only one origin-destination (OD) pair, pathfinding is stopped once the least cost path to the destination node is included in the cumulative set of all known least cost paths.

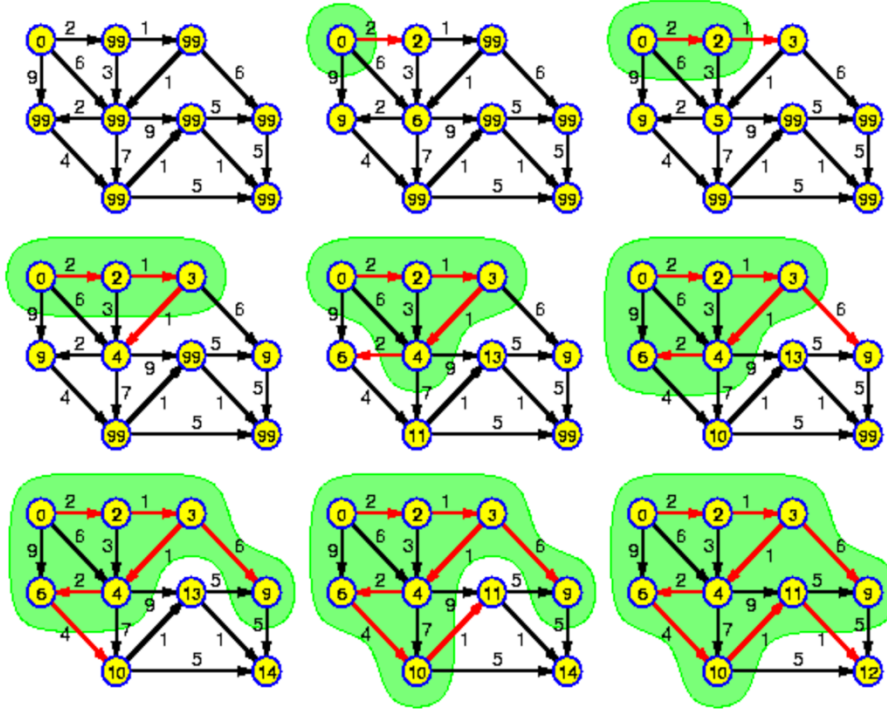


**Figure 4.** An illustration of the sequence of steps in finding least cost paths with Dijkstra's algorithm by Jasika et al. (2012).

When the size of the graph grows, the original form of Dijkstra's algorithm becomes computationally increasingly demanding. Thus, many studies have focused on optimizing the least cost path analysis itself by developing advanced algorithms (e.g. Ahuja et al., 1990; Goldberg & Harrelson, 2005; Noto & Sato, 2000). According to Noto & Sato (2000), the other two key methods for solving the simple least cost path problem are the A\* algorithm and genetic algorithms. A commonly pursued objective in enhancing least cost path finding has been reducing the total number of shortest paths that need to

be known before reaching the desired path (OD pair). Alongside other types of advanced pathfinding algorithms, this has resulted in faster ways of using Dijkstra's algorithm. One of the latter is A\* algorithm, that introduces Euclidean bounds around the origin and destination nodes and selects only a subset of the nodes to be visited. As Noto and Sato (2000) put it: “[A\* algorithm] eliminates fruitless searches by considering the distance to the destination”.

## 2.7 Exposure-based impedances in routing

This chapter features a short review of route planners for walking or cycling that consider environmental factors in addition to travel time. A related, yet omitted, emerging area of research is emissions optimization in vehicle routing problems (e.g. Qian & Eglese, 2016).

In accessibility research, travel time is often used as one of the key metrics of accessibility. Likewise, in also routing analysis, travel time seems to be the most often optimized variable. However, also other types of costs have been incorporated in routing analysis when using special criteria for pathfinding. Adjusted LCP analysis can be used to solve a variety of pathfinding problems, including finding paths of least environmental exposure. Several vivid names have been introduced to describe and promote different types of least-exposure paths. These names include e.g. green, healthy, happy, sustainable, safe and quiet paths (e.g. Bao et al., 2016, 2017; Hatzopoulou et al., 2013; Quercia, 2015; Quercia et al., 2014). In the context of this study, the concept quiet path is used to refer to routes of less noise exposure.

In route planners for walking and cycling, environmental exposure-based costs have been introduced in LCP analysis in order to find more pleasant and healthier routes for active transport. Both raster (surface) and graph-based routing methods have been used in exposure-based routing. In urban contexts, many of the studies have utilized graph-based methods since graphs apply well in modeling urban street networks. Many studies have demonstrated how graph-based LCP analysis can be used to minimize exposure to pollutants (e.g. Alam et al., 2018; Hasenfratz et al., 2015; Hertel et al., 2008; Sharker et al., 2012; Su et al., 2010).

Based on the discovered literature, raster-based LCP analysis methods (in exposure-based routing) were applied only in a few studies. For example, Davies and Whyatt (2009) used air pollution surfaces ( $PM_{10}$ ) and spatial data on traversable and non-traversable features of the study area to find least-exposure paths with common raster-based LCP functions. The decision to use raster-based method enabled them to incorporate continuous areas (e.g. parks) in the routing analysis. Their method

worked well for a relatively small study area but required careful data preparations to mask out all unwalkable features.

Incorporating dynamic exposures in LCP analysis has commonly required defining a custom cost function for calculating adjusted costs (i.e. impedances) by the exposures. For example, Ribeiro & Mendes (2013) used the concepts “contamination of distances” and “environmental impedance function” (EIF) to model exposure-based impedance from noise and air pollution ( $PM_{10}$ ). They assigned noise-based costs to edges of a graph according to contaminated distances of different noise levels, using predefined thresholds (dB) to decide whether a noise cost should be assigned or not. A commonly used way to balance between exposure-based impedances and travel-time has been to include distance as a base-cost in the EIF. In many studies, distance and travel time were considered as proportional, limiting complexity of the EIF. If exposures to multiple pollutants need to be integrated in a single EIF, or their relative weights in the cost function need to be adjusted (with respect to distance or to one another), EIF can also include additional cost coefficients. The idea of integrating multiple environmental exposures in a composite EIF is discussed further in chapter 5.8.

Despite the common goal of the exposure based EIFs presented in different studies, namely reducing dynamic exposure to pollutants, the composition of the cost functions has varied considerably between studies. This suggests that minimizing environmental exposures through routing analysis is more emerging than already well-established area of research. Many of the demonstrated methodologies have been influenced by different constraints on data availability but also by varying and subjective perceptions of impedances of different pollutants. Given this scientific background, a custom EIF for traffic noise was designed also in this study (see 3.5.2) and can be considered as one of the main outcomes of the thesis.

Many of the previously developed exposure-based routing methods (and applications) focus on dynamic exposure to air pollution. Means for finding least cost paths with respect to exposures to e.g.  $PM_{2.5}$  or  $PM_{10}$  particles have been developed in several studies (e.g. Davies & Whyatt, 2009; Hertel et al., 2008; Mahajan et al., 2019; Müller & Voisard, 2015; Möller & Lindley, 2015; Ribeiro & Mendes, 2013; Van den Hove et al., 2019; Zou et al., 2020). In these studies, considerable decreases (%) in the total exposure to the pollutants were found on the exposure-optimized paths, indicating a potential for green path route planners. Common to most of the prior studies on exposure-based routing, the alternative routes are presented with comprehensive statistics allowing comparison of differences in dynamic exposure, route length and travel time.

Some of the exposure-based LCP methods were developed further as web-based route planner services (e.g. Hatzopoulou et al., 2013; Su et al., 2010; Zou et al., 2020) or mobile applications (e.g. Caggiani et al., 2017; Hasenfratz et al., 2015). In these services, special attention has been paid on the visualization of the different route alternatives as well as presenting respective differences in exposures to pollutants and travel times. However, no visual representations of dynamic exposures to pollutants on the alternative routes were seen in most of the functional route planners at the time of writing this thesis. Instead, properties of the routes (e.g. exposures, travel time and distance) were often presented only numerically. To the author's knowledge, this is one of the critical shortcomings of most currently available (exposure-based) route planners and thus one of the motivations for creating a novel green path route planner application: to demonstrate how journey-time exposure on different routes could be better communicated also visually.

In the prior studies, publishing an exposure-based routing application as an online service has also required optimizing the efficiency of the LCP analysis to support responsive enough user experience. Hasenfratz et al. (2015) demonstrated how using static pollution maps and loading the whole LCP analysis application into the memory of a smartphone can provide very fast responses to user's actions. On the other hand, for example Su et al. (2010) implemented their route planner as a service based web application, where a distinct user interface application communicates with a exposure-based LCP service via asynchronous requests, leaving the user interface active even at times when routes are being calculated. By reviewing the discovered literature on exposure-based route planners, the latter approach was found more commonly utilized than building standalone mobile or desktop applications (such as the one by Hasenfratz et al. (2015)). A variety of viable technical implementations for such services seem to be available due to the increased opportunities that modern Web GIS technologies enable.

## 2.8 Web GIS concepts and developments

In this chapter, some concepts and developments of modern Web GIS are reviewed. In order to ensure that state of the art technologies are used in the technical implementation of the quiet path route planner, the focus is on the latest technological advancements that can empower highly interactive web map applications.

According to Agrawal & Gupta (2017) and Veenendaal et al. (2017), recent developments in Web GIS technologies and in their applications have happened in the context of emerging paradigms in common web technologies and increasing numbers of users. Alongside the growing number of web

users, also the ways people are using web services have changed. Increasing number of web users prefer mobile over desktop (Meeker & Wu, 2013, 2018), which has created new demand and opportunities for mobile-friendly web map applications (Veenendaal et al., 2017). In other words, it has been acknowledged that mobile users are the primary user group of many, if not most, new web applications. This shift has facilitated the adaptation of mobile-first principle and Responsive Web Design (RWD) in web development; the content and user interfaces (UIs) of modern web applications have been designed to look good on screens of all sizes (RWD), starting from the very smallest ones (mobile-first).

Emerging service-oriented architectures (SOA) have allowed distributing the most expensive data processing and analysis operations in dedicated machines. The concept has also been applied in Web GIS applications, enabling uninterrupted user interfaces and fast geospatial processing and analysis. Another benefit from SOA is scalability of web applications to support high but changing numbers of concurrent users. These developments can be seen as an adoption of a larger scale paradigm shift from independent applications to service-oriented architectures in Web GIS (Agrawal & Gupta, 2017). As per Lu (2005), “The service-oriented architecture is a very promising architecture for practical implementation of the next generation geographical information systems”. The shift towards SOA-based Web GIS solutions has occurred together with the emergence of cloud-computing platforms such as Amazon Web Services (AWS), Microsoft Azure cloud and ESRI ArcGIS Online (Veenendaal et al., 2017: 13). These services allow running GIS applications in appropriate infrastructure, either in hosted servers or using a serverless architecture. Then, distributed GIS services and data sources can be accessed via application programming interfaces (APIs) in similar manner as conventional web services. Complex GIS systems can be composed from a desired set of separate services and data sources, as illustrated by Veenendaal et al. (2017) in Figure 5.

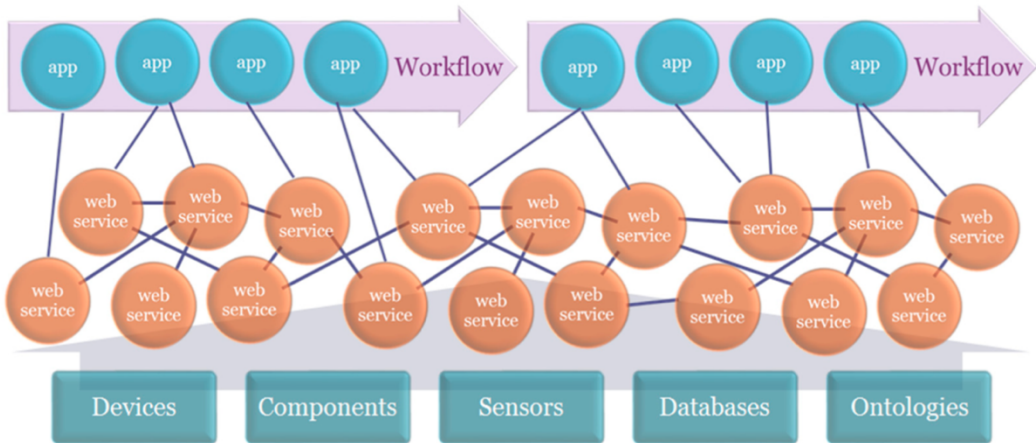


**Figure 5.** An illustration by Veenendaal et al. (2017) on interacting web services that feed into apps within application workflows.

The advantages of SOA for Web GIS systems also includes the ability to utilize services provided by public authorities and governments. Virtually any service that can be accessed through APIs can be integrated into Web GIS system using SOA. Integration of geospatial services has been facilitated with standardized geographical data formats and protocols such as web map service (WMS) and web feature service (WFS). Encouraged by SOA, the user interface of a Web GIS system can communicate with the supporting GIS services asynchronously (e.g. Neis & Zipf, 2017; Su et al., 2010), leaving the user interface layer always reactive to user's actions. This is a major difference (and improvement) compared to e.g. traditional desktop GIS software, which still often struggle to provide smooth user experience while executing geospatial analysis.

Some of the advancements in Web GIS technologies are enabled by the increased computational capabilities of users' devices and servers. Today, web browsers of personal computers and smart phones have access to increased computing power and graphics processing capabilities. Thus, modern web browsers enable running ever more vivid and interactive web map applications and also executing simple geospatial analysis right in the user's device (i.e. "client-side"). The limitations for running Web GIS applications in the browser are ever less set by the capabilities of the users' devices but then more by the available software that can utilize them.

Another aspect that has facilitated the advancing of Web GIS is the development of open source data formats and code for geospatial analysis and web-based visualizations (e.g. web map libraries, spatial databases and libraries for geospatial analysis). Many of these formats and software (e.g. Leaflet; OpenLayers & PostGIS) are actively developed by open source communities and some of them also financially supported by authorities of private companies.

A critical component of a Web GIS system is its user interface, which often is a web map application - if excluding pure Web GIS *services* such as geocoding and routing APIs. Many web map libraries are available for building customized interactive web map applications. They are usually implemented with JavaScript (JS) programming language as that is one of the few programming languages that is natively supported by most web browsers. While most web maps used to be (and probably still are) based on tiled raster maps (often called as basemap), some novel web map technologies have been introduced (Gaffuri, 2012; Lienert et al., 2012). The latest major revision of HTML (hypertext markup language), HTML5, added prominent capabilities for drawing increasingly rich and interactive vector-based visualizations. It has been demonstrated that HTML5-enabled technologies can be used in implementing web map applications with vivid vector graphics (e.g. Boulos et al., 2010; Farkas, 2019; Qiu & Chen, 2018). Also, HTML5 reduces the need for additional plugins (e.g. Adobe Flash Player) when dealing with interactive graphics. For example, one of the promising (HTML5-enabled) technologies for vector-based interactive web mapping, among other use cases, is WebGL. For example, one of the web map libraries that heavily utilize WebGL is Mapbox GL JS.

Apart from the technical advancements of the components of Web GIS, the broader picture of contemporary Web GIS has been studied with respect to various parallel developments, trends and opportunities. Veenendaal et al. (2017) illustrated this larger conceptual and technical framework (around Web GIS) with a pyramid of labelled Data, Information, Knowledge, Intelligence and Wisdom (DIKIW) (Figure 6). According to the review by Veenendaal et al. (2017), the advanced technical frameworks within and around Web GIS can facilitate providing users with both more personal and richer geospatial information.

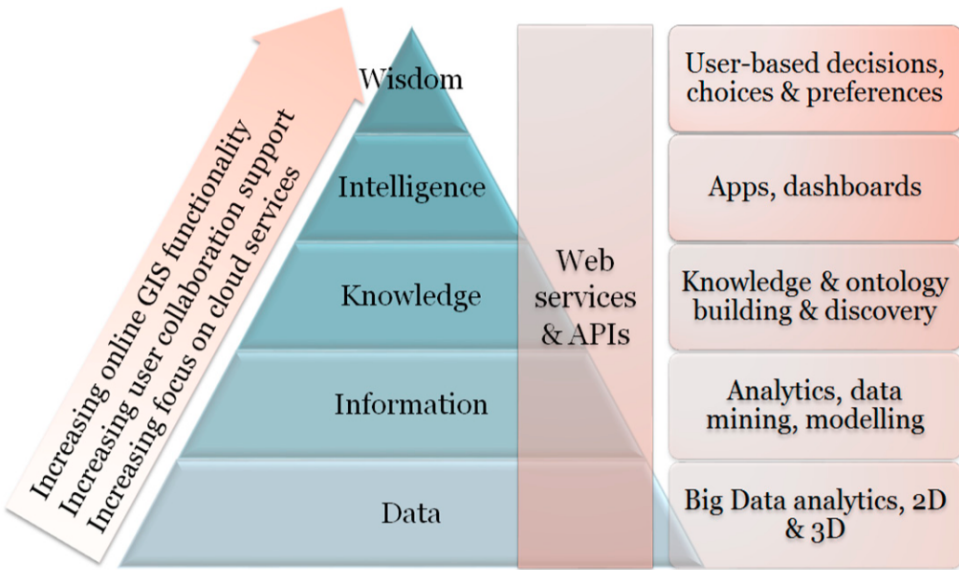


**Figure 6.** Illustration by Veenendaal et al. (2017): "Focus and trends in increasing web mapping functionality".

### III. DATA & METHODS

#### 3.1 Overview of the methods

Overview of the methods and their internal dependencies is illustrated in Figure 7. As shown in the figure, the three outcomes of the thesis depend on the routing application that optimizes both shortest and quiet paths. Assessments of pedestrians' exposure to traffic noise (1) and potential to reduce exposure to traffic noise (2) are linked to each other, as the achievable reductions are calculated using the same set of origin-destination walks determined in the first assessment. The web-based quiet path route planner (3) is a detached outcome from the first two and has additional dependencies to several Web GIS technologies.

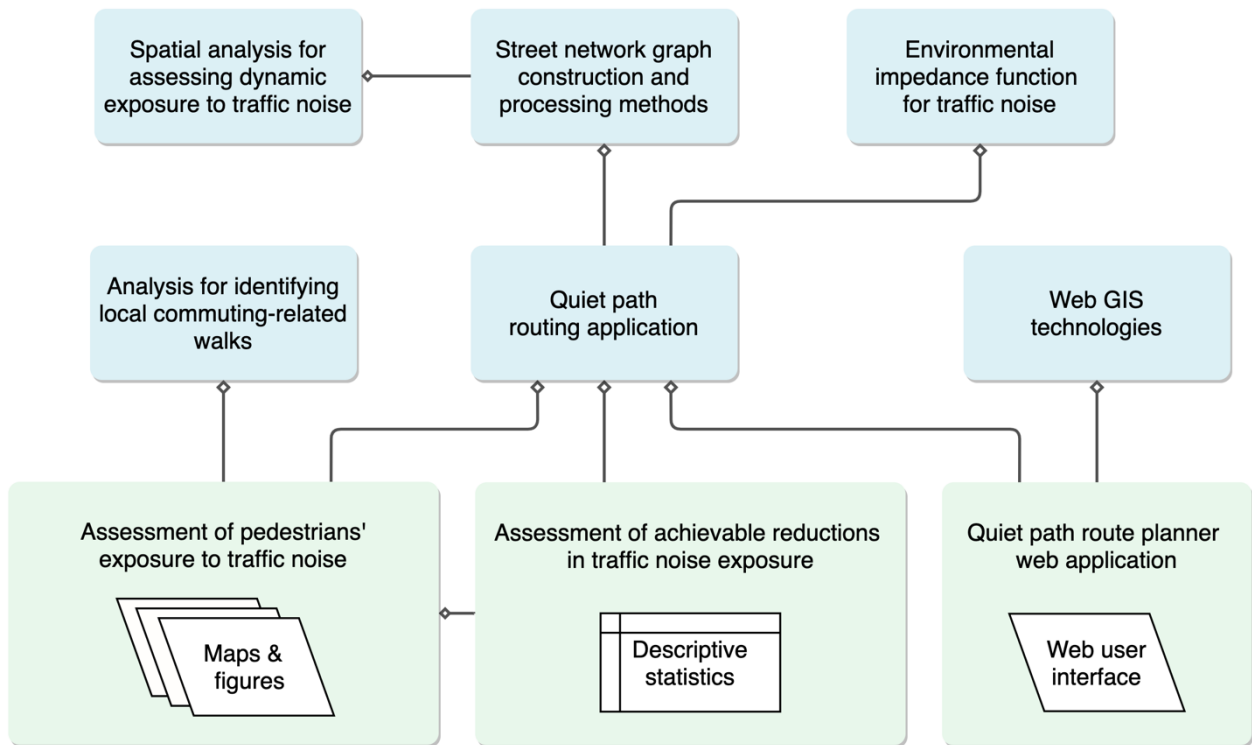


**Figure 7.** Illustration of the internal dependencies of applied methods and the results of the study.

#### 3.2 Study area

The study area of the case study of this thesis is Helsinki, as defined by the extent of the modeled traffic noise zones in Helsinki (Figure 8). Some of the islands in the very southern Helsinki were excluded from the study area as the traffic noise data does not cover them and they feature only minor and isolated street networks.

Helsinki is the capital of Finland and also one of the most important workplace hubs of the country. Its 653 835 inhabitants and 397 346 workplaces (Statistics Finland, 2020) make it a vibrant city with high flows of daily commuters. The majority of the trips in Helsinki are made by walking, cycling (Brandt et al., 2018) or with public transport organized by Helsinki Region Transport (City of Helsinki, 2020).

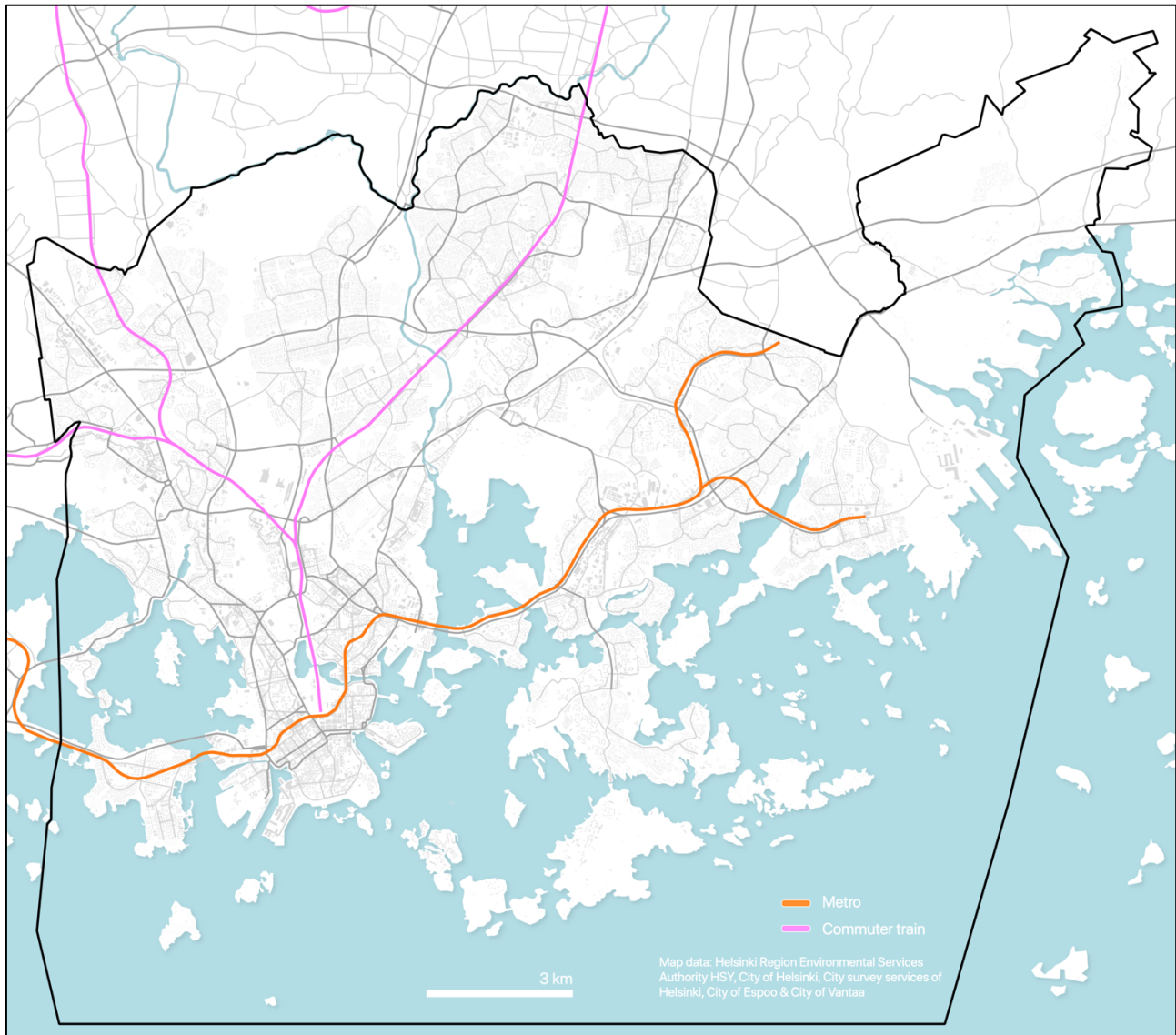


**Figure 8.** The study area and its key transportation networks.

### 3.3 Data

Several datasets were used in the study (Table 1). The developed routing application required only two input data, street network data from OpenStreetMap and modeled traffic noise zones, of which both were available as open data. On the other hand, the assessment of pedestrians' exposure to traffic

noise required a set of additional datasets of which the census-based commuting flow data was not openly available.

**Table 1.** Data that were used in the study.

Name	Source	Description	Use in the study	Open data
Traffic noise zones in Helsinki 2017	Urban Environment Division of city of Helsinki (Helsingin kaupunkiympäristöntoimiala)	Modeled traffic noise surfaces by different noise sources, e.g. A-weighted equivalent continuous sound pressure levels from traffic noise ( $L_{Aeq}$ ).	Dynamic exposures to noise pollution are assessed by the noise zones of this data.	Yes
250m statistical grid	Statistics Finland	250m * 250m polygon grid layer that is linked to YKR-commuting data.	Grid cells are used as origins and destinations in the analysis of pedestrians' dynamic exposure to traffic noise and in visualization of the results.	No
YKR-commuting data	Finnish Environment Institute (SYKE) / Statistics Finland	T06_tma_e_TOL2008_2016_hel – census-based commuting flows between 250m statistical grid cells. One row in the data reports the total number of commutes between a pair of grid cells.	Commuting-related walks are modeled by planning public transport itineraries for the commuting flows.	No
City districts in the Helsinki Metropolitan Area	Helsinki Region Environmental Services Authority HSY	City districts as polygons.	Centers of the city districts are used as destinations for distant workplaces in the itinerary planning analysis.	Yes
OpenStreetMap	© OpenStreetMap contributors	All walkable highways and paths as features of the street network.	A street network graph suitable for routing is constructed from the data.	Yes
Digitransit Routing API	Helsinki Region Transport (HRT)	A routing service for planning public transport itineraries via an application programming interface (API).	Itinerary planning for commuting flows was carried out using the routing API.	Yes

### 3.3.1 Modeled traffic noise data

As per Kephalopoulos et al. (2012: 11) (CNOSSOS-EU): “Since June 2007, EU countries are obliged to produce strategic noise maps for all major roads, railways, airports and agglomerations, on a five-year basis.”

I assessed dynamic exposures to traffic noise with respect to latest modeled traffic noise zones for Helsinki (City of Helsinki: strategic noise mapping, 2017). The noise modeling was carried out with a special software for the purpose (Datakustik CadnaA 2017) by Sito Oy as a commission from the city of Helsinki (City of Helsinki: strategic noise mapping, 2017). As per the documentation of the data, a wide range of factors affecting the ways and levels of noise were taken into account in the modeling. For example, these included noise source data of modeled traffic flows and speeds on different roads, the three-dimensional surface model of the city, buildings, sound barriers and acoustic properties of different surfaces (City of Helsinki: strategic noise mapping, 2017).

Prior to pre-processing the noise surface data, I inspected two parallel noise surface layers for vehicular traffic, one produced with CNOSSOS-EU modeling (Jarno Kokkonen et al., 2016; Kephalopoulos et al., 2012) and the other with joint-Nordic traffic noise estimation model (Jonasson & Storeheier, 2001; Nielsen, 1997). The latter was chosen for the study since its modeling height of 2 meters was closer to the typical walking altitude of pedestrians than the 4 meters from the ground used in CNOSSOS-EU model. However, since CNOSSOS-EU model has been described to have higher level of detail in both noise source and noise diffusion modeling (City of Helsinki: strategic noise mapping, 2017), choosing it could have been justified as well. Nonetheless, a visual comparison of the two noise layers did not reveal major differences between the two.

The noise surface data contained a few alternative noise indices. For this study, I chose the A-weighted equivalent continuous sound pressure level from vehicular traffic noise ( $L_{Aeq}$ ) for daytime (7am –22pm) as the primary noise index (layer: *2017\_alue\_01\_tielikenne\_L\_Aeq\_paiva*). A-weighting is used to consider the human ear's sensitivity to sounds of different frequencies (see 2.1). Then equivalent continuous sound pressure level is an averaging method for calculating a single sound pressure level from a time-varying sound pressure level during a defined time period (see chapters 2.1–2.3 for more information). As per Guski et al. (2017) and Van Kempen et al. (2018), both of these metrics (A-weighting and equivalent continuous sound pressure level) have been widely utilized in the studies on traffic noise and annoyance.

The data included modeled traffic noise surfaces attached with attribute data on the minimum and maximum traffic noise levels ( $L_{Aeq}$ ) as per a pre-defined set of 5-decibel ranges. The modeled traffic noise levels ranged from 45 dB(A) to 80 dB(A). I made three map visualizations of the noise surfaces to illustrate the high spatial precision of the modeling (Figure 9, Figure 10 & Figure 11). For example, the effect of buildings as effective noise barriers can be seen when comparing the noise surfaces

between Figure 10 and Figure 11; in the first map the +60 dB(A) noise surfaces spread hundreds of meters from the highways whereas in the latter they are more restricted between the buildings.

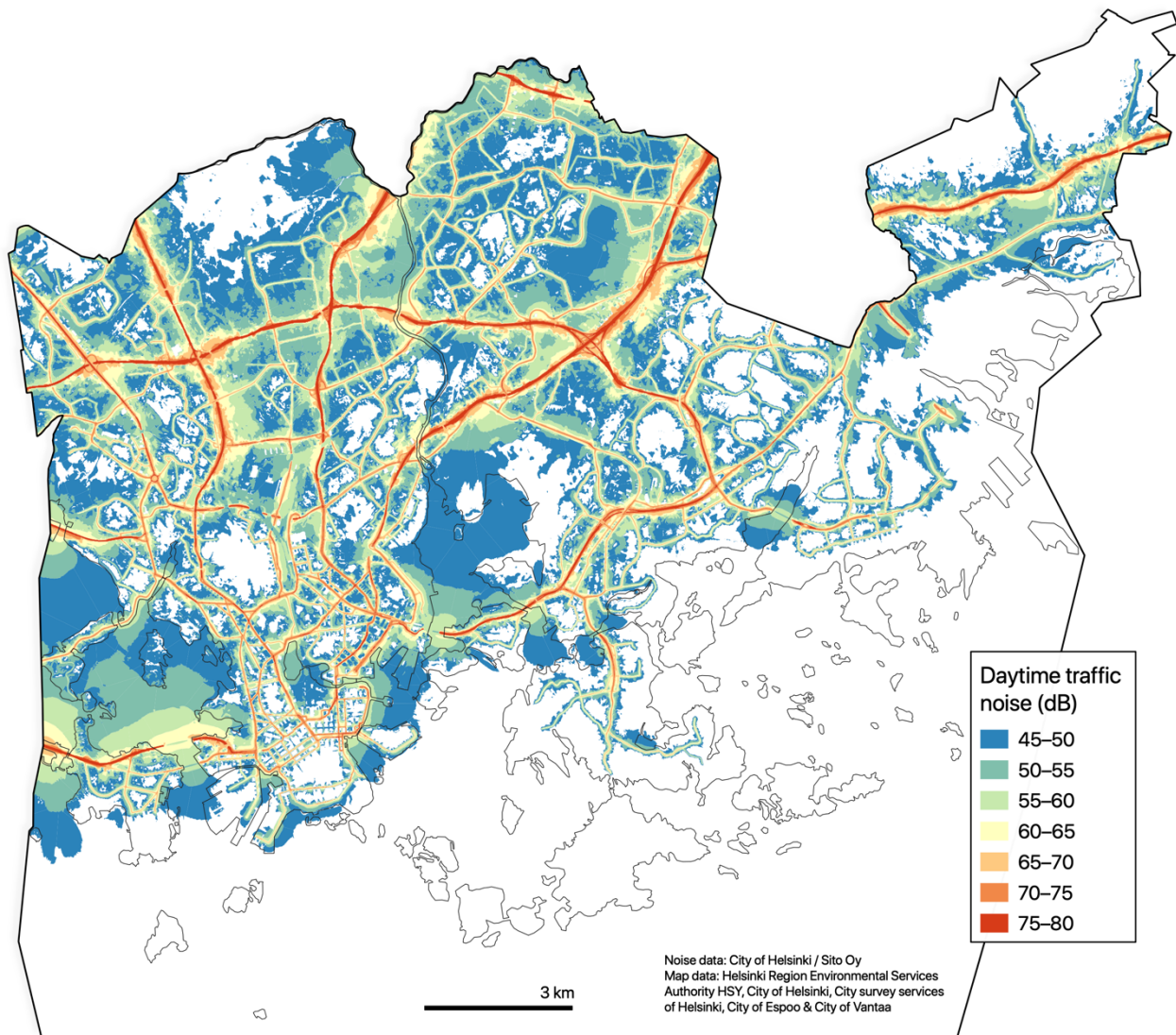


**Figure 9.** Modeled daytime traffic noise levels (dB(A)) in Helsinki (City of Helsinki: strategic noise mapping, 2017; visualization by the author).

Only small amount of pre-processing was needed prior to utilizing the noise surface data in the study. I found a few topological errors in the data (revealed first in the assessment of pedestrians' dynamic exposure to traffic noise and then in the validation of the spatial join); in some cases, two or more noise surfaces intersected with each other, resulting areas with multiple (parallel) noise index values. These topological anomalies were not fixed, but instead considered when spatially joining the noise values to street network data. When two or more competing noise values were found in the spatial join, only the maximum value was extracted (see 3.5.1). I validated this practice through a visual inspection of the noise surface data: the surfaces representing higher noise levels appeared

considerably more logically with respect to the presumed noise sources than the intersecting (underlying) ones of lower noise levels.

It should be noted that the decision to use noise data of only noise source (vehicular traffic) in the dynamic exposure assessment is arguably in line with the *Environmental noise guidelines for the European Region* (Kephhalopoulos et al., 2012). The guidelines and the supplementary literature state that the thresholds for harmful noise levels vary between different noise sources. Also, the mitigation actions for dealing with different types of community noises vary, making the results of separate exposure assessments more valuable for planning purposes. In this study, the main focus is on dynamic exposure to vehicular traffic noise, excluding exposure to noise from rail and air traffic and industrial sites. Despite that this approach may be appropriate for the dynamic noise exposure assessment, the noise exposure-based routing application could benefit from integration of also other noise sources in the routing analysis. The prospects for integrating multiple environmental exposures (including different noise sources) in exposure-based routing are discussed further in chapter 5.8.

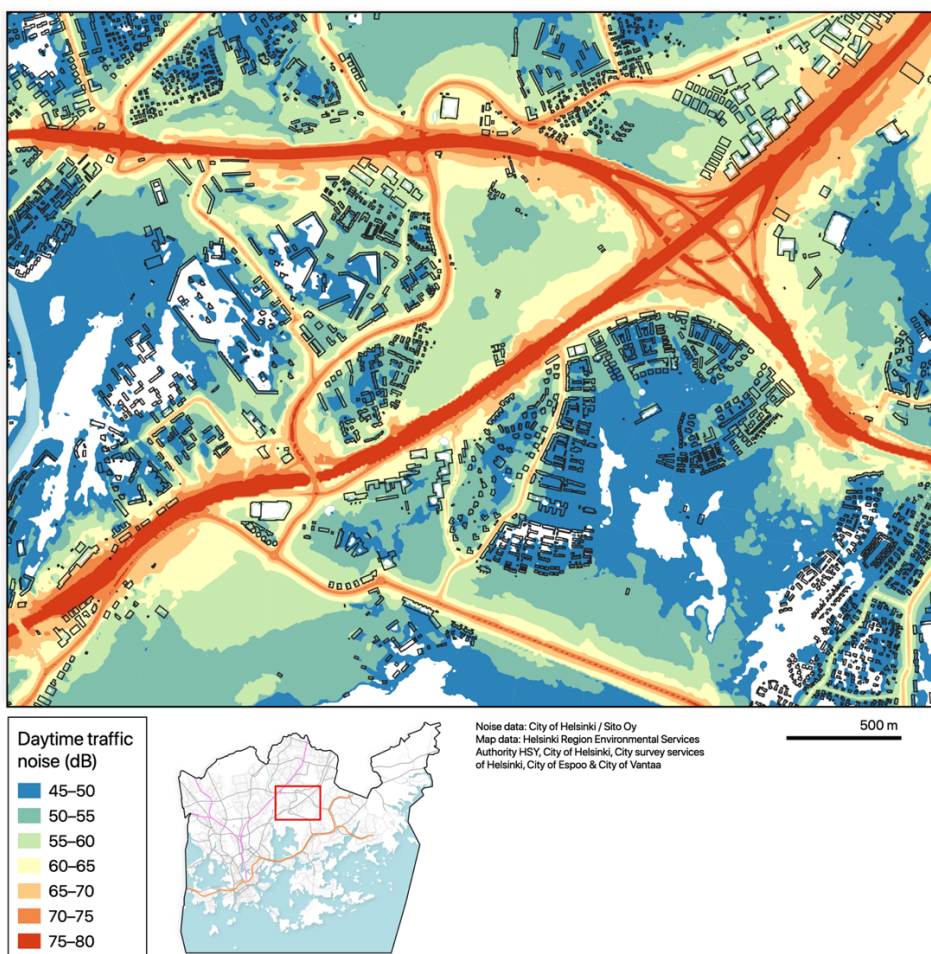


**Figure 10.** Modeled daytime traffic noise levels (dB(A)) in Viikki (City of Helsinki: strategic noise mapping, 2017; visualization by the author).

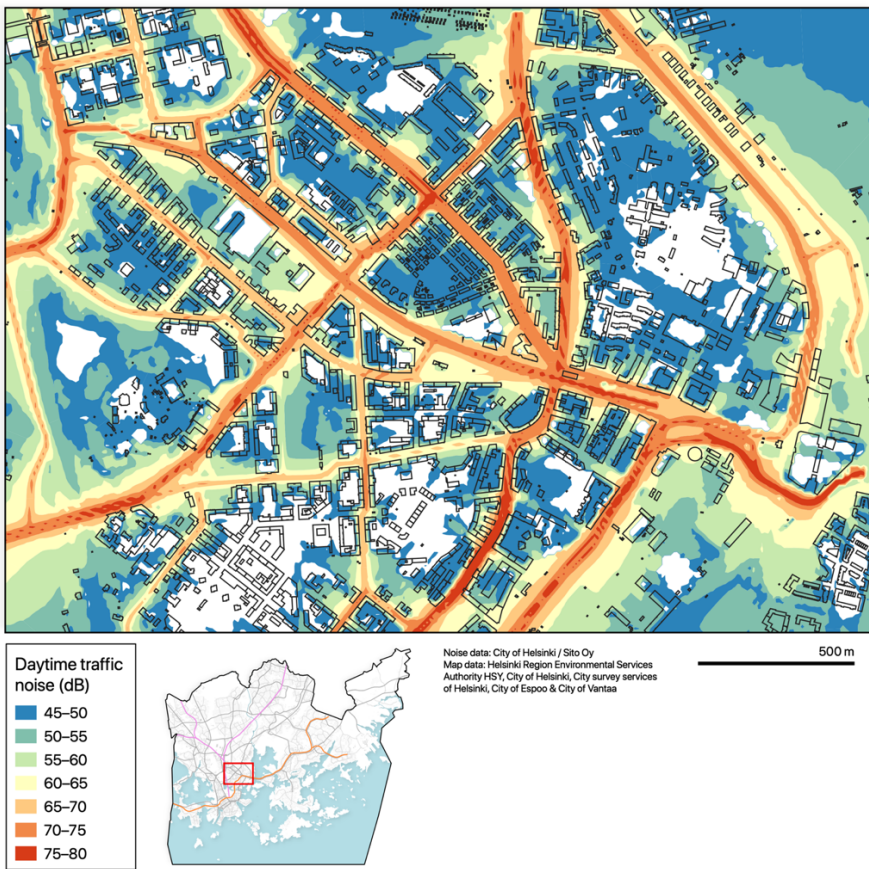


**Figure 11.** Modeled daytime traffic noise levels (dB(A)) in Kallio and Vallila (in Helsinki) (City of Helsinki: strategic noise mapping, 2017; visualization by the author).

### 3.3.2 OpenStreetMap data

I downloaded a large dataset of street network features from OpenStreetMap (OSM) for walkable street network graph construction. The data was queried from Overpass API (2019) which allowed using a custom query string to request only the appropriate features based on their attributes. The python library OSMnx (Boeing, 2017) provided a practical way for accessing the API and using a customized query string. The query string was based on the default query string of OSMnx for walkable street features but adjusted to exclude several unwalkable features (Table 2).

Yet, some unwalkable street features were needed to be filtered out from the graph only after creating it due to limitations in the querying capabilities of OSMnx. Hence, a subsequent download of unwalkable street network data was required.

Choosing OSM data as the basis of the walkable street network graph can be justified with at least three arguments. As demonstrated by a number of studies, e.g. Zielstra & Hochmair (2011, 2012), OSM often contains a comprehensive set of walkable street features of major cities, since the data is

updated by active local OSM communities (1). The street network data used in the official route planner application of Helsinki Region Transport (HRT/HSL) authority is solely based on OSM data. Therefore, OSM data of the area is kept up to date by also professional mappers (2). Moreover, the use of OSM data allows easier adopting of the methodology in other study settings and areas (3).

**Table 2.** Query strings for street network data downloads to be used with Overpass API and OSMnx python library.

Graph description	Query string
Walkable street network graph	<code>["area"!~"yes"]["highway"!~"trunk_link motor proposed construction abandoned platform raceway"]["foot"!~"no"]["service"!~"private"]["access"!~"private"]</code>
Additional graph of unwalkable street segments (e.g. service tunnels)	<code>["area"!~"yes"]["highway"!~"trunk_link motor proposed construction abandoned platform raceway"]["foot"!~"no"]["service"!~"private"]["access"!~"private"]["highway"~"service"]["layer"~-1 -2 -3 -4 -5 -6 -7"]</code>

### 3.3.3 Register based origin-destination (OD) commuting data

I acquired census-based commuting data (T06\_tma\_e\_TOL2008\_2016\_hel) for the study to enable public transport itinerary planning from homes to workplaces. The planned itineraries were needed for the assessment of pedestrians' exposure to traffic noise. The commuting data was produced by Statistics Finland and provided by the Finnish Environment Institute. It is commonly referred to as YKR-commuting data ("Yhdyskuntarakenteen seurannan aineistot"). In the data, daily commutes are reported by aggregated origin-destination (OD) flows between 250 m statistical grid cells covering the whole country. Essentially, a commuting flow for one OD (cell) pair is reported with one row in the data. The data only includes commutes for which the coordinates of both origin and destination are known. Thus, presumably small share of all commutes was omitted in the analysis. Assessing the accuracy and quality of the commuting data were left outside the scope of the thesis. The only pre-processing that I did for the data was extraction of commuting flows that originated in the study area.

### 3.3.4 Online routing service of the local public transport authority

I used the online route planner service of Helsinki Region Transport (HSL) authority in planning public transport itineraries for the commutes (Digitransit Routing API -

<https://digitransit.fi/en/developers/apis/1-routing-api/>). The service was accessed via its application programming interface (API) to allow efficient and reproducible itinerary planning. The planned itineraries were needed in two phases of the study: 1) in finding local (commuting-related) walking routes for the assessment of pedestrians' exposure to traffic noise (see 3.7.2), and 2) in assessing the quality of the shortest paths calculated with the quiet path routing method in comparison to the reference paths returned from the API (see 5.5).

### 3.4 Technical framework and architecture

The technical framework of the study is composed of several internal and external dependencies (Figure 12). I implemented the majority of the data analysis and the quiet path routing method in Python programming language. Thus, the main external dependencies of the study cover several Python libraries that I used in processing and analyzing statistical, geospatial and graph data (e.g. Pandas, GeoPandas, NetworkX and OSMnx). The used libraries and packages have also their own external dependencies which are now shown in the figure.

I favored modular design pattern in developing the methods as a Python project. This meant establishing common utilities to be used in different phases of the analysis as well as by the quiet path routing application. I distributed functions to separate Python modules with distinct responsibilities to make finding and using them practical. The detailed technical description of the external dependencies (i.e. libraries) of the Python environment is attached as Appendix 1. Sharing of the methods as openly available source codes is described in chapter 4.5.

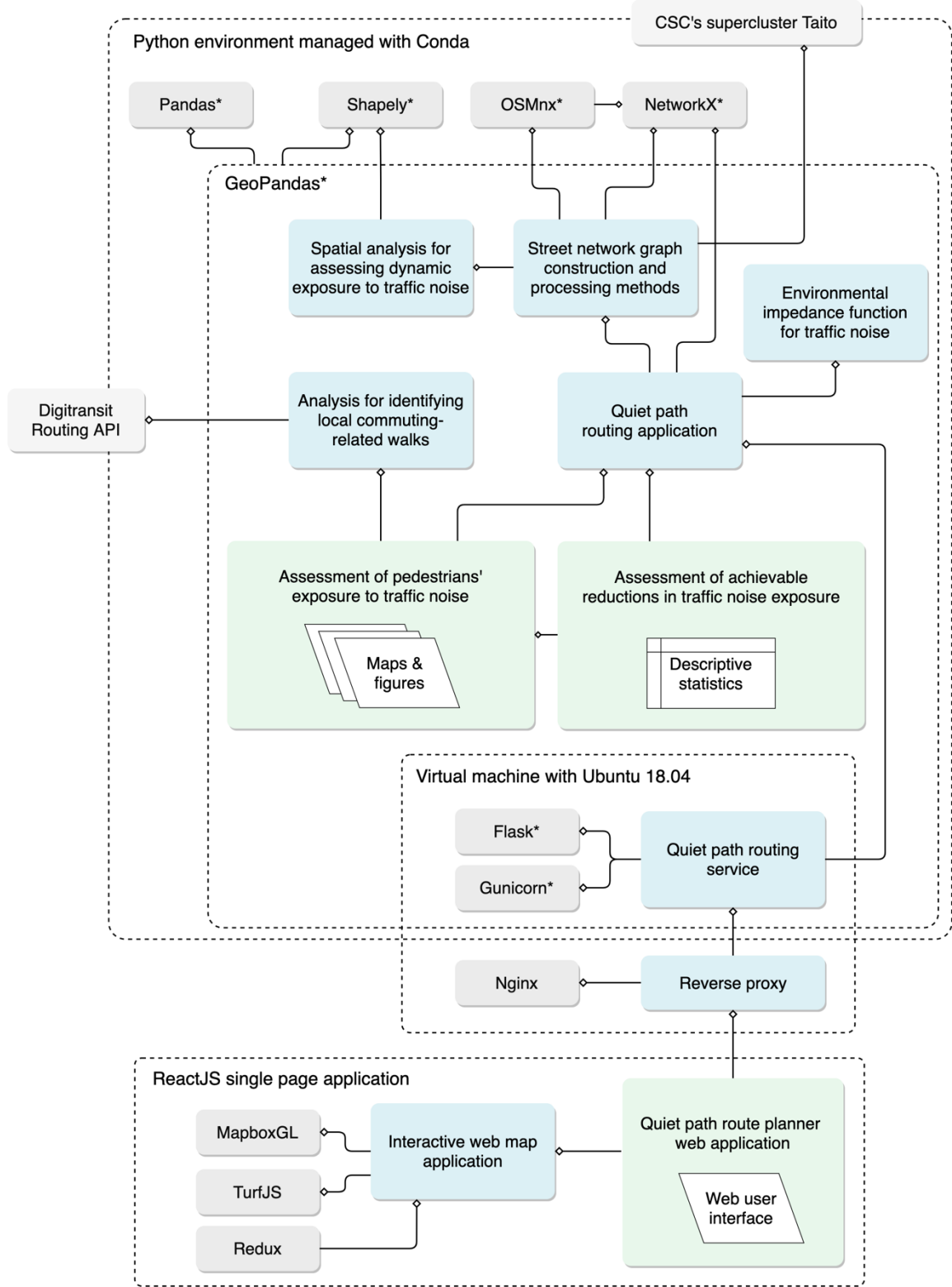


**Figure 12.** Technical framework of the study: internal (blue) and external (grey) technical dependencies (\* = Python library). The several external dependencies of the used Python libraries are not included in the graph.

### 3.5 Quiet path routing method

### **3.5.1 Network acquisition and manipulation**

I included the following three steps in acquiring and processing street network data to a graph suitable for noise exposure based routing analysis:

- 1) Walkable street network data acquisition and graph construction (Figure 13);
- 2) Determining contaminated distances with different noise levels: spatially joining noise surface data to edges (Figure 14);
- 3) Calculating noise exposure based costs to the graph with an environmental impedance function for noise (see 3.5.2, 3.5.3 & Figure 16).

I used the Python library OSMnx to download walkable street network data from OSM and to build a graph from it in NetworkX format (as described in chapter 3.3.2). OSMnx was also used to convert the directed graph to an undirected one, as street segments can be traversed to both directions by walking. Undirected graphs also require less computing power and memory for processing. After initial graph construction, straight line geometries were added to edges that were missing them, based on locations of the origin and destination nodes of the edges.

A temporary graph of unwalkable edges (e.g. service tunnels) was constructed in similar manner as the main graph but by using an altered query string (Table 2). The unwalkable edges were matched with the edges of the main graph by both *osm\_id* and geometrical overlay analysis. Both matching methods were needed since *osm\_id* is not guaranteed to be unique in all cases. The edges that were matched and identified as unwalkable were then removed from the graph. Finally, I made sure that no inaccessible edges or nodes were left in the graph as subgraphs (due to lost connections between nodes).

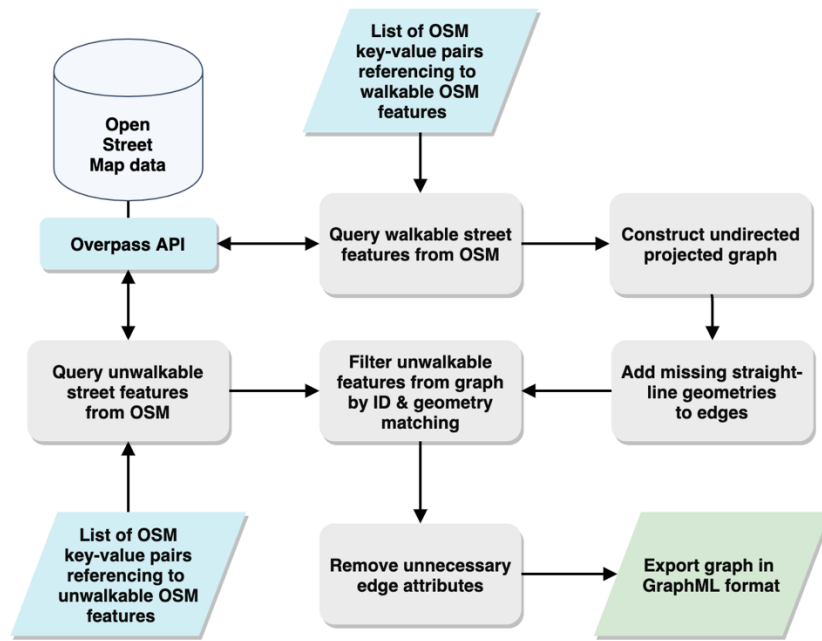


**Figure 13.** Workflow of street network graph acquisition and construction.

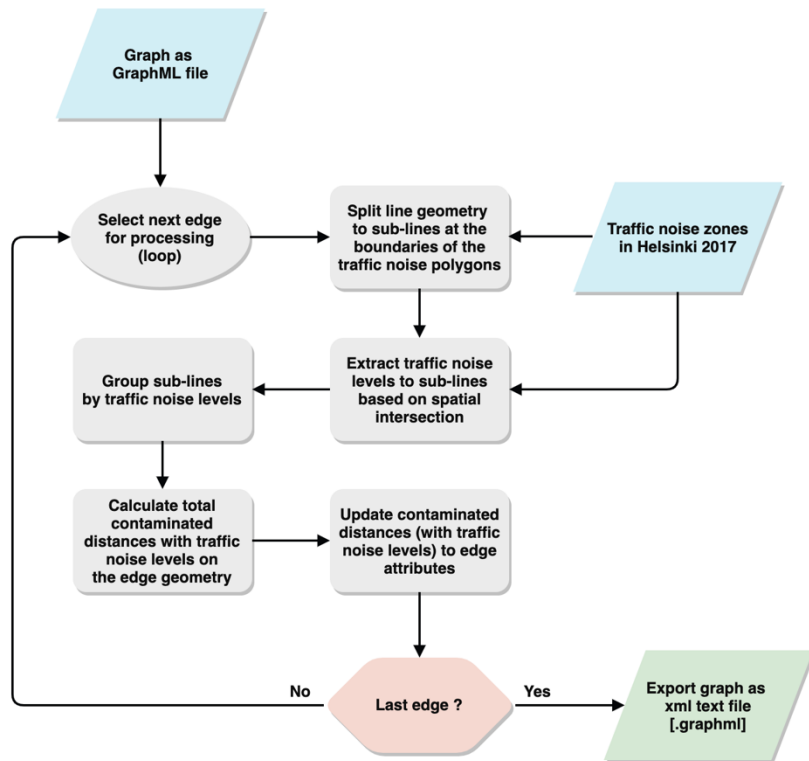


**Figure 14.** Workflow of extracting exposures to traffic noise (contaminated distances) to the edges of the graph.

A lossless spatial join of noise data ( $L_{Aeq}$ ) to the edges of the graph was carried in three phases (Figure 14). First, the edge geometries were split at the boundaries of the traffic noise surfaces by intersection

analysis. Second, underlying traffic noise data was extracted to the split edge geometries by their center point using vector-based point sampling in GeoPandas. Third, the split edges were aggregated by their original edge IDs and contaminated distances with different noise levels were added up for each edge. The result of the spatial join was validated by checking that the sum of the contaminated distances to different noise levels never exceeded the total length of the edge. This validation revealed the few topological inconsistencies in the noise surface data (see 3.3.1) and was fixed by only considering the maximum noise value when multiple values were sampled by a single sampling point.

Due to the high number of edges (180647), a challenge of the spatial join was its high demand for computing power and high memory consumption. Hence, I ran the first iteration of the analysis in a CSC's (IT Center for Science Ltd.) supercluster Taito, where 20 processing cores and plenty of memory were reserved for the run. However, the Python implementation of the spatial join could be further optimized which allowed running it also on a normal desktop computer. The more efficient analysis included 1) utilizing spatial indexing and GeoDataFrames, 2) organizing the edges as lists of edges (i.e. edge-chunks) and 3) processing the edge-chunks in parallel. I used the standard multiprocessing library of Python for the parallel processing both on desktop- and CSC's computer.

### 3.5.2 Environmental impedance function

An environmental impedance function (EIF) for noise was designed to enable exposure-based routing analysis. I defined the equation for calculating composite edge costs from length and dynamic noise exposure as:

$$C_e = d_e + C_{en} \quad (1)$$

where  $C_e$  is the total composite cost of the edge;  $d_e$  is the length of the edge (i.e. base cost) and  $C_{en}$  is an additional noise exposure -based cost (by an EIF). In the later parts of the thesis, the noise exposure -based cost is referred to as noise cost. The concept of contamination of distances (Ribeiro & Mendes, 2013) was applied in calculating the noise costs. However, instead of using a few fixed thresholds (dB) in assigning the costs (as in Ribeiro & Mendes, 2013), I developed the following EIF to calculate them on a continuous scale:

$$C_{en} = \sum_{i=db_{min}}^{db_{max}} d_{dB_i} \times a_{dB_i} \times s \quad (2)$$

where  $dB_i$  refers to a 5 dB range from  $dB_i$  to  $dB_i + 5$  dB (e.g. dB<sub>55</sub> refers to the dB-range of 55 dB to 60 dB),  $d_{dB_i}$  is the total contaminated distance (m) with the dB-range  $dB_i$  (e.g. 14 m of dB<sub>55</sub>) on the edge geometry,  $a_{dB_i}$  is a dB-specific noise cost coefficient and  $s$  is an arbitrary noise sensitivity coefficient (e.g. on range of 0.1 to 40).

Arguably, the critical, yet conceptually most challenging, component of the EIF is the dB-specific noise cost coefficient ( $a_{dB_i}$ ). Ideally, the noise cost coefficient should reflect the perceived loudness and annoyance of a given L<sub>Aeq</sub>. According to Guski et al. (2017), assessing exposure to A-weighted equivalent continuous sound level (e.g. L<sub>Aeq</sub>) has been the standard metric in the studies on static noise exposure and annoyance. However, based on their review, no widely accepted linear or non-linear relationship seem to exist between A-weighted sound pressure level (SPL) and perceived loudness (or particularly annoyance), regardless of the several sound attempts to find one (e.g. Miedema & Oudshoorn, 2001). Furthermore, as the reviewed papers focus on static exposure (e.g. L<sub>Aeq</sub> at home location), the applicability of their findings in assessing annoyance of dynamic traffic noise exposure is somewhat limited. Given this uncertainty on modeling loudness or annoyance by L<sub>Aeq</sub>, I tested two alternative functions for calculating the noise cost coefficients. First of the functions (3) assumes a linear relationship between loudness and L<sub>Aeq</sub> and sets the noise costs on a (linear) range from 0.0 to 1.0 with respective L<sub>Aeq</sub> range of 40 dB(A) to 75 dB(A):

$$a_{dB_i} = \frac{dB_i - 40 \text{ dB}}{75 \text{ dB} - 40 \text{ dB}} \quad (3)$$

The second function (4) introduces a power law between loudness and sound pressure level based on what Parmanen (2007: 60) reformatted from widely used Stevens' power law (Stevens, 1960):

$$a_{dB_i} = 10^{\frac{0.3 * dB_i}{10}} \quad (4)$$

where  $dB_i$  is the lower limit of a 5-dB interval and the minimum  $dB_i$  is 40 dB. Despite having its basis in noise research, the applicability of the Stevens' power law is probably limited in this context since it was not originally designed to work with averaged A-weighted sound pressure levels (but with simple intensity metrics). The respective noise cost coefficients by both functions for  $dB_i$  values from 45 dB to 75 dB are presented in Figure 15 and Appendix 2 (as table).

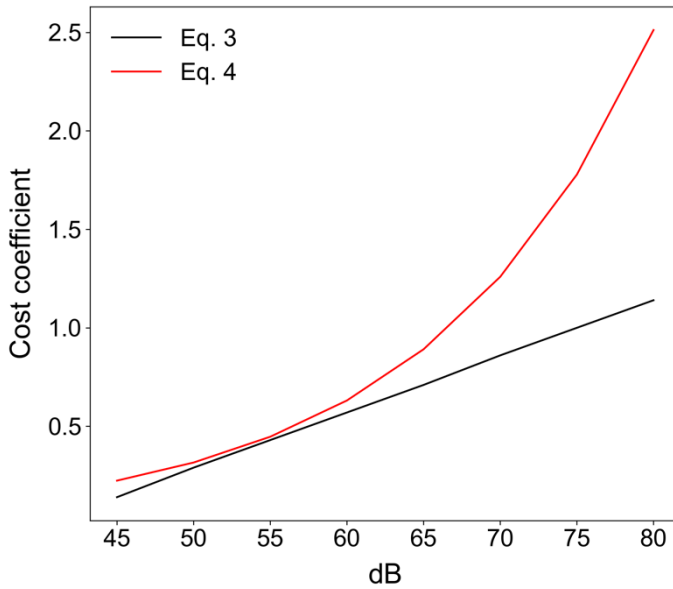


**Figure 15.** Noise cost coefficients for dB range 45–75 dB calculated with two different equations: linear (3) and power (4). Noise cost coefficient is a key component of the environmental impedance (EIF) function for noise.

I selected Equation 4 for calculating the noise cost coefficients. The power law doubles the cost (loudness) roughly at every 10-dB increase, hence giving significantly higher costs to the highest noise levels. This could be seen as a desired feature of the function, as the highest noise levels ( $> 65$  dB) are considered as most harmful to people. The power function may also be partially supported by interpretation of the nonlinear HA%/L<sub>den</sub> curves displayed in Figure 2 by Guski et al. (2017): a majority of the annoyance/SPL curves took the form “J” instead of a straight line, suggesting that an increase in SPL at higher noise level may have an amplified effect on the perceived annoyance compared to an equivalent increase in SPL at lower noise levels.

However, when I tested both functions for noise cost coefficient in developing the quiet path routing application, almost identical quiet paths options were found in most cases. It may be that the sensitivity index and the overall availability of alternative paths (between origin and destination) override the effect of the small differences in noise costs between the two noise cost functions. Uncertainties in noise-annoyance-loudness -relationships are considered further in chapter 5.8.

### 3.5.3 Quiet path routing application

In this chapter, operation and main functions of the quiet path routing application are described. The developed application features three key capabilities: 1) it optimizes shortest paths, 2) it optimizes quiet paths and 3) it assesses dynamic exposure to noise on the paths. The operation of the application is delineated by explaining the sequence of actions that are executed during:

1. Starting the application (steps 1–2 below);
2. Creating origin and destination nodes in the graph for one OD pair (steps 3–7);
3. Solving a single shortest and quiet path routing problem (steps 8–12);
4. Filtering out duplicate paths by length and geometry (steps 13–14).

The application first loads a processed graph from a GraphML file to a NetworkX graph object (step 1) and then calculates noise exposure -based costs to edges attributes (step 2). The environmental impedance function for noise (see 3.5.2) is applied in calculating the noise costs from contaminated distances with different noise levels (Figure 16). Parallel noise costs are calculated by different noise sensitivity coefficients. The final set of noise sensitivity coefficients that were selected for the quiet path routing application was defined as [0.1, 0.15, 0.25, 0.35, 0.5, 1, 1.5, 2, 4, 6, 10, 20, 40]. I found this set to provide an appropriate balance between performance and path variability. In most cases, multiple identical or nearly identical quiet paths were found, indicating that adding more sensitivity coefficients would not have resulted in finding more unique alternative (quiet) paths.

Calculation of the noise costs is not computationally very demanding and could hence be set to run at runtime (initialization) of the application as opposed to loading the costs from the static graph file. This setup facilitated testing of different variants of the environmental impedance function and noise sensitivity coefficients.

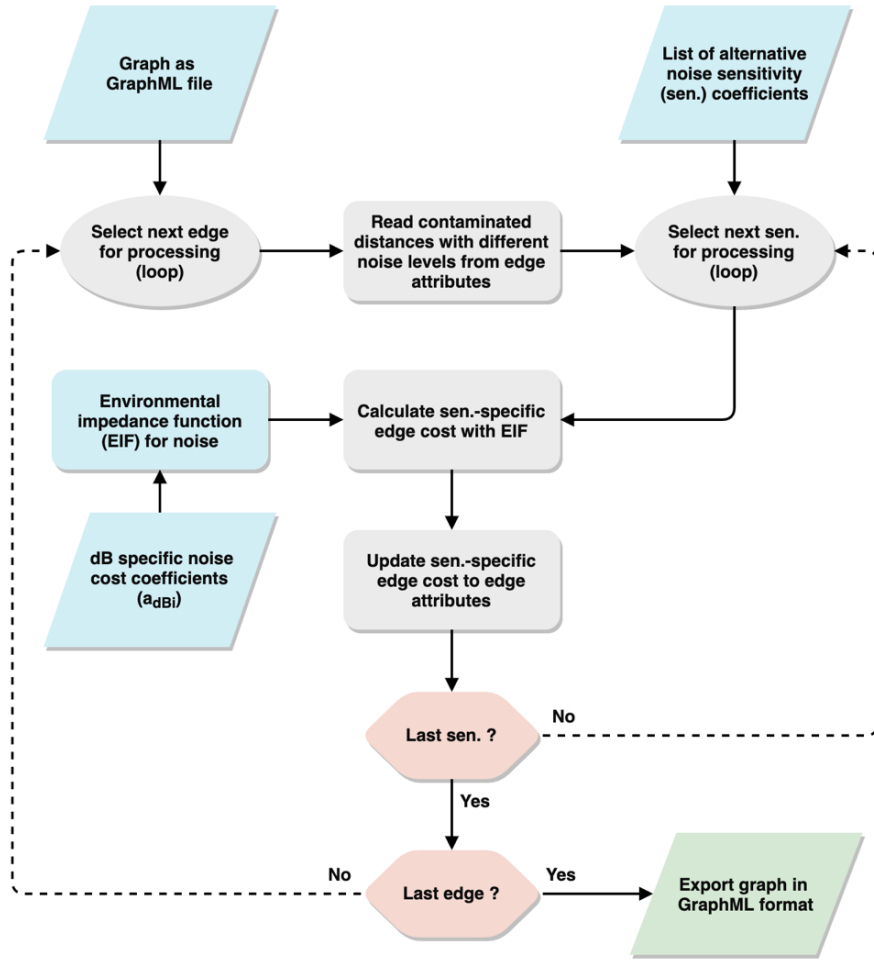


**Figure 16.** Workflow of calculating and adding noise sensitivity specific edge costs as new edge attributes.

To enable finding origin and destination nodes for a given OD pair fast, geometries of nodes and edges of the graph are collected to GeoPandas GeoDataFrames. The spatial indexes of the GeoDataFrames are used to quickly narrow down the candidates for nearest edge and node at a given location. Subsequently, the very nearest features are determined by using the geometrical distance functions from the Shapely package (step 3).

In most cases, the distance to the nearest edge is smaller than to the nearest node. Then, a new node needs to be created to the graph at the nearest point on the nearest edge (step 4). Subsequently, two linking edges need to be created to the graph to connect the newly created node to the origin and destination nodes of the nearest edge (step 5). Again, geometrical functions from the Shapely package are used in splitting the edge at the nearest point. Contaminated distances with different noise levels are then estimated for the linking edges as fractions of the contaminated distances of the nearest edge, by the ratio of the length of the linking edge to the length of the nearest edge (step 6). Then, noise costs (by different noise sensitivity coefficients) are calculated and updated to the edge attributes of

the linking edges, allowing them to be used in the LCP analysis in the same way as all other edges (step 7).

The complete sequence of higher-level actions included in solving one quiet path routing problem is illustrated in Figure 17. As illustrated, after creating new nodes for origin and destination, LCP analysis is carried out to find the shortest and a set of quiet paths for the given OD. First, the shortest path is calculated by using length as the cost variable (step 8). Then, a set of quiet paths are calculated by the noise costs that were calculated to the graph when the application was started (step 9), resulting a collection of paths represented by sequences of node IDs. At this stage, the number of paths is equal to the number of noise sensitivity coefficients. Then, the respective edges of the paths are fetched from the graph object by the sequences of node IDs (step 10). Subsequently, attributes of the edges are aggregated for each path. The line geometry of each path is constructed from the separate line geometries of its edges (step 11). Also, total lengths and contaminated distances with different noise levels and statistics on dynamic noise exposure (see chapter 3.5.4) are calculated from the aggregated edge attributes (step 12).

Finally, paths having unique geometry are filtered out from the full set of (quiet) paths. The filtering is done in two phases. First, the paths having exactly same length are filtered out (step 13). Then, a simple overlay analysis is performed to filter out paths with nearly identical geometries (step 14):

For one path at a time, all paths that fall completely within a 30 m radius (buffer) around the path are collected. The collected paths must also have a length difference of less than 30 m. Then, the best path of the collection is determined by the normalized noise exposure index (see 3.5.4). Only the best path of the collection is retained, and others are discarded. Iterating the filtering results a set of fewer but geometrically more unique paths. One of the desired effects of this filtering step is to discard one of the two paths that use the same road but different sidewalks by it. Another one is to discard the path that uses the center line of a road if there is an alternative path using an adjacent sidewalk. The shortest path is also included in this filtering process, and hence may get “replaced” with a nearly identical quiet path.

Once the paths are fully processed, they are returned either as a GeoPandas GeoDataFrame or GeoJSON. The first format was used in the assessment of pedestrians’ exposure to traffic noise and the second one in used in the web-based quiet path application programming interface (i.e. quiet path routing API). The attributes and schema of the shortest and quiet paths are described further in the next chapter (3.5.4) and in the documentation of the quiet path API (see 4.1).

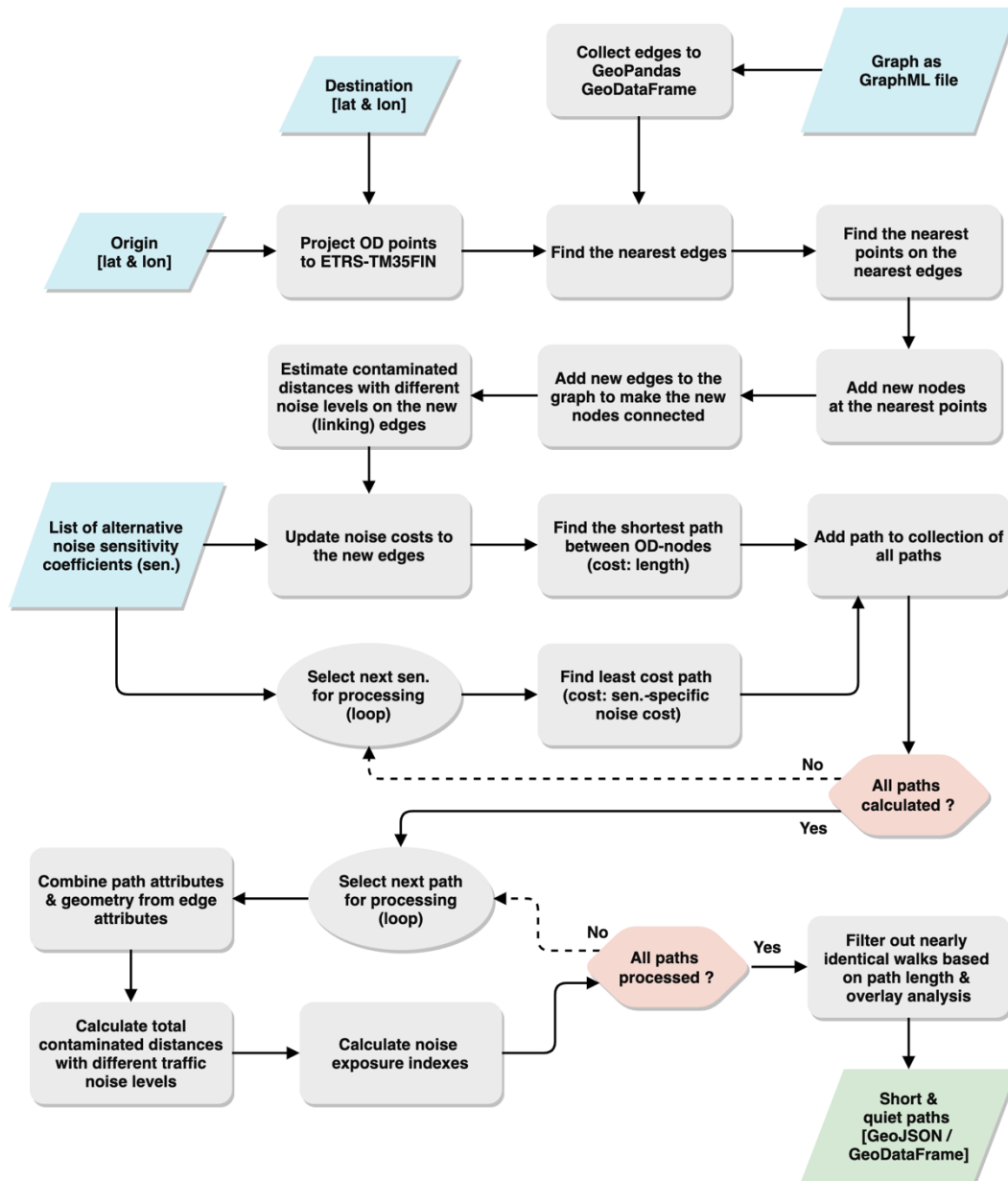


**Figure 17.** The sequence of high-level actions included in solving a common pathfinding problem with quiet path routing application.

### 3.5.4 Noise exposure assessment of short and quiet paths

I developed several metrics and indices for assessing and comparing dynamic exposure to traffic noise on short and quiet paths (Table 3). The indices presented in this chapter play a key role in comparing alternative quiet and short paths both in the web-based quiet path route planner and in the analysis of pedestrians' opportunities to reduce exposure to traffic noise (i.e. achievable reductions in traffic noise exposure). The challenge in developing such indices was compressing the information

from contaminated distances with different traffic noise levels ( $ED_{dB_i}$ ) to simple but descriptive indices of traffic noise exposure.

The simplest of the indices ( $ED_{+dB_i}$  – Equation 6 in Table 4) describes the total cumulative contaminated distance (i.e. distance of exposure) with noise levels higher than a fixed threshold, for example the exposure to noise levels higher than 65 dB. Then, the ratio of  $ED_{+dB_i}$  to the total length of a path can be calculated as a *dB-specific noise exposure ratio* ( $ER_{+dB_i}$  – Equation 7). This index can already be used to compare paths of different lengths, as it is distance normalized. The mean noise level ( $dB_{mean}$ ) is calculated simply by adding up the products of contaminated distances and the respective noise levels and dividing the sum with the total length of the path (Equation 8).

I applied the environmental impedance function for noise (i.e. noise cost function; Equation 4) to define a general *noise exposure index* (EI – Equation 9). EI aims to model the total noise-related environmental impedance of a path. Only a simple form of the EIF was needed here, excluding the base-cost (length) and the noise sensitivity coefficient ( $s = 1$ ). Also, a distance normalized version of the index was defined as *distance normalized noise exposure index* ( $EI_n$  – Equation 11). It varies from 0.0 to 1.0, as it is calculated by dividing the noise exposure index of a path with the theoretical maximum noise exposure index of a path with equal length. Furthermore, the difference in EI can be calculated for a quiet path compared to the shortest path, to measure reduction in EI (Equation 10).

**Table 3.** The noise exposure indices that were defined for measuring dynamic traffic noise exposure and reduction in noise exposure on quiet paths.

Metric	Equation	Description
Contaminated distance with noise level $dB_i$ (m)	$ED_{dB_i} = d_{dB_i}$	(5) The total (cumulative) exposure to noise level $dB_i$ on the path
Total contaminated distance with noise levels higher than $dB_i$ (m)	$ED_{+dB_i} = \sum_{i=+dB_i}^{dB_{max}} ED_{dB_i}$	(6)
Percentage of total contaminated distance with noise levels higher than $dB_i$ of the total path length (%)	$ER_{+dB_i} = \frac{\sum_{i=+dB_i}^{dB_{max}} ED_{dB_i}}{d} * 100$	(7)
Mean dB on the path	$dB_{mean} = \frac{\sum_{i=dB_{min}}^{dB_{max}} ED_{dB_i} * dB_i}{d}$	(8)
Noise exposure index (i.e. total noise-based environmental impedance)	$EI = \sum_{i=dB_{min}}^{dB_{max}} ED_{dB_i} * a_{dB_i}$	(9) Similar to environmental impedance function (2) but without noise sensitivity coefficient ( $s = 1$ )
Reduction in noise exposure index (%)	$EI_{diff} = \frac{\Delta EI}{EI_s} * 100 = \frac{EI_q - EI_s}{EI_s} * 100$	(10) Reduction (%) in noise exposure index between short and quiet path
Distance normalized noise exposure index (index)	$EI_n = \frac{EI}{EI_{max}} = \frac{EI}{a_{max} * d} = \frac{EI}{a_{75dB} * d}$	(11) EI of the path normalized by dividing it with maximum theoretical EI for a path of same distance

$dB_i = 5$  dB range with  $dB_i$  as the lower value (e.g. 55 dB refers to noise range of 55–60 dB)

$ED_{dB_i}$  = total contaminated distance with noise level of  $dB_i$  (e.g. 14 m of 55–60 dB noise)

$a_{dB_i}$  = dB-specific noise cost coefficient (as in Equation 4)

### 3.6 Web-based quiet path route planner

To demonstrate the potential utility of the quiet path routing method in practical situations, I developed a proof of concept web-based quiet path route planner. Also, it accelerated developing and

adjusting the quiet path routing method, as different variants of the street network graph and environmental impedance function could be easily tested.

The technical implementation of the quiet path route planner is composed of three components (Figure 18): graph processing for quiet path routing, server-side quiet path routing application and client-side route planner user interface. The interface between the graph processing scripts and the routing application is a static GraphML file. On the other hand, the client-side web application communicates with the routing application via a RESTful API exposed by the server application. The capabilities of the quiet path routing API are documented in more detail in the results chapter (see 4.1).

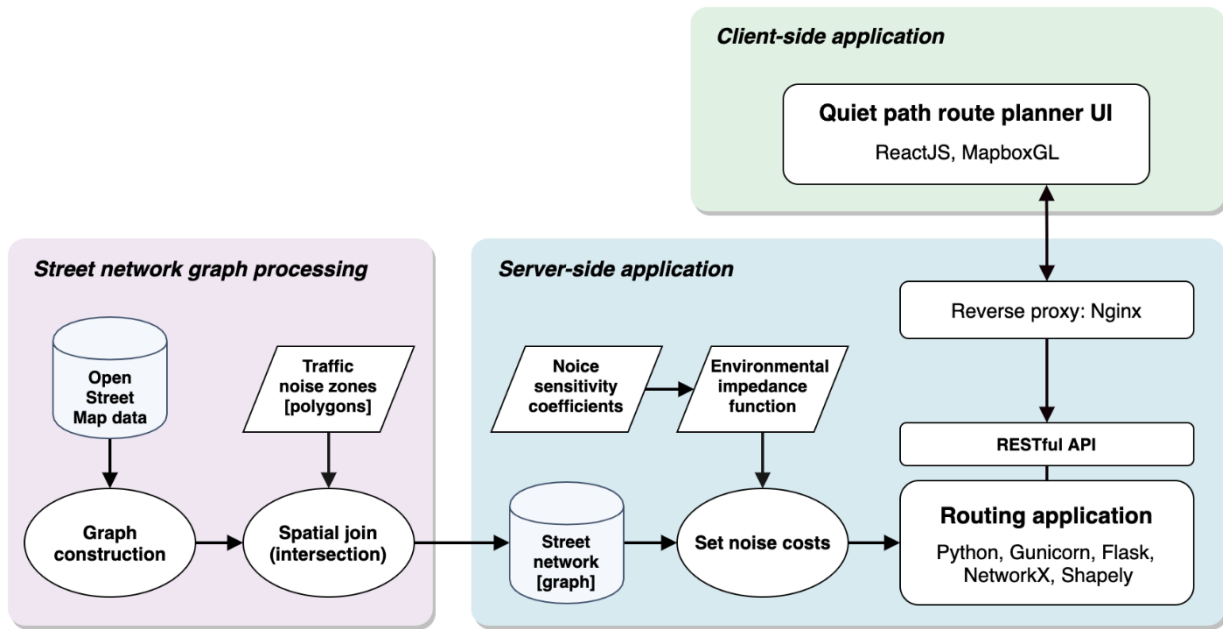


**Figure 18.** Technical architecture of the quiet path route planner web application.

I acquired a virtual machine for hosting the quiet path routing application as a web service. In addition to the normal scientific and geospatial Python libraries, the library Flask was installed to enable accessing the functionality of the routing application with RESTful web requests. Since Flask is not recommended for production environments, the library Gunicorn was configured to run the Python-Flask application in more efficient and secure manner. Essentially, this meant running several instances of the application in parallel to be able to quickly handle many simultaneous routing requests.

I developed an interactive web map application to serve as the user interface for the quiet path routing service. The application was developed as a progressive web application (PWA), to allow using it by

simply opening a web page. PWA is a collection of web development patterns and common web technologies for delivering applications directly through the web as opposed to e.g. Google Play store (for Android apps) or Apple's App Store (for iOS apps). The application was implemented with ReactJS library as a single page application (SPA). Mapbox GL JS was chosen as the web mapping library due to its great support for visualizing vector data interactively. Mapbox Studio was used to design a custom, light-colored, basemap to allow visualizing multiple paths with varying colors clearly on top of it. ReactJS SPA, as a technical framework, enabled building highly customized and reactive web map application for the purpose. Communication between the web map application and the routing service was implemented with asynchronous requests; after the routing request is sent from the client, a callback function (at the client) is invoked once the paths are returned from the routing service. The design and features of the user interface are presented in more detail in the results chapter (see 4.2).

During the making of this thesis, components of the web-based quiet path routing application, particularly the user interface, were developed iteratively based on the comments and suggestions from a small group of test users. Closer to the end of the thesis project, the focus in developing the routing application was guided also by the project HOPE – Healthy Outdoor Premises for Everyone. Thus, the support for assessing and minimizing exposure to also real-time air pollution was implemented in the routing application. Also, to enable significantly faster routing analysis for longer OD distances, the routing analysis was converted to utilize the graph library igraph (Csardi & Nepusz, 2006) instead of NetworkX. The links to the source-codes and further documentation of both versions of the routing application are presented in the results chapter (see 4.1, 4.2 & 4.5).

### **3.7 Case study: pedestrians' exposure to traffic noise in Helsinki**

#### **3.7.1 Overview of the analysis**

To test the routing applications' feasibility in large-scale noise exposure assessments, I carried out a case study where I assessed pedestrians' dynamic exposure to traffic noise during commuting related walks in Helsinki. I made three major assumptions in the case study in regard to the used data and commuting related mobility:

- 1) YKR commuting flow data (see 3.3.3) accurately indicates the origins and destinations of commutes originating from Helsinki;

- 2) All commutes from Helsinki to Helsinki Metropolitan Area (i.e. Helsinki, Espoo, Vantaa and Kauniainen) use public transport;
- 3) Most interesting and significant component of total dynamic exposure to noise occurs during the first walks of the travel chains (i.e. on walks from homes to public transport stops).

I made the third assumption to focus the assessment on the most local walks of each origin and thus provide information on the differences in dynamic exposure to noise between different areas. Using all walks of the travel chains in the exposure assessment would have resulted in more truthful results in commuters' exposure to traffic noise but less meaningful results on local walking conditions.

The exposure assessment consisted of two parts:

- 1) Estimation of origin (i.e. home) – PT stop (or commuting destination) walking routes and their utilization rates (Figure 19, chapter 3.7.2);
- 2) Assessment of pedestrians' exposure to traffic noise on shortest paths from origins to local PT stops or commuting destinations (Figure 20, chapters 3.7.3 & 3.7.4).

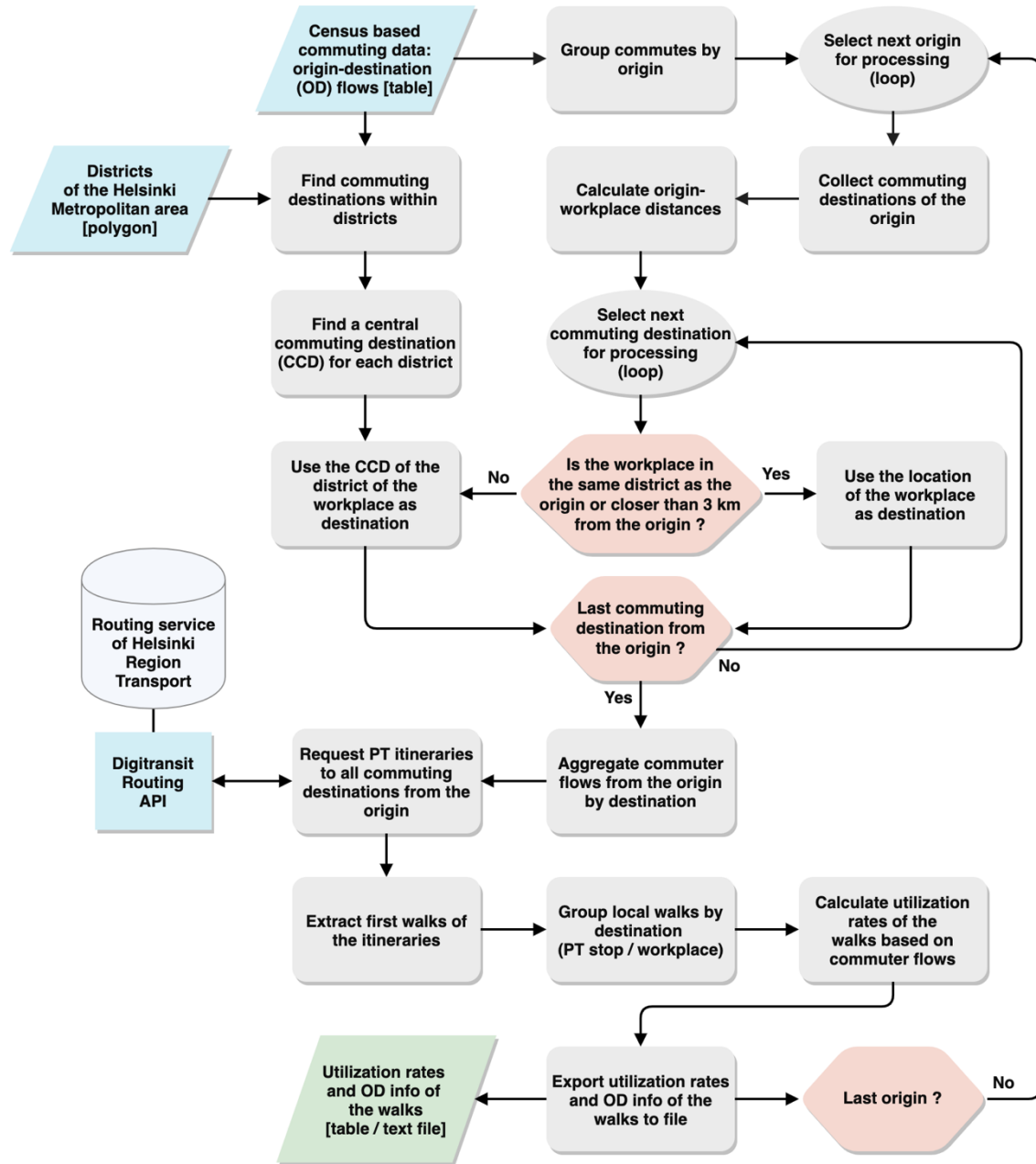


**Figure 19.** Workflow of the analysis for modeling origin – PT stop (or commuting destination) walking routes and estimating their utilization rates based on commuter flows (as in 3.7.2). I analyzed census based commuting flow data and extracted the first walks of planned public transport itineraries to commuting destinations. These first walks are referred to as *local walking routes* in the study.

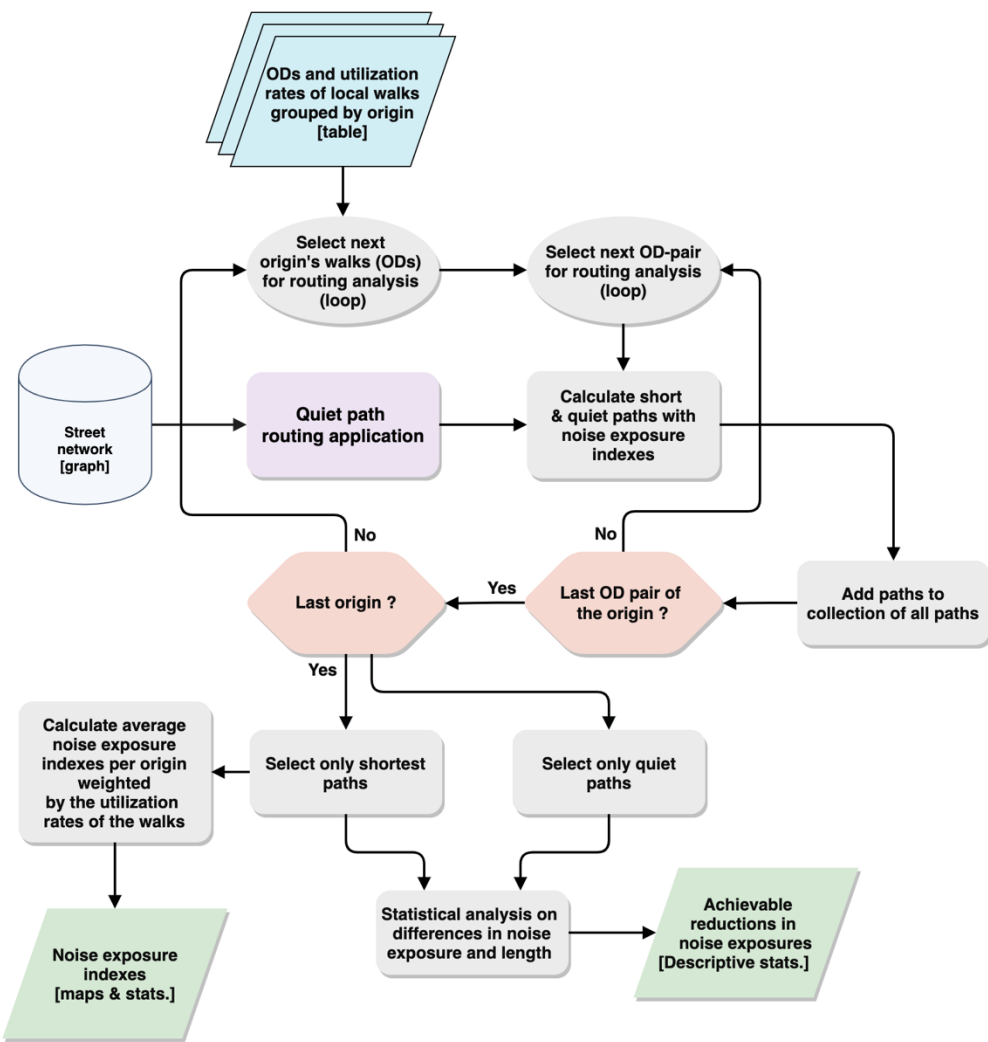


**Figure 20.** Workflow of the analysis for 1) calculating short and quiet paths for local walking routes (3.7.3), 2) assessing exposures to traffic noise on the paths (3.7.4) and 3) assessing achievable reductions in traffic noise exposure by taking quiet paths (3.8).

### 3.7.2 Estimating local walking routes by PT commutes

Local walking routes to public transport stops (PT stops) or commuting destinations were estimated as a result of an extensive public transport itinerary planning analysis (Figure 19). In this chapter, the necessary steps that were required for determining commuting destinations from *one* origin (i.e. home location) are described. The full iteration of the analysis (for all origins) is illustrated in Figure 19.

The real commuting destinations (by the commuting data) were selected as destinations for all commuting destinations closer than 3 km from the origin. In order to limit the number of routing requests to Digitransit API (i.e. the route planner service of HRT), distant commuting destinations (farther than 3 km from the origin) were aggregated by city districts. The centers of the districts were

then used as the commuting destinations for the distant workplaces (Figure 21). The following sequence of GIS analysis was used to adjust the center of each district to better represent a “central workplace location” and to ensure that it is located in an accessible part of the street network:

- 1) Create a convex hull polygon by the commuting destinations of the district;
- 2) Calculate a center of gravity for the convex hull polygon;
- 3) Calculate distances from the commuting destinations (of the district) to the center of gravity;
- 4) Select the “central workplace location” as the commuting destination closest to the center of gravity.

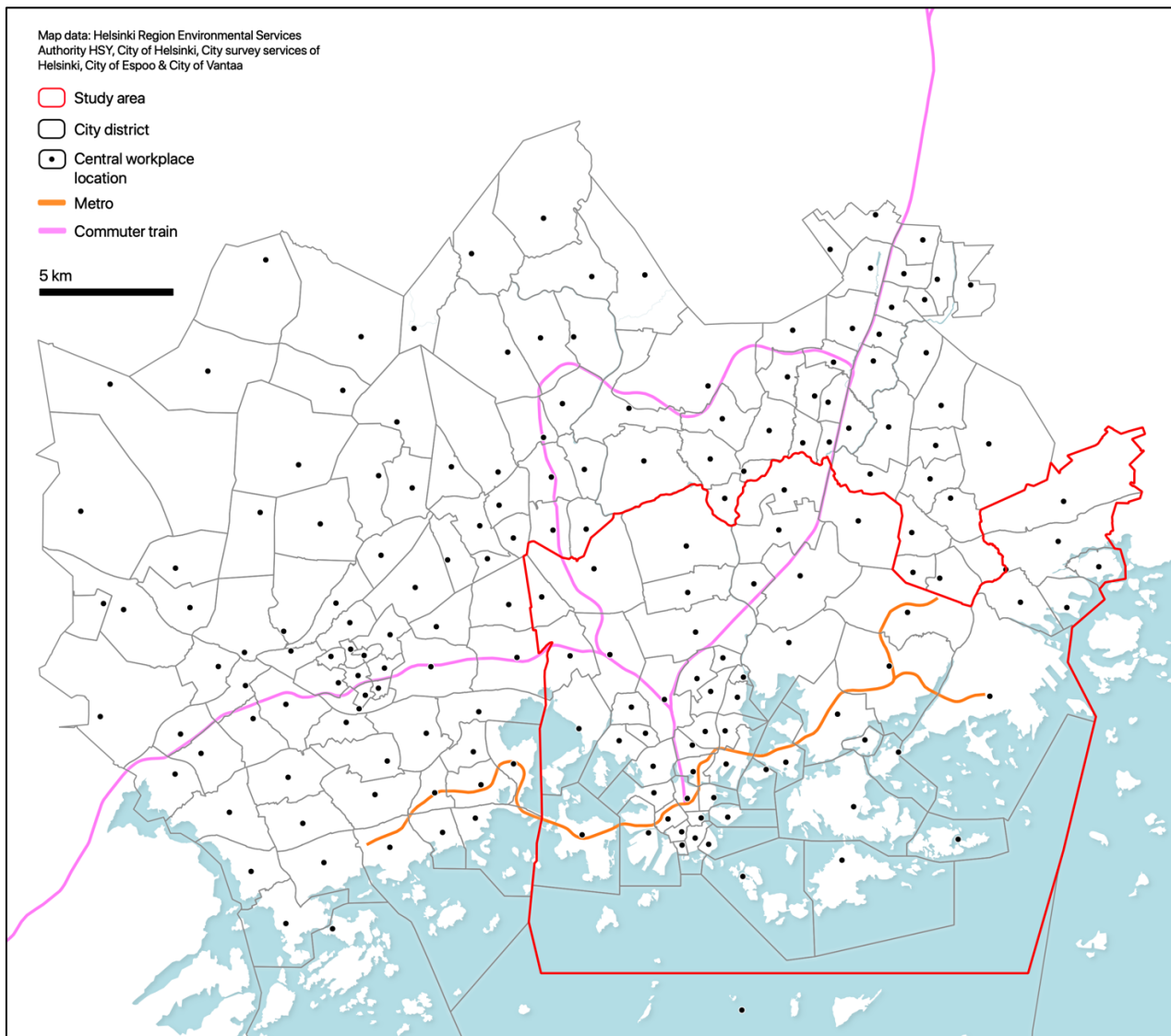


**Figure 21.** Extent of the itinerary planning analysis by commuting flow data. In the Helsinki case study, I assessed exposure to noise during commutes originating within the municipality (marked with red). In the analysis, public transport itineraries were planned for all commutes and first walks of the travel chains were extracted for noise exposure assessment. The point symbols represent “central workplace location” of each city district.

For each origin-destination pair (commuting flow), three public transport itineraries were requested from Digitransit routing API. The open routing API is provided by the local public transport authority Helsinki Region Transport (HRT/HSL). In the routing requests, walking speed was set as 70 m/min (as in Jäppinen et al., 2013; Toivonen et al., 2014). Default values were used for other routing parameters to match typical user preferences (Table 4). In cases where the routing request did not result any itineraries, origin or target location was slightly adjusted in order to reach the underlying street network.

**Table 4.** Parameters used in public transport itinerary planning with Digitransit routing API.

Parameter	Value
Origin	Center of the YKR grid cell
Destination	Destination of the commute
Date	Monday 8:30 am, 05/27/2019
Walking speed	70 m/min
Means of transport used	All except city bikes
Transfer safety margin	0 min
Number of itineraries to suggest	3

The resulting itineraries were aggregated by origin. The first walks of the itineraries were extracted and grouped by their destinations. Walks of two kinds were found: 1) walks from origins to PT stops and 2) direct walks from origins to commuting destinations. The walks from each origin were aggregated by their destination and combined utilization rates of the aggregated walks were calculated (Figure 22).

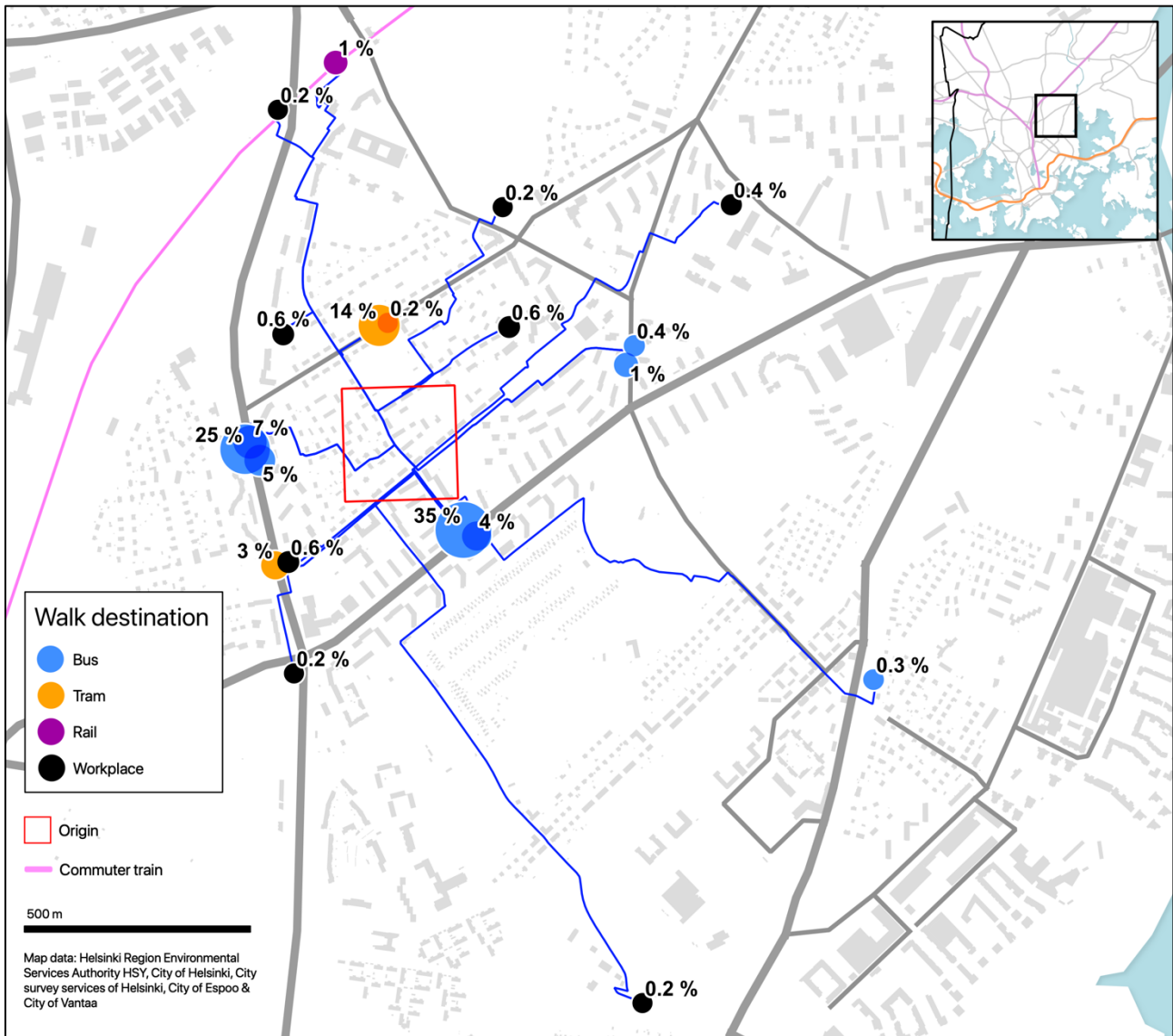


**Figure 22.** An example of projected walking routes and their utilization rates from one origin to public transport stops and workplaces. The walking routes are extracted from planned public transport itineraries (travel chains) to all commuting destinations from the origin as per census based commuting flow data.

To validate the results of the itinerary planning analysis, I compared the sums of the utilization rates of the walks to the total flow of commutes from each origin by the original commuting flow data. Of the total number of commutes originating in the study area (296470), 83 % were included in the analysis. The mean inclusion of commutes per origin was 81% with a standard deviation of 14 %. The analysis performed well at most central and residential areas, but considerable share of the commutes from several remote and coastal areas were excluded, as illustrated in Figure 23. Comparison of the number of commutes against the inclusion of the commutes (in the analysis) by origin revealed that the lower inclusion of commutes occurred mainly at origins with fewer commutes

(Figure 24). Further inspection of the commuting statistics at origin-level revealed that of the origins with less than 50 % inclusion of commutes, none had more than 12 commutes in total.

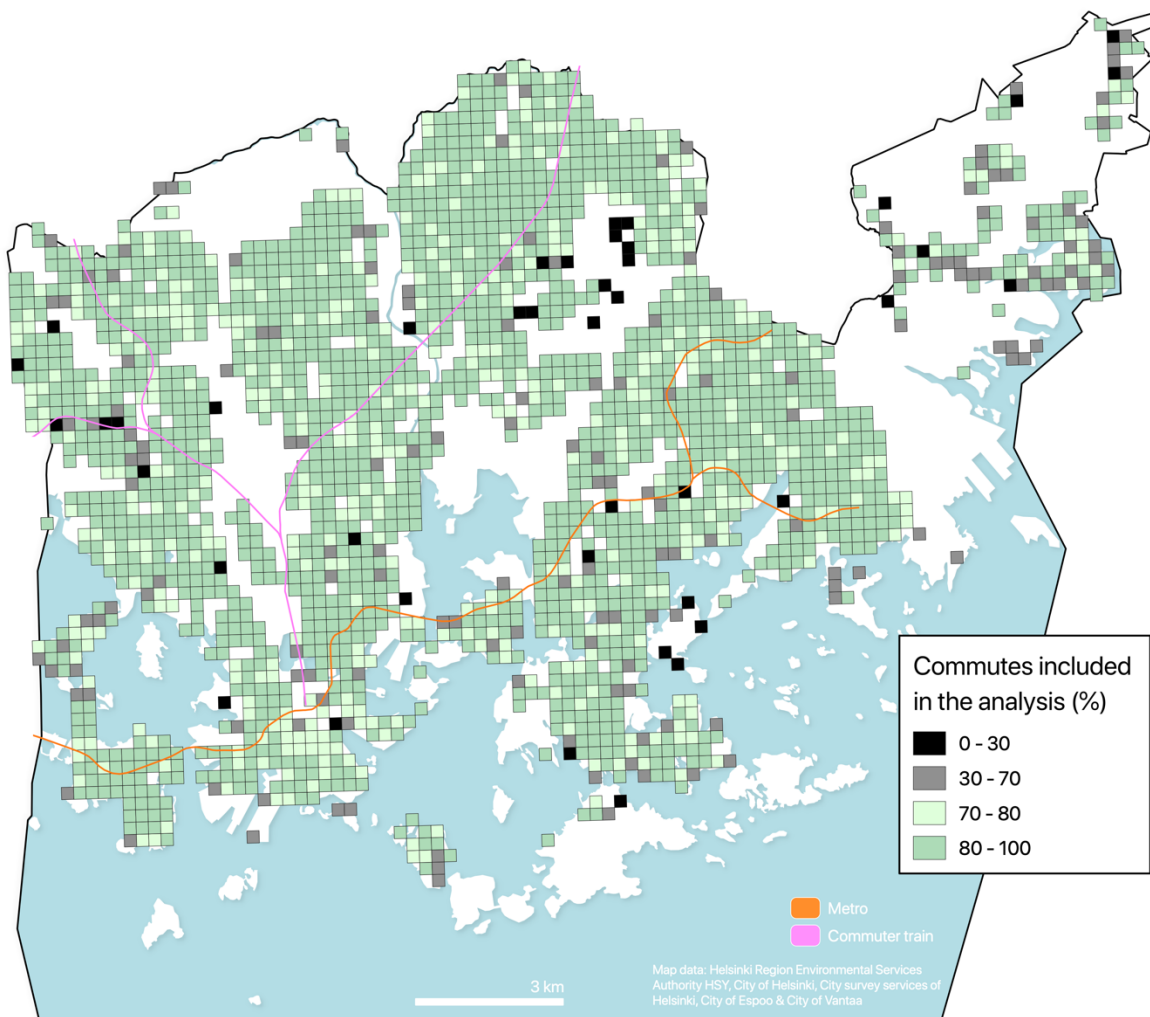


**Figure 23.** Inclusion (%) of commutes per origin in the itinerary planning analysis for finding local walking routes to PT stops and commuting destinations. Only commuting destinations located in Helsinki Metropolitan Area, or max. 3 km from origins, were included in the analysis. Consequently, for some origins, significant shares of commutes were excluded in the analysis (shown with grey and black squares on the map). For these origins, the accuracy of the assessment was thus limited. Yet for majority of the origins, more than 70 % of all commutes were included in the analysis (green squares).

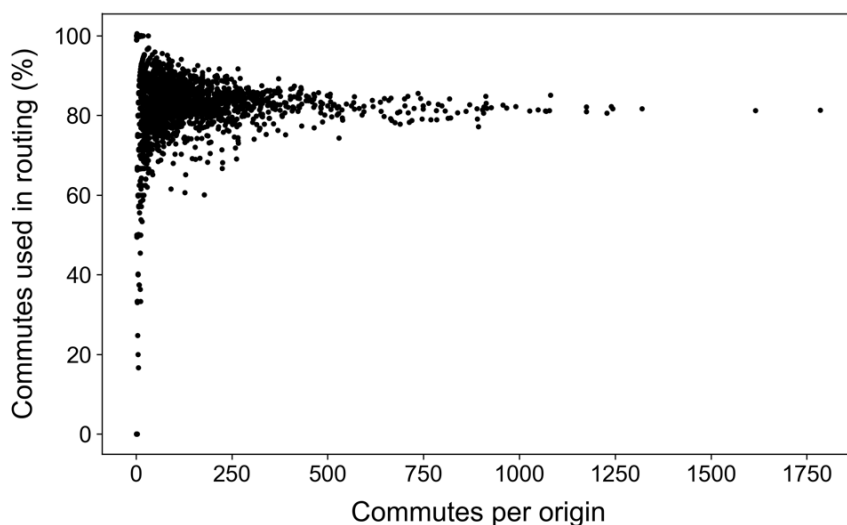


**Figure 24.** Number of commutes vs. commutes included in the itinerary planning analysis (%) per origin.

### 3.7.3 Least cost path calculations: short and quiet paths

I routed shortest and quiet paths for all walking routes (determined in the previous phase of the analysis) with the quiet path routing application (3.5) developed in the study (Figure 20). The utilization rate of each route was inherited as attribute information to the respective short and quiet paths. It was needed in later parts of the analysis when weighted statistics of noise exposures were calculated. Once all paths were routed, I calculated descriptive statistics of the lengths of the shortest paths (Table 5). Figure 25 illustrates the spatial variation in the volume of the shortest paths.

**Table 5.** Descriptive statistics of the length of the shortest paths to PT stops and commuting destinations (i.e. workplaces), both separately and combined (n=31291).

Path length (m)	Mean	Median	SD	p10	p25	p75	p90
All (n=31291)	491	408	338	136	234	670	964
To PT stops (n=18716)	472	397	318	132	230	649	924
To workplaces (n=12575)	883	771	486	333	453	1209	1582

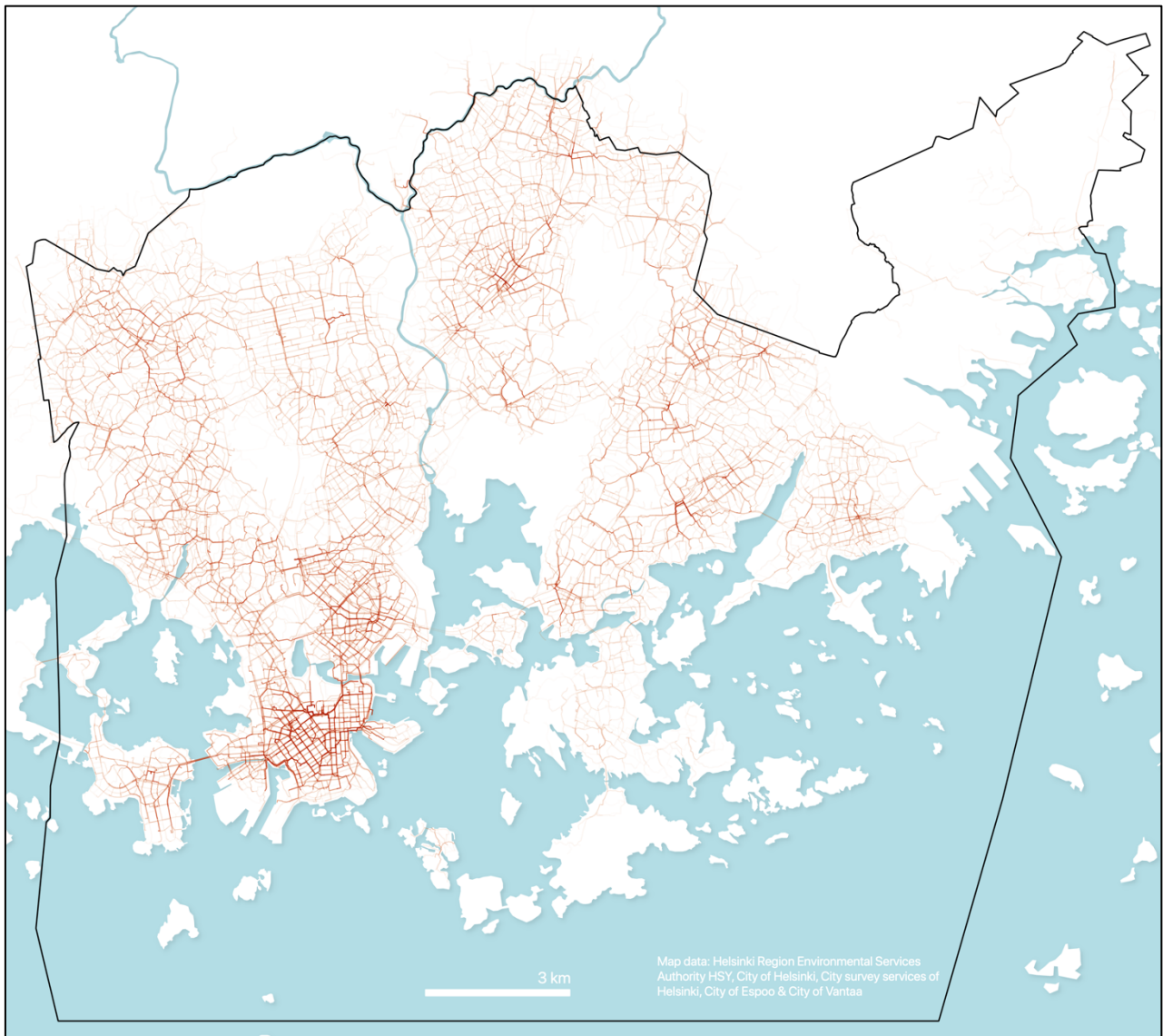


**Figure 25.** All shortest paths visualized with feature blending method: overlapping paths show darker on the map. I routed shortest and quiet paths for all local walking routes to PT stops (and workplaces) modeled in the previous phases of the assessment.

### 3.7.4 Assessment of dynamic exposure to traffic noise

As dynamic noise exposure assessment was already a built-in feature of the quiet path routing application, no separate analysis for determining exposures to traffic noise on the paths was needed. I calculated weighted descriptive statistics of the noise exposure attributes (Table 3) of the paths. The weighting was done with the modeled utilization rates of the walks. I calculated the descriptive statistics separately for all paths and for a subset of only origin–PT stop paths (excluding origin – commuting destination paths).

Also, I calculated origin-level statistics of noise exposure indices to enable exploring possible spatial patterns in the dynamic noise exposures. For this analysis, I included only the origin–PT stop paths to focus the assessment on the most local walks of the origins. Paths that were not completely inside the extent of the noise surface data were also filtered out in the analysis. The total utilization rates of the paths that were included in the analysis were added up per origin, to assess the statistical significance of the results (per origin). Again, I weighted the descriptive statistics by the utilization rates of the walking routes. Therefore, the (weighted) mean noise exposure index can indicate the expected noise exposure on an *average walk* from each origin.

### 3.8 Assessment of achievable reductions in exposure to traffic noise

In the case study (3.7), I routed both shortest and quiet paths for 31291 commuting-related walks with the quiet path routing application. The same paths were used to assess also achievable reductions in dynamic noise exposure on the quiet paths (i.e. the performance of the quiet path routing functionality).

After filtering out paths that were outside the extent of the traffic noise data and a few other problematic paths, I assessed the achievable reductions in noise exposure for 12180 OD pairs having the shortest path in the length range from 300 to 1300 m. The achievable reductions in exposures were calculated per OD pair, by comparing different noise exposure indices of the quiet paths to the corresponding indices of the shortest path. The achieved reductions in noise exposures were evaluated with respect to the following properties of the paths:

- 1) Distance between origin and destination (O-D distance);
- 2) Noise exposure indices of the shortest path;
- 3) Length difference between quiet and shortest path.

Two subsets of the paths (grouped by OD) were selected to assess the effect of the length of the shortest path (O-D distance) in the achievable reductions in noise exposure. Paths in the length range from 300 to 600 m were added to the first set (*short paths*) and paths in the length range from 700 to 1300 m to the second set (*longer paths*).

The reductions in noise exposures were measured against a set of thresholds for maximum length differences. The noise exposure indices of each shortest path were compared to the noise exposure indices of the corresponding quiet paths with maximum length difference of 100, 200 and 300 meters, respectively. Accordingly, for each OD pair, three metrics of achievable reductions in noise exposure indices were obtained, one for each length difference threshold. Subsequently, descriptive statistics

were calculated for all (achievable) reductions in noise exposure indices by the maximum length difference thresholds (100, 200 and 300 meters). In addition, scatterplots of the achievable reductions in exposures and length differences were made to explore the relationship between length difference and achievable reductions in noise exposures. Also, numbers of the quiet paths were compared to the lengths of the shortest paths with scatterplots and boxplots - it was anticipated that more quiet path alternatives are found for longer O-D distances.

Another aggregation of the paths was done by selecting several subsets of the OD-level statistics by the exposure indices of the shortest paths. Thus, the magnitude of the achievable reductions in noise exposures could be assessed also with respect to the initial noise exposures of the walks (by the shortest paths). Moreover, a simple linear regression analysis was carried out between the reductions in the exposure indices and the initial values of the indices (on the shortest paths). It was anticipated that for a higher noise exposure on a shortest path, also higher achievable reductions would be achievable on the respective quiet paths.

## IV. RESULTS

### 4.1 Quiet path routing API

At the time of writing this thesis, the web-based quiet path route planner service (3.6) is accessible via the quiet path routing API at [www.greenpaths.fi/](http://www.greenpaths.fi/). The API is open and thus accepts requests over https from any client. The specific path for requesting quiet paths is [www.greenpaths.fi/quietpaths/{origin}/{destination}](http://www.greenpaths.fi/quietpaths/{origin}/{destination}). This endpoint expects the origin and destination in decimal coordinates in WGS84 coordinate system. For example, a valid request to the API is: [greenpaths.fi/quietpaths/60.20772,24.96716/60.2037,24.9653](http://greenpaths.fi/quietpaths/60.20772,24.96716/60.2037,24.9653).

The API responds to requests simply by returning either a collection of paths in the GeoJSON FeatureCollection format or a descriptive error message. The collection of paths includes both shortest path and quiet paths (if any were found). GeoJSON is a standard format for representing geographical features and their non-spatial attributes. It is an adaptation of the JavaScript Object Notation (JSON) format and can thus be easily used in a variety of data-interchange applications.

The returned short and quiet paths are equipped with several attributes on noise exposure and length (Table 6). Some of the attributes describe difference in noise exposure compared to the shortest path and thus have non-null values only for quiet paths. An example of a FeatureCollection of two paths is presented in Figure 26. Since the paths are returned in a standard GeoJSON format, they can be easily viewed by common web mapping libraries and most desktop GIS applications (e.g. QGIS). More detailed documentation of the quiet path routing API can be viewed at: [https://github.com/DigitalGeographyLab/hope-green-pathserver/blob/develop/docs/green\\_paths\\_api.md](https://github.com/DigitalGeographyLab/hope-green-pathserver/blob/develop/docs/green_paths_api.md)

**Table 6.** Descriptions of the path properties returned by the quiet path routing API.

Property	Type	Nullable	Description
type	string	no	Type of the path: either “short” or “quiet”.
id	string	no	Unique name of the path (e.g. “short” or “qp_0.2”). For quiet paths, the name is formatted as “qp_xx”, where xx is replaced with the noise sensitivity coefficient of the path.
length	number	no	Length of the path in meters.

cost_coeff	number	no	Noise sensitivity coefficient with which the quiet path was calculated.
len_diff	number	no	Difference in path length compared to the shortest path in meters.
len_diff_rat	number	yes	Difference in path length compared to the shortest path in percentages.
missing_noises	boolean	no	A boolean variable indicating whether noise data was available for all edges of the path (experimental attribute).
mdB	number	no	$\text{dB}_{\text{mean}}$
mdB_diff	number	yes	Difference in $\text{dB}_{\text{mean}}$ compared to the shortest path.
nei	number	no	Noise exposure index (EI).
nei_norm	number	no	Distance-normalized noise exposure index ( $\text{EI}_n$ ).
nei_diff	number	yes	Difference in noise exposure index ( $\text{EI}_{\text{diff}}$ ) compared to the shortest path.
nei_diff_rat	number	yes	Difference in noise exposure index ( $\text{EI}_{\text{diff}}$ ) as percentages compared to the shortest path.
noises	object	no	A dictionary containing contaminated distances with different noise levels. Keys of the dictionary represent noise levels (dB) and values distances in meters.
noise_range_exps	object	no	Exposures (m) to noise level ranges where noise levels exceeding 70 dB and lower than 50 dB are aggregated (separately). Keys represent noise levels and values distances (m).
noise_pcts	object	no	Relative exposures (%) to different noise level ranges (noise_range_exps). Keys represent noise levels and values shares.
noises_diff	object	yes	Exposures to different noise levels. Keys represent noise levels and values distances (m).
path_score	number	yes	Ratio of difference in noise exposure index to difference in length compared to the shortest path - i.e. reduction in noise exposure index per each additional meter walked.

The quiet path routing API allows anyone to query short and quiet paths in Helsinki and assess dynamic exposure to noise on the paths. Therefore, the routing API can facilitate both scientific dynamic noise exposure assessments and building route planner applications for people (both demonstrated in this study). However, due to the limited computing power of the current server setup,

the recommended way to route large numbers of paths is to run a self-hosted instance of the quiet path routing application, as instructed in the documentation of the codebase (see 4.5).

```

Path_FC: {
  type: "FeatureCollection",
  features: [
    {
      geometry: { coordinates : [...], type: "LineString" },
      properties: {
        type: "short",
        id: "short",
        length: 5107.54,
        cost_coeff: 0,
        len_diff: null,
        len_diff_rat: null,
        missing_nosies: "false",
        mdb: 70.5,
        mdb_diff: null,
        nei: 3654.4,
        nei_norm: 0.72,
        nei_diff: null,
        nei_diff_rat: null,
        noises: { 45: 246.68, 50: 285.14, 55: 229.9, 60: 296.49,
                  65: 135.53, 70: 1782.62, 75: 2082.59 },
        noise_range_exps: {...},
        noise_pcts: {...},
        noises_diff: null,
        path_score: null
      },
      type: "Feature"
    },
    {
      geometry: { coordinates : [...], type: "LineString" },
      properties: {
        type: "quiet",
        id: "q_0.2",
        length: 5189.25,
        cost_coeff: 0.2,
        len_diff: 81.7,
        len_diff_rat: 1.6,
        missing_nosies: "false",
        mdb: 61.3,
        mdb_diff: -9.2,
        nei: 2126.5,
        nei_norm: 0.41,
        nei_diff: -1527.9,
        nei_diff_rat: -41.8,
        noises: { 45: 1196.12, 50: 194.09, 55: 204.74, 60: 622.92,
                  65: 1081.62, 70: 1452.68, 75: 103.07 },
        noise_range_exps: {...},
        noise_pcts: {...},
        noises_diff: { 40: 0, 45: 949.44, 50: -91.05, 55: -25.16, 60: 326.43,
                      65: 946.09, 70: -329.94, 75: -1979.52 },
        path_score: 18.7
      },
      type: "Feature"
    },
    {...}, {...}, ... ]
  }
}

```

**Figure 26.** A FeatureCollection containing two paths returned from the quiet path routing API.

## 4.2 Quiet path route planner

At the time of writing this, the interactive web map user interface (UI) of the quiet path route planner is accessible at: <https://green-paths.web.app/>. To facilitate testing and using the application in real-life (i.e. real-time) situations, namely on mobile phones, both Responsive Web Design (RWD) and mobile-first principle are applied in the design of the UI. Figure 27 represents a basic user story covering the typical sequence of actions for requesting, receiving and comparing route suggestions for one pathfinding problem. Since the main objective of the route planner application was to serve as a proof of concept of the quiet path routing method, only the most essential functionalities were implemented. Hence, for example, address geocoding functionality is not supported but the user can select the origin and destination only from the map. However, some minor features and functionalities are implemented in the UI to improve the overall user experience (Table 7).

To make the application more intuitive to use, most of the noise exposure indices (see 3.5.4) are not shown in the UI as they would have required additional explanations. Instead, dynamic exposures to different traffic noise levels are visualized with dB-specific colors both on the map and in the list of paths. In the list, the ratios of the exposures to different traffic noise levels (%) are visualized as a colored bar chart. For quiet paths, the difference in traffic noise exposure index compared to the shortest path ( $EI_{diff}$ ) is presented simply as reduction (%) in *noise* (despite the conceptual difficulty).

Figure 28 (A–C) and Figure 29 (A–C) represent the quiet path route planner in two practical situations. In the first figure, only two paths are shown for the OD pair. In Figure 28 (C) and Figure 29 (B), a quiet path has been opened from the list and more detailed noise exposure information is shown for the path:

- 1) Exposures to different traffic noise levels (%) as colored bar charts for both the opened (quiet) path and the shortest path;
- 2) Durations of exposure to different traffic noise levels on the opened (quiet) path.

In Figure 29, routing was performed for a longer OD-distance, resulting more alternative quiet paths (A). To reduce the number of the displayed paths, user can select a maximum length for the paths via the filter button (Figure 29: C).

**Table 7.** Minor features and functionalities of the route planner UI that aim to improve the overall user experience of the application.

Trigger	Action
---------	--------

User clicks the “Find quiet paths” -button and routing is started	Map zooms automatically to fit both origin and destination in the view
User selects “Use current location” as origin	Map zooms automatically to user location
Routing results multiple quiet path alternatives of which some are calculated with high noise sensitivity coefficient	Longest quiet paths are filtered out by default if they were calculated with high noise sensitivity coefficient (user can show them by disabling filtering by length from the filter-button)
Routing results include quiet paths that are only slightly longer than the shortest path	The shortest quiet path is automatically selected if it is only slightly longer than the very shortest path
Path is selected from the map by clicking	The list of paths automatically “jumps” to display the selected path
An error occurred during routing	A descriptive error message is shown, e.g. “Error in routing”
User selects an origin or a destination outside the supported area	The UI prevents routing and shows an error message “Origin [or destination] is outside the supported area”
User is trying to select a path from the map on mobile device but does not click directly on the path	A small search radius is used when selecting paths from the map to ease selecting paths on mobile phones (i.e. without a mouse)
User changes the orientation of the mobile device (i.e. to landscape or portrait mode) or switches to a device of different size	The UI reacts to the dimensions of the screen in order to show practical layout on devices of any sizes (especially on mobile)
User triggers the “add to home screen” functionality of the web page in the browser of a mobile device	The web application is added to the “home screen” of the user’s phone. When opened from home screen, the application can be used similarly as installed apps: it runs in full screen mode without address and bookmark bars of the browser (see <b>Figure 30</b> ) and avoids the need to be refreshed. This feature is enabled by specific HTML meta tags and a custom-made “app icon”.

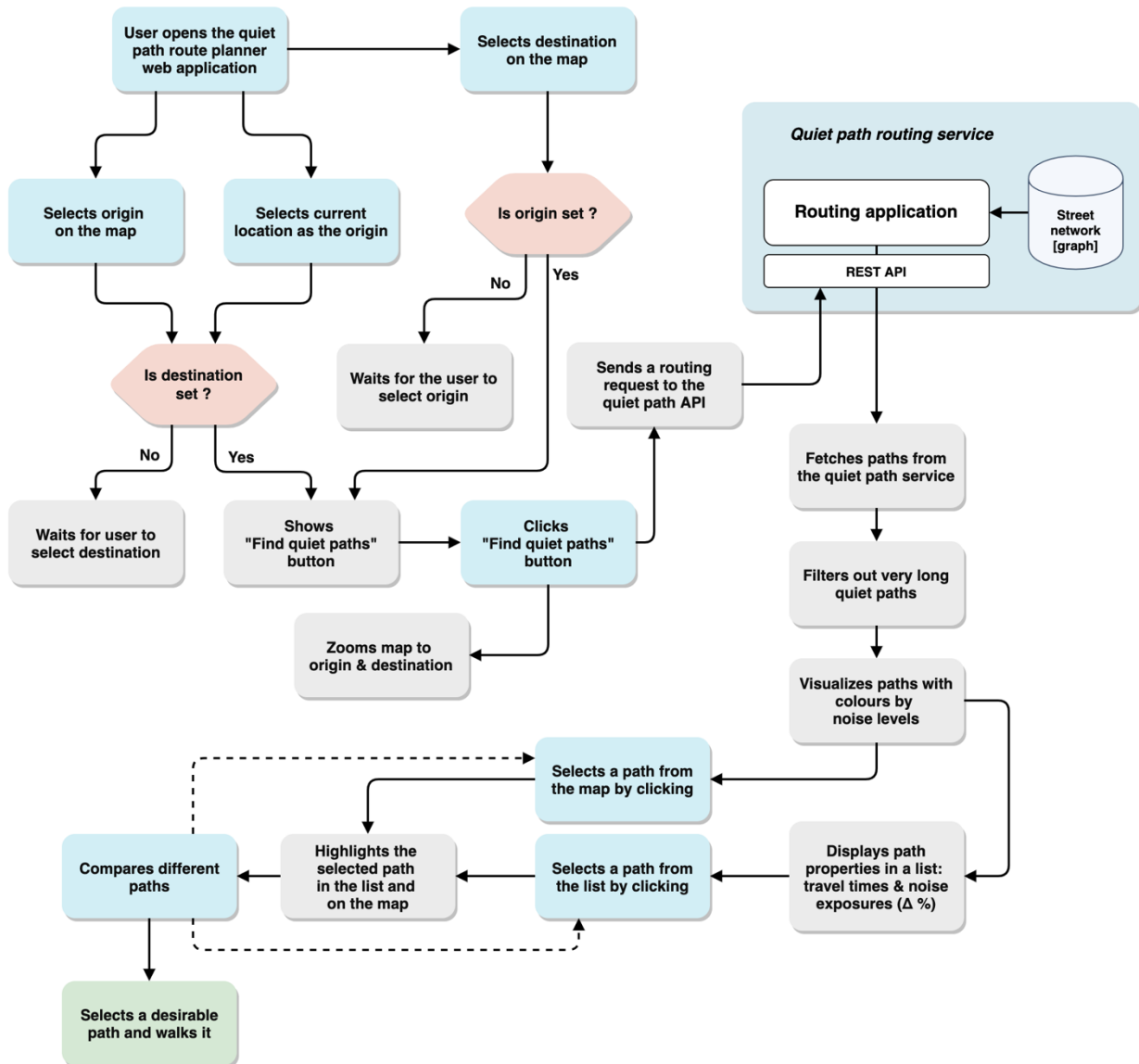


**Figure 27.** A typical sequence of actions included in solving one pathfinding problem from the perspective of the route planner application (grey) and user (blue).

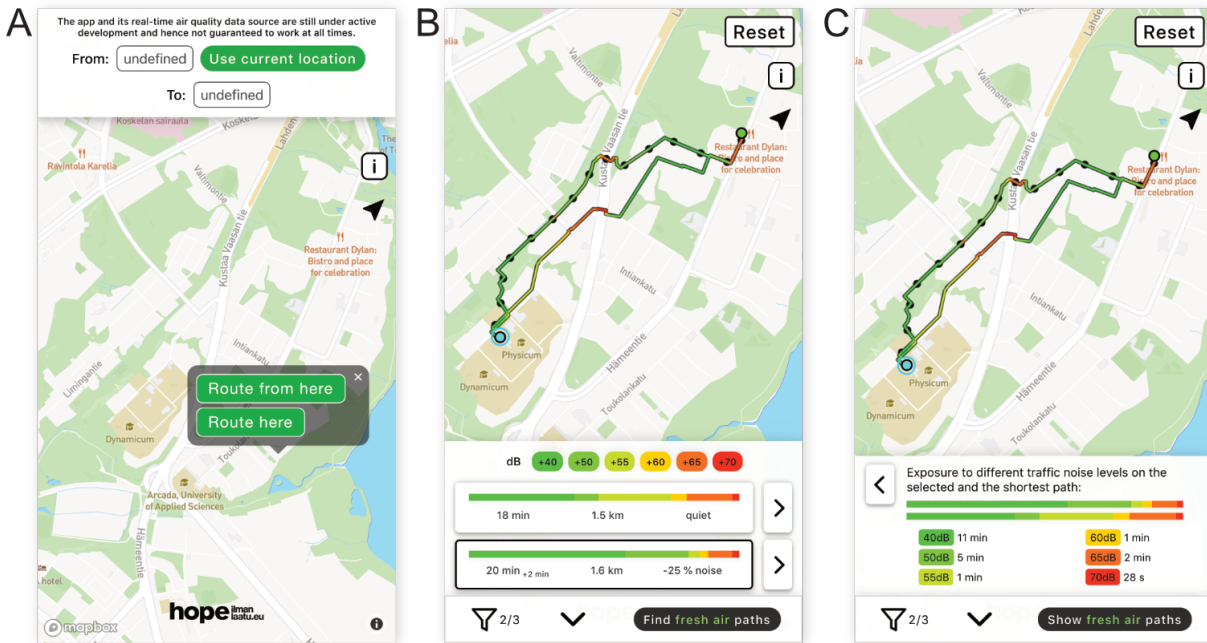


**Figure 28.** The user interface of the quiet path route planner when (A) user first opens the application, (B) showing two alternative paths (one shortest path and one quiet path) and (C) showing dynamic exposures to noise on a selected path.

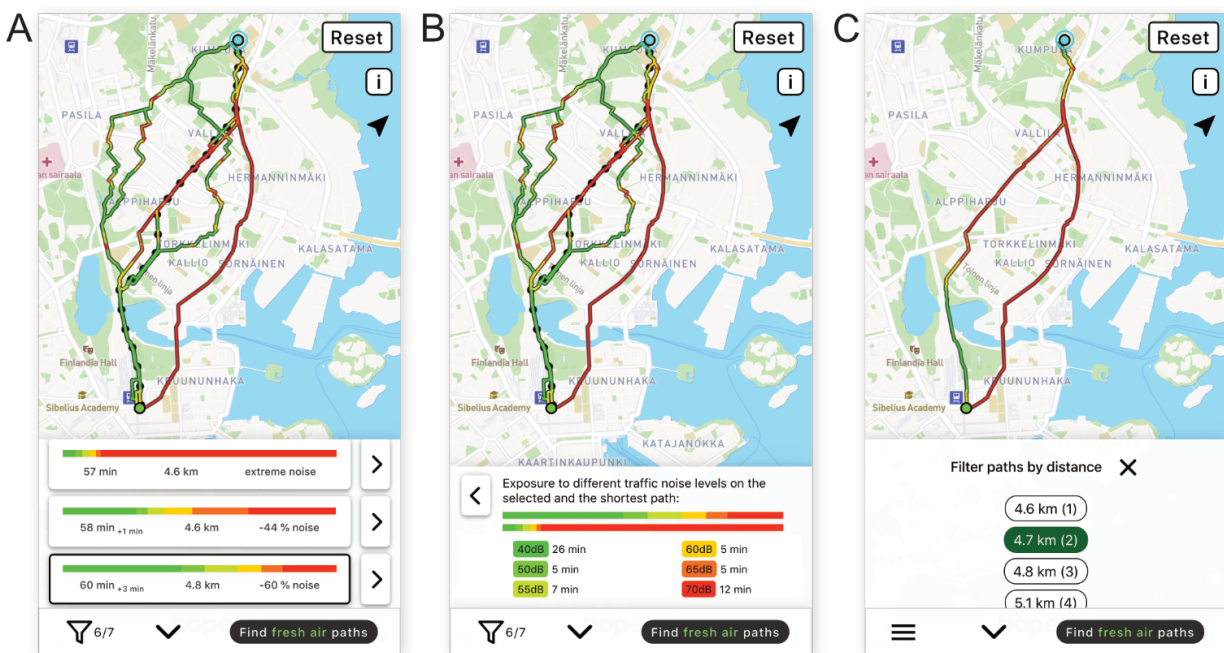


**Figure 29.** The user interface of the quiet path route planner when (A) showing several alternative paths (one shortest path and six quiet paths) and (B) showing exposure to noise on a selected path. Longest paths can be filtered out (hidden) by a user-defined length threshold (C).

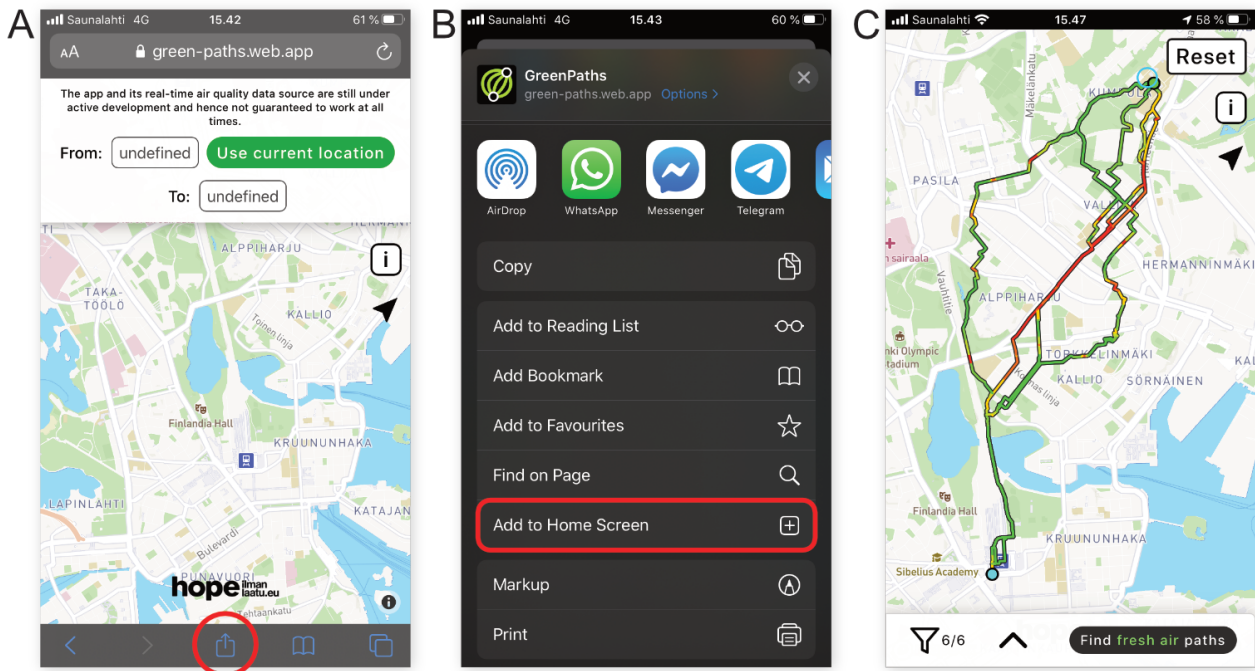


**Figure 30.** “Add to home screen” -functionality of the web application; the quiet path route planner can be “installed” on user’s phone (A & B) to appear similarly as installed apps (i.e. without web browser and address bar) (C).

## 4.3 Case study: Pedestrians’ exposure to traffic noise in Helsinki

### 4.3.1 Pedestrians’ exposure to traffic noise

Pedestrians’ exposure to traffic noise on shortest walking routes is highly variable. On average, almost half (46 %) of the total distance of a walk is exposed to traffic noise levels higher than 60 dB (Table 8) (e.g. more than 460 m of 1 km), suggesting that walking conditions are often suboptimal.

Table 8 represents both average exposures and variance in exposures to traffic noise on all shortest walking routes from all origins (including home–PT stop and home–workplace walks). Table 9 shows the same information only on local walking routes to PT stops (excluding direct walks to workplaces). The noise exposures on the paths were assessed by several noise exposure indices (see 3.5.4: Table 3). The noise level thresholds 60 dB, 65 dB and 70 dB were selected for the threshold-based indices in order to assess exposures to the highest traffic noise levels. The statistics are weighted by the modeled utilization rates of the walks and hence better represent average exposures to traffic noise. The paths included in Table 9 were shorter, on average, than the ones in Table 8, as per the descriptive

statistics of path lengths presented in Table 5 (see 3.7.3). Accordingly, the unnormalized noise exposure indices show higher values (on average) for the longer paths (Table 8).

The average exposures to the very highest noise levels ( $> 70$  dB) are considerably smaller compared to the exposures to lower noise levels ( $ED_{+65dB}$  &  $ED_{+60dB}$ ). High standard deviations of the exposure indices indicate highly unequal exposures to traffic noise between different walks. For both EI, ED and ER indices, excluding the highest noise level threshold (70 dB), the standard deviations of the indices are of the same magnitude as their means (i.e. relatively high). The average traffic noise level on all walks is 58 dB but it varies considerably from quiet to noisy ( $SD = 7$  dB).

**Table 8.** Descriptive statistics of exposure to traffic noise on the first walks of public transport itineraries to workplaces and on direct walks to nearby workplaces (n=30160).

Variable	Mean	Median	SD	p10	p25	p75	p90
EI	255	193	226	47	100	340	543
EI <sub>n</sub>	0.31	0.29	0.17	0.1	0.19	0.41	0.52
dB <sub>mean</sub>	58	58	7	48	52	63	67
ED <sub>+60dB</sub> (m)	214	144	219	13	64	295	510
ED <sub>+65dB</sub> (m)	137	75	178	0	21	179	352
ED <sub>+70dB</sub> (m)	52	7	101	0	0	63	146
ER <sub>+60dB</sub> (%)	47	42	33	4	19	74	100
ER <sub>+65dB</sub> (%)	30	21	30	0	5	47	79
ER <sub>+70dB</sub> (%)	11	2	20	0	0	14	36

**Table 9.** Descriptive statistics of exposure to traffic noise on the first walks of public transport itineraries to workplaces (direct walks to nearby workplaces are filtered out, n=17891).

Variable	Mean	Median	SD	p10	p25	p75	p90
EI	245	189	210	47	98	329	518
EI <sub>n</sub>	0.31	0.29	0.17	0.1	0.19	0.41	0.52
dB <sub>mean</sub>	58	58	7	48	52	63	67
ED <sub>+60dB</sub> (m)	206	141	207	15	64	288	480
ED <sub>+65dB</sub> (m)	131	74	166	0	21	173	335

ED <sub>+70dB</sub> (m)	49	7	94	0	0	62	139
ER <sub>+60dB</sub> (%)	47	42	33	5	19	75	100
ER <sub>+65dB</sub> (%)	30	21	30	0	5	47	79
ER <sub>+70dB</sub> (%)	11	2	20	0	0	14	36

### 4.3.2 Spatial patterns in pedestrians' exposures to traffic noise

The results of the origin-level dynamic noise exposures show significant spatial variation between different areas (Figures 32–36). The choropleth maps presented in this chapter represent mean traffic noise exposure indices at origin-level, weighted with the estimated utilization rates of the walks. Thus, three analogous ideas: 1) *average local walk*, 2) *typical local walk* and 3) *expected local walk* can be applied in interpreting the results. The three concepts aim to consider the spatial and statistical nature of the choropleth maps; as the indices are weighted with the utilization rates of the walks, they can estimate the *expected* traffic noise exposure on an average or arbitrary (commuting-related) walk from each origin.

Figure 31 represents spatial variation in the mean walking distance from origin to its (local) PT stops. Figure 32 represents mean traffic noise level ( $\text{dB}_{\text{mean}}$ ) on the walks from each origin (for origin-level STD of  $\text{dB}_{\text{mean}}$ , see Appendix 5). Figure 33 and Figure 34 represent mean exposures (m) to traffic noise levels exceeding 65 dB(A) and 70 dB(A) thresholds ( $\text{ED}_{+65\text{dB}}$  &  $\text{ED}_{+70\text{dB}}$  as in 3.5.4: Table 3). Respectively, Figure 35 and Figure 36 represent mean relative exposures (%) to traffic noise levels exceeding the thresholds as proportions of the total lengths of the paths ( $\text{ER}_{+65\text{dB}}$  and  $\text{ER}_{+70\text{dB}}$  as in 3.5.4: Table 3). Choropleth maps of noise exposure index (EI) and normalized noise exposure index ( $\text{EI}_n$ ) are attached only as Appendix 3 and Appendix 4, as they are conceptually more difficult but show mainly similar spatial patterns as ED and ER.

Some spatial patterns in the noise exposure indices are visible on the maps. Exposure to the highest noise levels by  $\text{dB}_{\text{mean}}$  occur often on the walks from the origins near the major roads in the city. Similarly, the highest mean  $\text{ED}_{+65\text{dB}}$ ,  $\text{ED}_{+70\text{dB}}$ ,  $\text{ER}_{+65\text{dB}}$  and  $\text{ER}_{+70\text{dB}}$  appear often near the major roads of the city, but with considerable spatial variation. Some correlation between the average walking distances from the origins and the respective  $\text{ED}_{+65\text{dB}}$  and  $\text{ED}_{+70\text{dB}}$  indices can be seen by visual comparison of the maps (Figure 31; Figure 33 & Figure 34), as expected. Exposures to the very highest noise levels are distributed unequally in the study area. For some neighborhoods (e.g. Itä-Pakila, Kruunuhaka and Koskela), the indices  $\text{ED}_{+65\text{dB}}$  and  $\text{ED}_{+70\text{dB}}$  are considerably higher than the

average of all walks (Table 9). Despite that these indices are likely to co-vary with the mean walking distances (as mentioned above), also the relative traffic noise indices  $ER_{+65dB}$  and  $ER_{+70dB}$  show higher values in the same areas. For a substantial share of the areas (including the previously mentioned), the mean traffic noise level of the average walk is higher than 65 dB(A). Considering these findings, the results indicate that major dynamic exposures to unhealthy traffic noise levels are relatively common in the study area.

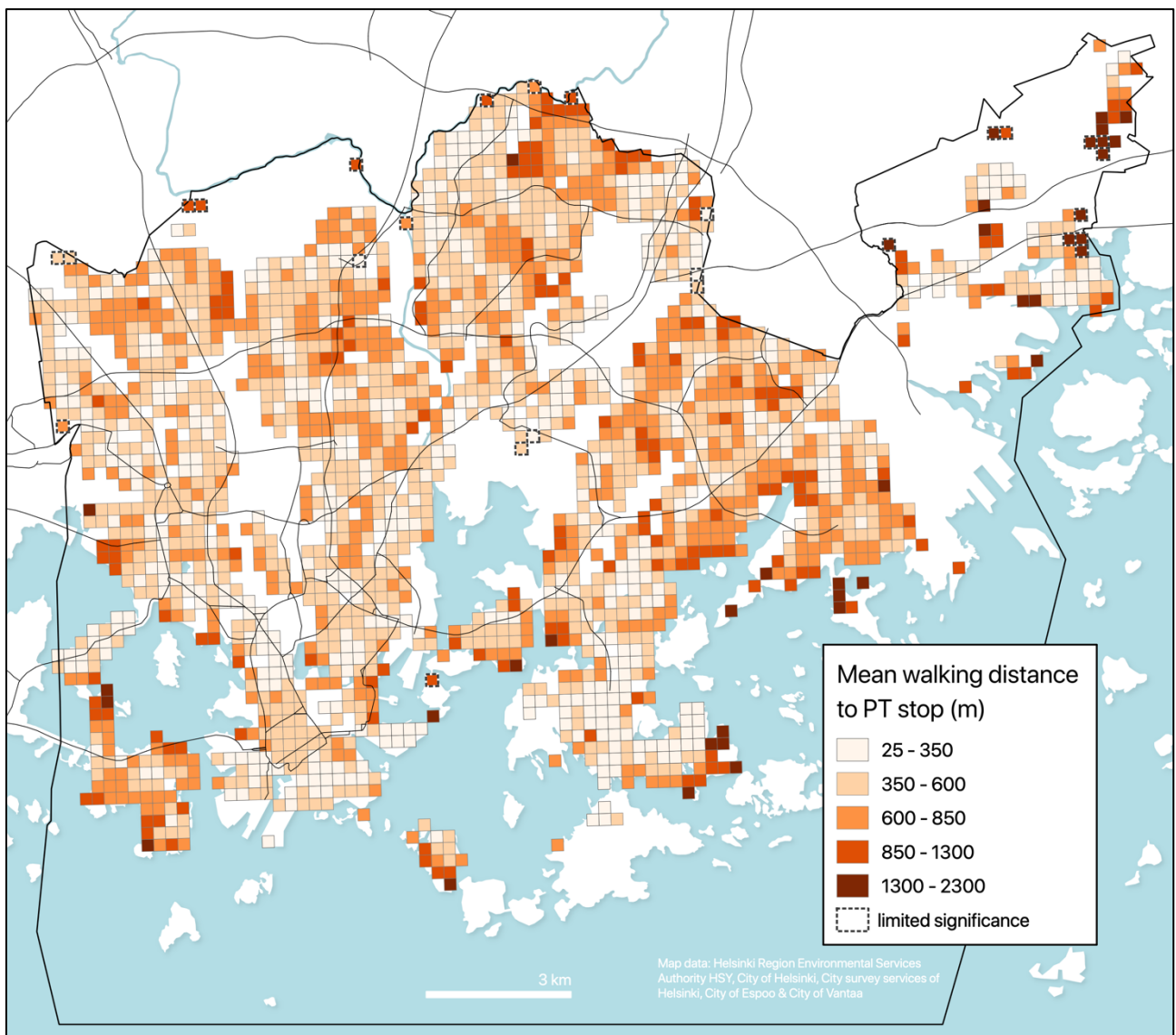


**Figure 31.** Mean walking distances from homes to closest public transport (PT) stops. The averages are weighted with the estimated utilization rates of the walks based on the total flow of commutes using each origin – PT stop pair.

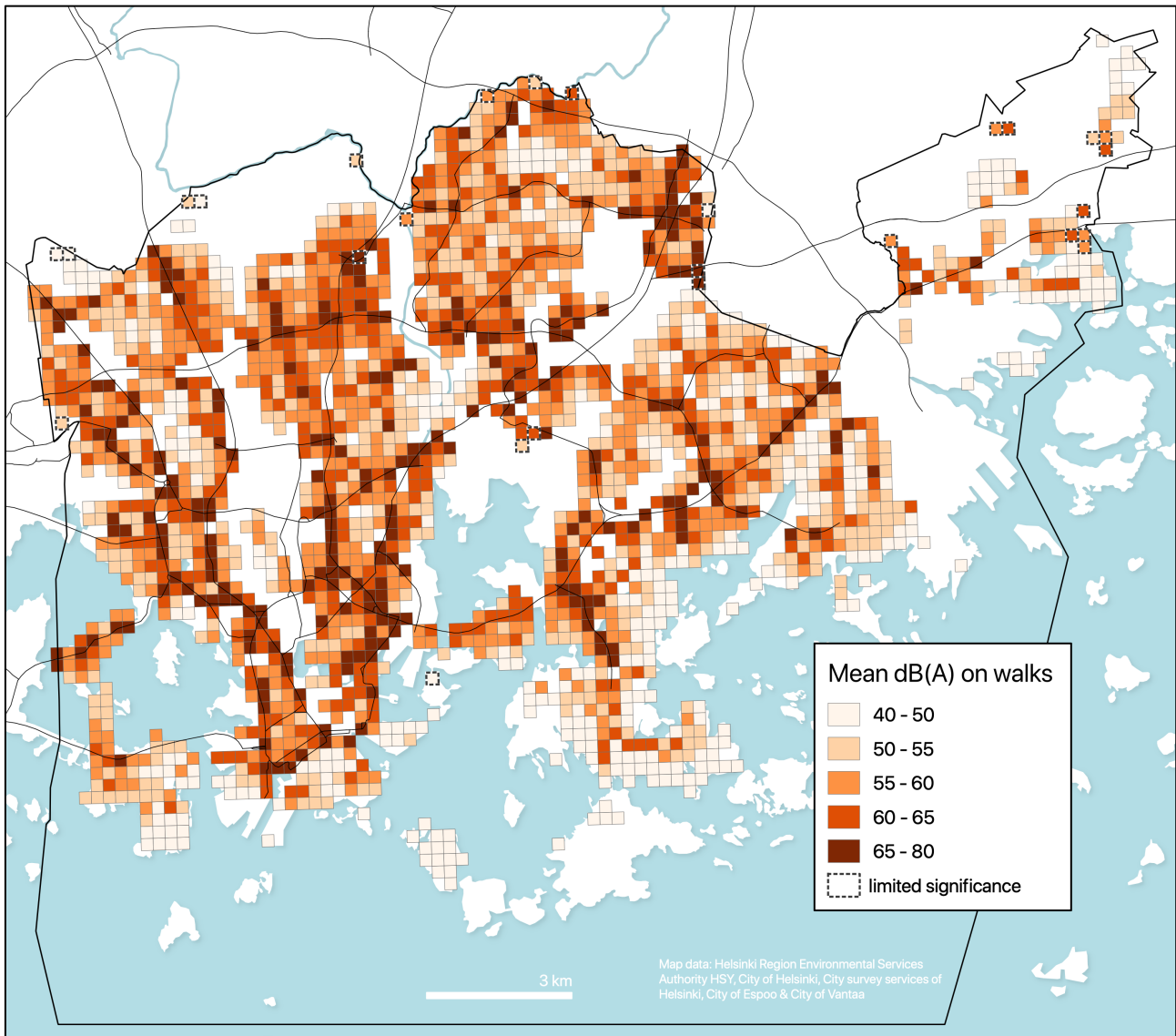


**Figure 32.** Mean traffic noise level (dB(A)) on walks from homes to closest PT stops. The averages are weighted with the estimated utilization rates of the walks based on the total flow of commutes using each origin – PT stop pair.

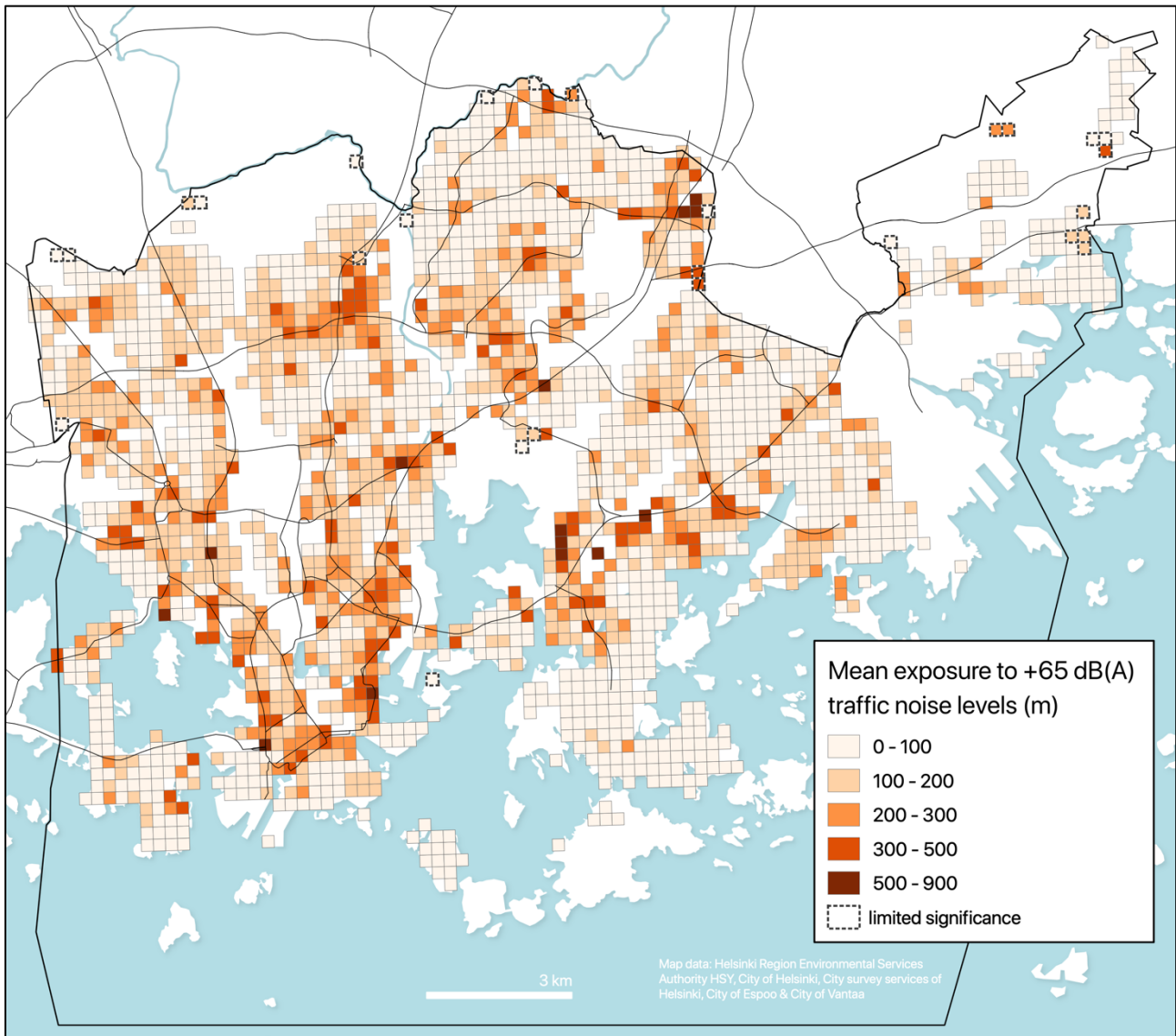


**Figure 33.** Mean exposures to +65 dB(A) traffic noise levels (m) on walks from homes to closest PT stops. The averages are weighted with the estimated utilization rates of the walks based on the total flow of commutes using each origin – PT stop pair.

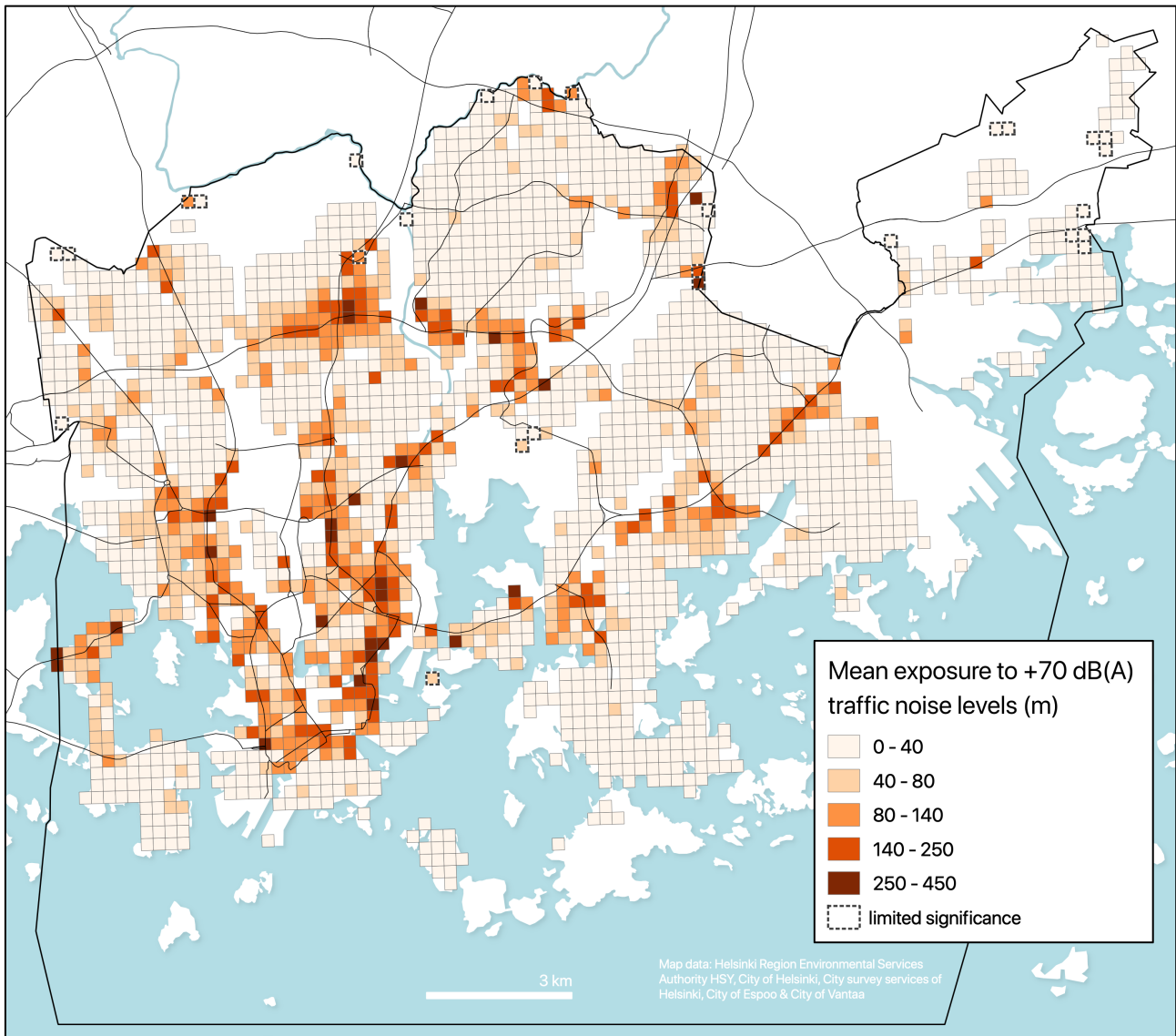


**Figure 34.** Mean exposures to +70 dB traffic noise levels (m) on walks from homes to closest PT stops. The averages are weighted with the estimated utilization rates of the walks based on the total flow of commutes using each origin – PT stop pair.

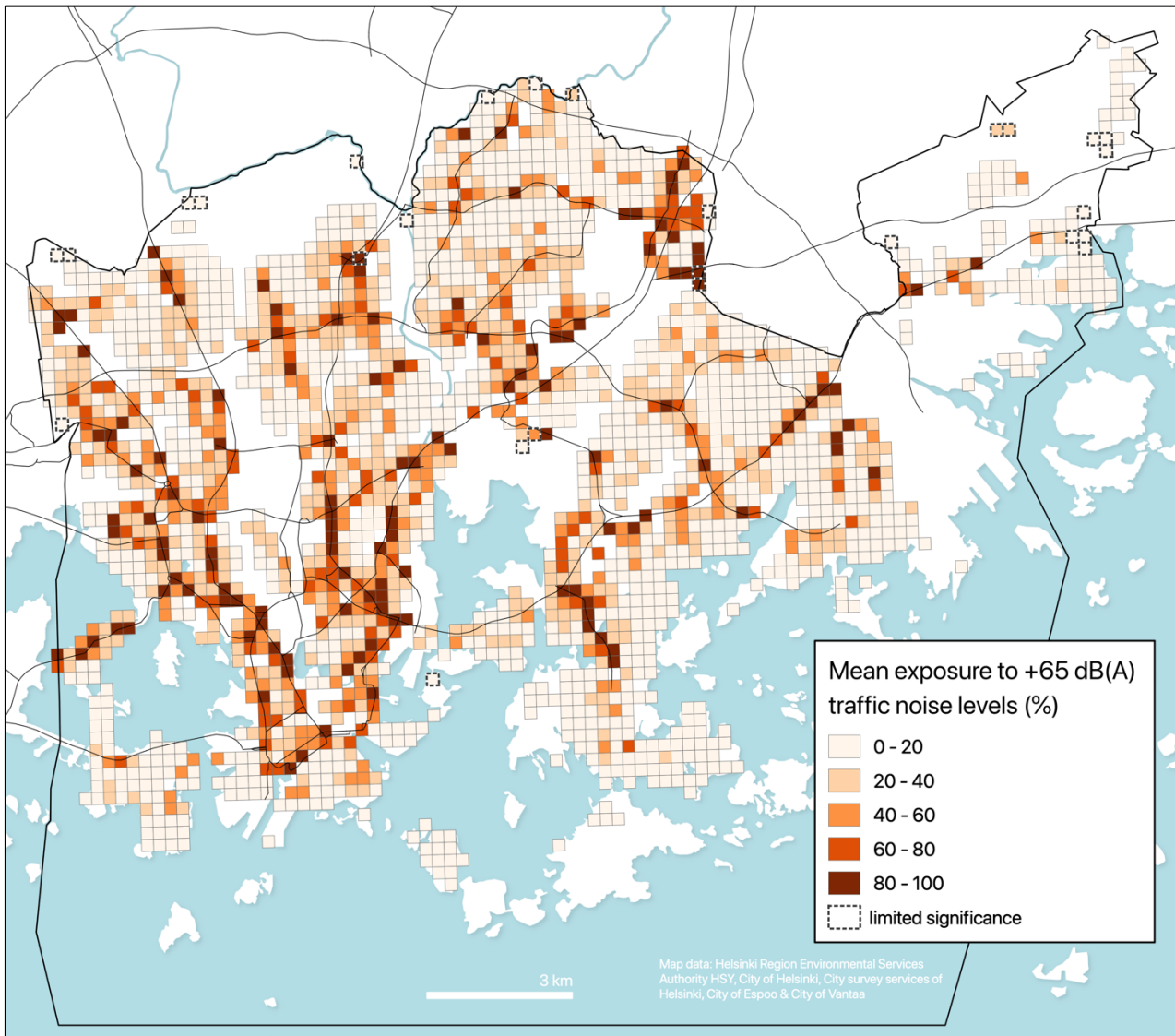


**Figure 35.** Mean exposure (%) to traffic noise levels higher than 65 dB(A) on walks from homes to closest PT stops as (mean) percentage of total lengths of the walks (i.e. mean  $ER_{+65dB}$  as defined in 3.5.4: Table 3). The origin-level averages are weighted with the estimated utilization rates of the walks based on the total flow of commutes using each origin – PT stop pair.

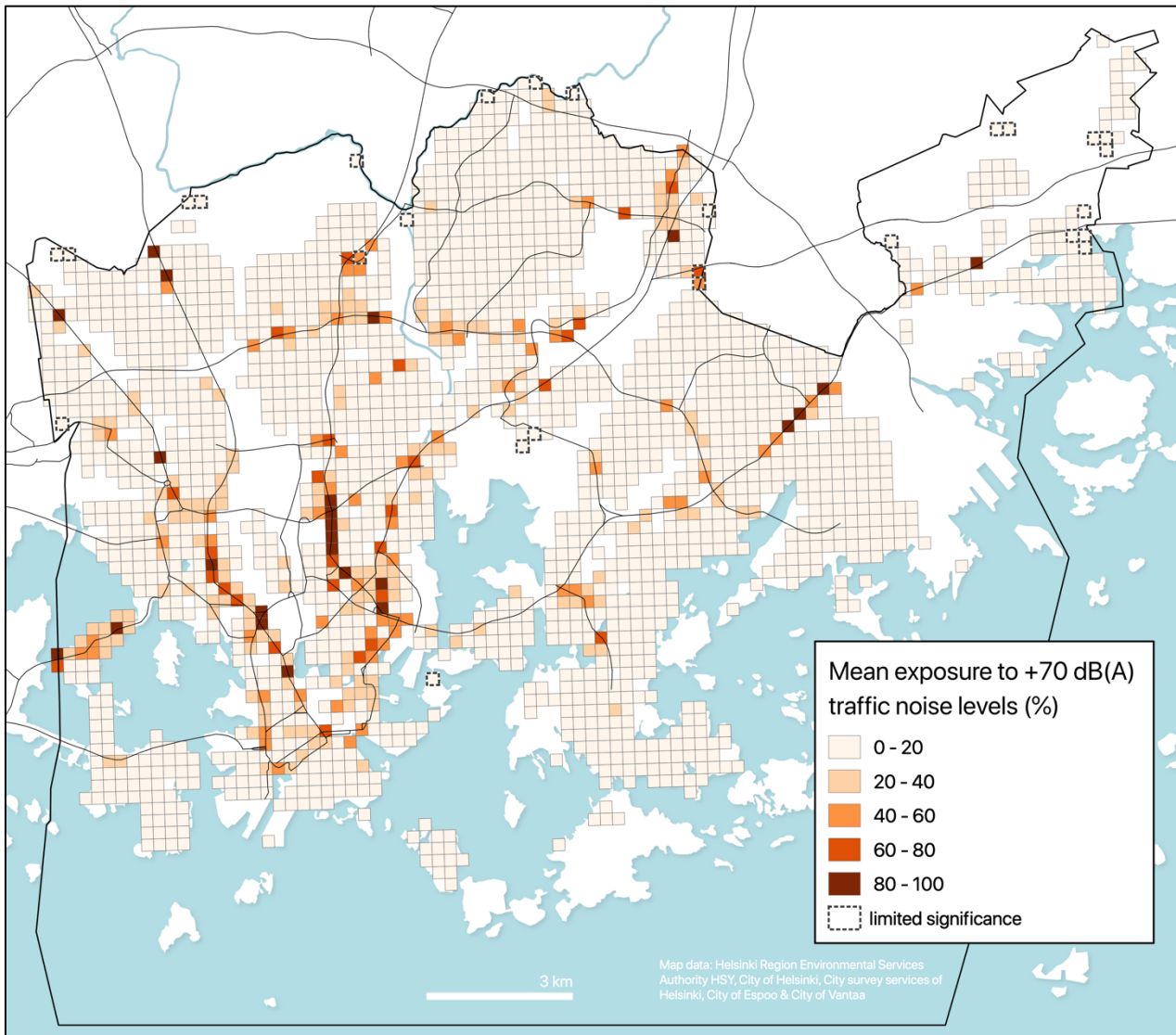


**Figure 36.** Mean exposure (%) to traffic noise levels higher than 70 dB(A) on walks from homes to closest PT stops as (mean) percentage of total lengths of the walks (i.e. mean  $ER_{+70dB}$  as defined in 3.5.4: Table 3). The origin-level averages are weighted with the estimated utilization rates of the walks based on the total flow of commutes using each origin – PT stop pair.

#### 4.4 Achievable reductions in exposure to traffic noise

I assessed the performance of the quiet path routing by exploring achievable reductions in traffic noise exposures (see 3.8). The results of the performance assessment show that significant, but highly variable reductions in dynamic noise exposure can be achieved by choosing alternative, quiet paths.

In this chapter, the achievable reductions are presented by the following six noise exposure indices (for definitions, see 3.5.4: Table 4):

- 1)  $dB_{mean}$  (i.e. mean noise level on the path);

- 2) ED<sub>+60dB</sub> (i.e. distance of exposure to noise levels higher than 60 dB);
- 3) ED<sub>+65dB</sub> (i.e. distance of exposure to noise levels higher than 65 dB);
- 4) ER<sub>+60dB</sub> (i.e. percentage of exposure to noise levels higher than 60 dB);
- 5) ER<sub>+65dB</sub> (i.e. percentage of exposure to noise levels higher than 65 dB);
- 6) EI (i.e. noise exposure index).

The term *initial noise exposure index* is used to refer to the noise exposure index of a shortest path of a given OD pair. Figure 37 represents scatterplots of achievable reductions in the noise exposure indices and the initial noise exposure indices for first subset of paths (short paths). For each index, three scatterplots were created by the three length difference (addition) thresholds for quiet paths (100, 200 and 300 m). In addition, the results of the simple linear regression analysis are shown in the figure for each scatterplot. Figure 38 represents the same set of scatterplots and metrics as Figure 37, but for the longer paths (700–1300 m). Three important observations can be made from the scatterplots and the results of the regression analysis:

- 1) Higher exposure to noise on the shortest path predicts higher achievable noise reduction (by quiet paths);
- 2) Greater additional length of the quiet path (compared to the length of the shortest path) seem to predict higher reduction in exposure to noise;
- 3) The statistical relationships between reductions in noise exposure indices and the initial noise exposure indices are stronger for the longer paths (Figure 37 vs. Figure 38).

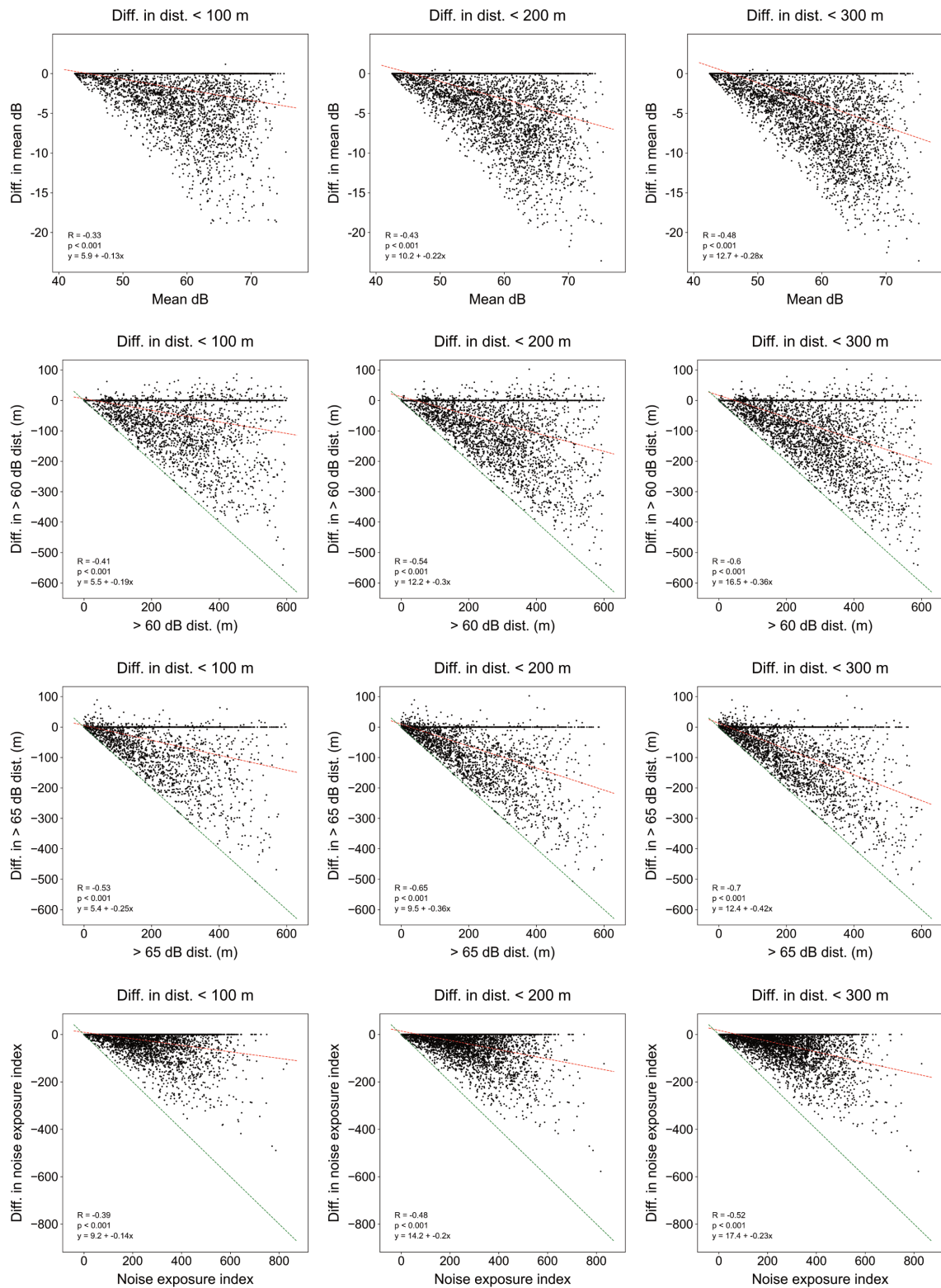


**Figure 37.** Regression analysis between the reductions in traffic noise exposures on quiet paths and the initial traffic noise indices. The analysis covers shortest paths in the length range of 300 to 600 m and the respective quiet paths. The red lines represent the regression lines of the regression analysis and the green lines show the theoretical maximum reductions in the noise exposure indices.

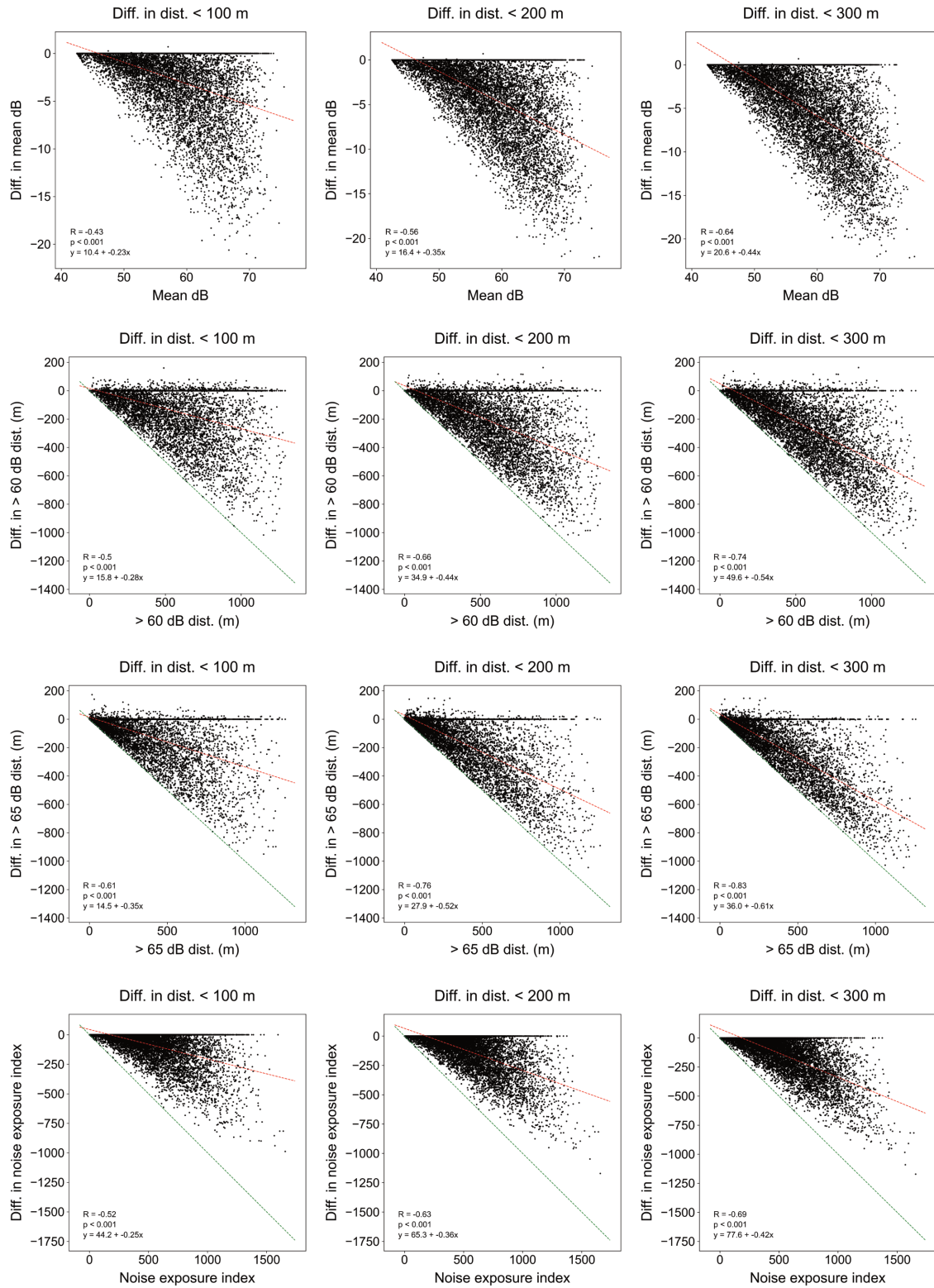


**Figure 38.** Regression analysis between the reductions in traffic noise exposures on quiet paths and the initial traffic noise indices. The analysis covers shortest paths in the length range of 700 to 1300 m and the respective quiet paths. The red lines represent the regression lines of the regression analysis and the green lines show the theoretical maximum reductions in the noise exposure indices.

Table 10 and Table 11 represent the descriptive statistics of the achievable reductions in traffic noise exposure indices ( $ER_{+65dB}$  and  $dB_{mean}$ ) for a set of path subsets. Since no quiet paths shorter than the maximum allowed length difference (100, 200 or 300 m) were found in many cases, the average length differences of the quiet paths were substantially lower than the allowed maximum length difference (threshold) in each group. For this reason, averages of the length differences of the quiet paths are also included in the table (“quiet path length difference”). At least five observations, partly overlapping with the previous ones, can be made by exploring the statistics:

- 1) Achievable reductions in traffic noise exposure seem to be higher for longer (shortest) paths;
- 2) Initially higher noise exposures (on shortest paths) seem to predict also higher achievable reductions in them;
- 3) Higher length addition of quiet paths seems to predict higher reduction in noise exposure;
- 4) Higher mean and median length differences of quiet paths were found for longer shortest paths (700–1300 m), indicating that more quiet paths are found for longer O-D distances;
- 5) Accordingly, the lower median length differences of the quiet paths for shorter paths (300–600 m) indicate that in many cases few (or no) quiet paths are found for short O-D distances.

The mean reductions in  $ER_{+65dB}$  are consistently and significantly higher for the longer paths (22–57 % vs. 12–38 %). Similarly, higher mean reductions in  $dB_{mean}$  were found for the longer paths (2.4–9.6 dB vs. 1.6–6.4 dB).

**Table 10.** Descriptive statistics of the achievable reductions in noise exposure index  $ER_{+65dB}$  on different subsets of the paths. The subsets were defined by 1) the length of the shortest path, 2) the length difference of the quiet path and 3) the initial  $ER_{+65dB}$  ( $n_{300-600m} = 4338$ ,  $n_{700-1300m} = 7842$ ).

Path length (m)	Quiet path length difference (m)	Subset of paths by $ER_{+65dB}$					
		10–40 %	40–70 %	70–100 %	Difference (%) in $ER_{+65dB}$ (mean, median, SD)		
Range	Max	Mean	Median	SD			
300–600	< 100	18	0	28	-12, 0 (26)	-24, -0 (31)	-22, -0, (28)
300–600	< 200	41	6	56	-16, -0 (29)	-33, -29 (33)	-33, -30, (30)
300–600	< 300	60	17	81	-17, -0, (29)	-37, -36 (34)	-38, -40, (30)
700–1300	< 100	31	21	32	-22, 0 (30)	-35, -33 (32)	-32, -28, (30)
700–1300	< 200	74	64	64	-29, -20 (33)	-49, -53 (31)	-48, -54, (30)

700–1300	< 300	117	103	95	-32, -26, (33)	-56, -60 (28)	-57, -64, (27)
----------	-------	-----	-----	----	----------------	---------------	----------------

**Table 11.** Descriptive statistics of the achievable reductions in noise exposure index  $\text{dB}_{\text{mean}}$  on different subsets of the paths. The subsets were defined by 1) the length of the shortest path, 2) the length difference of the quiet path and 3) the initial  $\text{dB}_{\text{mean}}$  ( $n_{300-600\text{m}} = 4103$ ,  $n_{700-1300\text{m}} = 6925$ ).

Path length (m)	Quiet path length difference (m)	Subset of paths by $\text{dB}_{\text{mean}}$			
		55–60 $\text{dB}_{\text{mean}}$	60–65 $\text{dB}_{\text{mean}}$	65–80 $\text{dB}_{\text{mean}}$	
Range	Max	Mean	Median	SD	Difference (dB) in $\text{dB}_{\text{mean}}$ : mean, median (SD)
300–600	< 100	19	0	29	-1.6, -0.0 (2.7)    -2.6, -0.0 (4.0)    -3.0, -0.0, (4.3)
300–600	< 200	43	8	57	-2.3, -0.5 (3.2)    -4.1, -2.3 (4.7)    -5.1, -3.8, (5.3)
300–600	< 300	64	21	83	-2.7, -0.0, (3.4)    -4.9, -3.8 (5.0)    -6.4, -5.8, (5.8)
700–1300	< 100	32	22	33	-2.4, -1.4 (2.8)    -3.9, -2.8 (4.1)    -5.0, -3.6, (5.0)
700–1300	< 200	77	70	64	-3.6, -3.0 (3.2)    -5.9, -5.6 (4.5)    -7.8, -7.9, (5.5)
700–1300	< 300	122	113	94	-4.2, -3.9, (3.4)    -7.2, -7.3 (4.5)    -9.6, -10.2, (5.4)

## 4.5 Sharing of the methods and results

All content and methods developed in the thesis are shared with a permissive MIT license via a public GitHub repository: <https://github.com/hellej/quiet-paths-msc>. Unfortunately, some of the data sources consisted of too big files (e.g. graph data) or had restrictive license (e.g. YKR-commuting data) and hence could not be shared along with the source-code (for list of the used datasets, see Table 1). However, the complete method for downloading and processing OSM street network data for graph construction is included in the repository. Hence, a “noise-aware” walkable street network graph can be easily generated for any area of interest, as long as traffic noise data for the given area is available. After generating a graph for the area of interest, the quiet path routing application can be run on a personal computer (as opposed to a server-based setup).

During the study, the quiet path routing application was developed further within the HOPE project (Healthy Outdoor Premises for Everyone). A parallel version of the quiet path routing application was created by “forking” the source-code from: <https://github.com/hellej/quiet-paths-msc> to a new

repository under the GitHub community of the Digital Geography Lab: <https://github.com/DigitalGeographyLab/hope-green-path-server>. While developing the quiet path routing method further, the source code was also heavily refactored and documented. Also, to enable significantly faster routing analysis for longer OD distances, the routing analysis was migrated to utilize the routing library igraph (Csardi & Nepusz, 2006) instead of NetworkX. The name of the application was changed from *quiet paths* to *green paths*. The source-code for the user interface application is accessible at: <https://github.com/DigitalGeographyLab/hope-green-path-ui>. Instructions for getting the application up and running locally are included in the README.md files at the root of both repositories (hope-green-path-server & hope-green-path-ui). Both repositories utilize GitHub releases that enable creating snapshots of the repositories at a specific time. At the time of writing this, the latest release for the hope-green-path-server is v1.3 and for hope-green-path-ui: v1.2. New releases of both projects will be published as they are developed further.

## V. DISCUSSION AND CONCLUSIONS

### 5.1 Significant but varying reductions in traffic noise exposure can be achieved by routing quiet paths

In this study, I developed a quiet path routing method (and application) to address three objectives: 1) to assess dynamic exposure to noise, 2) to support a proof of concept quiet path route planner and 3) to assess achievable reductions in traffic noise exposure by route choices in Helsinki. The third was needed to demonstrate the potential utility of the quiet path routing application in practical situations.

To the best of my knowledge, achievable reductions in dynamic exposure to traffic noise have not been studied in such a large scale in previous studies. Instead, a common approach has been to compare exposures of interest on alternative paths between several known OD pairs. For example, Ribeiro & Mendes (2013) found somewhat similar reductions in mean dB(A) (2.2–6.4 dB) as were discovered in this study, but by only studying three OD pairs. On the other hand, achievable reductions in exposure to air pollution have been assessed in many studies and also by higher number of OD pairs. Mahajan et al. (2019), for example, used somewhat similar approach for quantifying potential reductions in PM2.5 exposure as I (for reductions in traffic noise exposure), composed of 1) routing several thousands of shortest and exposure-optimized paths, 2) grouping of shortest paths by several distance ranges and 3) assessing the reductions in exposure with respect to distance increase. In the assessment they use arbitrary origins destinations for the paths, as also many others (e.g. Mölter & Lindley, 2015; Zou et al., 2020), whereas I used more realistic origins and destinations from the analysis of census based commuting data. Thus, the advantage of the assessment of this study is combining large sample size ( $n=12180$ ) and more realistic ODs.

To summarize the main findings of the assessment, three factors seem to predict higher reduction in traffic noise exposure on a quiet path. Higher traffic noise exposure on the shortest path sets the initial amount of noise exposure higher, likely resulting in higher probability for presence of alternative, quieter paths (1). Longer distance between origin and destination seem to increase the total number of alternative paths, thus (again) increasing the probability for finding quiet paths (2). Undoubtedly, also greater additional length of the quiet path results in higher reduction in noise exposure – as per the basic principle of LCP routing analysis (3).

The results of the statistical analysis show 12–57 % mean reduction in exposure to noise levels higher than 65 dB and 1.6–9.6 dB mean reduction in mean dB, depending on at least the three factors

described above. The standard deviations of the reductions were of the same magnitude as the mean reductions themselves, indicating high variation in opportunities for choosing quiet paths (at least in Helsinki): while in most cases a significant share of the total noise exposure of the shortest path could be avoided by choosing an alternative, quiet path; in some cases no applicable quiet paths were found for the OD pair. Despite the high variances of the achievable reductions, the averages can be interpreted as significant *expected* achievable reductions in traffic noise exposure. As per these results, it can be concluded that the quiet path routing method does have the potential to find considerably quieter yet only slightly longer paths in many common situations. This further justifies the need for a web-based quiet path route planner with which individuals can reduce their journey time exposure to traffic noise in real-worlds situations.

Again, similar argument has been used in developing air pollution based routing analysis further (e.g. Hatzopoulou et al., 2013; Mahajan et al., 2019; Zou et al., 2020); as significant reductions in air pollution can be achieved with exposure optimized routing, there seem to be potential for also mobile and web applications that allow these potential reductions to be realized by individuals’.

## **5.2 Publishing a green path routing application online can facilitate citizens to choose healthier paths**

While it could be reasoned that pedestrians and cyclists often try to minimize their exposure to unhealthy environments, there is a likely “exposure awareness gap” as suggested by Ueberham et al. (2019): individuals may not be aware of their dynamic exposure to pollutants. As demonstrated by a number of studies (e.g. Lwin & Murayama, 2011, 2013; Quercia, Schifanella, & Aiello, 2014; Ribeiro & Mendes, 2011), considering environmental factors in routing analysis seem to have the potential to find healthier or in other ways more pleasant routes. Therefore, there is a clear need and motivation for developing user-friendly route planners to facilitate reducing pedestrians’ and cyclists’ journey-time exposure to pollutants.

In this study, I developed a web-based proof of concept quiet path route planner to demonstrate the utility of the quiet path routing method in real-life situations. A small number of test users used the route planner during the project, but no structured survey was carried out to assess the users’ experiences. However, the general feedback on the usability was consistent: the quiet path route planner is relatively intuitive to use and it can help finding alternative, quieter paths. As per the feedback, particularly coloring the geometries of the paths by noise levels eases comparing alternative paths with respect to noise exposure.

The route planner was developed to be highly mobile friendly, to facilitate on-demand route planning especially on the move. Also, it was designed to be so simple that no additional instructions are needed. Thus, no noise exposure indices other than the self-explanatory ones are shown in the user interface. The difference in noise exposure index (between a shortest and a quiet path) is shown simply as a reduction in *noise* (%). This way, the complexity of the underlying EIF for noise does not limit the usability of the application.

It is important to help individuals to find paths that suits their personal needs and time-dependent circumstances. An important feature, or possibly a limitation, of the quiet path route planner are the fixed settings for routing: user does not get to decide the relative importance of noise exposure and travel-time before routing. Instead, the route planner always suggests several alternative quiet paths (by different weightings) along with the shortest path. This approach works well in an application that only minimizes one type of exposure, since it allows the user to decide the best path (as opposed to a route planner that finds only one path). However, a different approach is probably more suitable for route planners that take into account multiple criteria in routing. In the route planner developed by Novack et al. (2018), for example, the user needs to set the relative importance of several factors (e.g. green areas, quietness and distance) already prior to routing, by using a set of slide-bars in the user interface. A weakness to this functionality is posed by the unknown default weighting of the different criteria; when the user sets multiple factors equally important, the relative weights of the different factors are essentially decided by the developers of the route planner. Therefore, instead of fixing all settings prior to routing, presenting the user a set of alternative suggested paths may well be a reasonable approach.

A popular green path route planner may be one of the most effective ways to reduce pedestrians' and cyclists' dynamic exposure to pollutants. The better the green path route planner can meet users' needs and expectations, the more likely it is to become popular. Technical prospects of developing the quiet path route planner further, and towards a more general green path route planner, are reviewed in the next chapter (5.3). On the other hand, challenges in combining multiple environmental exposures in routing analysis are discussed in chapter 5.8.

### **5.3 Alternative quiet paths need to be calculated to suit different situations and personal preferences**

Since the environmental impedance function (EIF) could not be formulated to accurately model the health effect of a walk, the final decision on choosing the healthiest, nor best, path could not be

implemented inside the quiet path routing application. Furthermore, since sensitivity to noise and time-constraints depend on the person and the situation, no attempt was made to choose the *optimal* trade-off between reduction in noise exposure and addition in travel time with pure application logic. Thus, one of the most essential features of the quiet path routing application is finding several alternative quiet paths for an OD pair to let the user to make the final decision on choosing the most desirable path.

The alternative quiet paths are calculated by gradually increasing the noise sensitivity coefficient in the environmental impedance function in parallel (iterative) pathfinding calculations. The defined set of noise sensitivity coefficients ranges from 0.1 to 40. The highest coefficients effectively override the weight of length in the composite cost and produce paths of *least noise exposure*. Thus, with the highest sensitivity coefficients, considerably longer quiet paths may be calculated when opportunities for walking in quiet are limited. On the other hand, many of the quiet paths calculated with the lowest sensitivity coefficients are almost identical with the shortest path. Therefore, when alternative paths calculated with different sensitivity coefficients are presented (to a user), it is critical to clearly communicate the following three properties of the paths: 1) how noisy is the shortest path, 2) what is the achievable reduction in noise exposure on the quiet paths and 3) how much longer are the quieter paths compared to the shortest path.

As per the results of the assessment of achievable reductions in exposure to traffic noise, the number of quiet paths seem to increase when OD-distance increases. When several paths have the same length and only little variation in noise exposure, the importance of letting the user to choose the path further increases. In these situations, also other factors that affect walkability and pedestrians' personal preferences presumably start to play bigger role in the route selection.

## **5.4 Advanced routing features and higher performance require revised technical implementation**

In the further developments of the quiet path routing application, also temporally more dynamic, or even real-time pollutant data should be integrated in the exposure-based routing analysis. Since real-time data on traffic noise levels is often not available, noise levels for different times of the day could be interpolated from modeled daytime and night-time noise levels by statistical means.

However, in the case of Helsinki, for example, availability of real-time air quality data is improving. Within the HOPE project, in which the quiet path route planner is being developed further (at the time of writing this), a novel modeled real-time air quality index (AQI) data was integrated in the

routing analysis. This posed a challenge for the performance of spatially joining exposure data to street network graph. In this thesis, I carried out a lossless, but not very fast, spatial join between noise surface data and total 180 647 line geometries of street edges. Since the processing was needed only once, accuracy of the join was prioritized over performance. For real-time pollutant data, however, the appropriate balance between accuracy and performance of processing the data depends on several factors, including update interval, spatial accuracy and format (raster/vector) of the data. In the HOPE project, hourly pollutant data was accessible in raster format via an API. I revised the spatial join to use point sampling, which gave a performance boost of 2–3 orders of magnitude in processing time, from 20–40 minutes to a few seconds.

From a technical standpoint, a route planner should be robust enough to support a high number of concurrent users. The route planner developed in the study demonstrates the use of modern Web GIS technologies and a simple service-oriented architecture, where the user interface works as an independent web map application and communicates with the routing service with asynchronous requests. Generally speaking, a somewhat similar architecture has been applied in many previous studies (e.g. Novack et al., 2018; Su et al., 2010). This design facilitates the development of such service, as new features can be developed to either or both of the applications depending on where the changes are needed. If more computing power is needed, the routing service can be moved to another server or infrastructure, requiring only minimal changes to the user-interface.

The possible features of a green path routing application are ultimately bound to its technical implementation, including the used programming environment and the chosen libraries. For a proof of concept route planner, as the one developed in this study, a relatively simple Python implementation (and igraph library) was adequate for the routing application. However, when advanced features such as turning costs and traffic light penalties are needed, the limitations of existing graph libraries, such as NetworkX and igraph, may likely become obstacles. Thus, at some point, developing the quiet path route planner further probably requires either implementing a customized LCP application (i.e. not using existing graph-libraries) or extending an existing routing application with exposure-based routing features. Another option would be to use one routing application (e.g. OpenTripPlanner) for creating a more advanced street network graph and then another for the implementation of the green path routing functionalities. In addition, street network graph creation should be automated and scheduled, so that changes in the street network are included in the routing application without a considerable delay. For OSM-based routing applications, such as the quiet path route planner and OpenTripPlanner, this should be achievable with moderate effort.

## 5.5 Usability of the quiet path routing application depends also on the quality of the shortest paths

This study shows that a functional route planner for exposure-based routing can be built using exclusively open-source technologies and OpenStreetMap data. However, the true usability of the developed quiet path routing application would have remained uncertain if the quality of the paths was not assessed. Hence, in addition to the assessment of achievable reductions in exposure to traffic noise (i.e. performance of the quiet path routing method), also the quality of the shortest paths was evaluated.

Lengths of the shortest paths were compared to the reference paths calculated with the route planner service of HRT (i.e. Digitransit Routing API). As per Table 12, the mean and median difference in path lengths are negative but minor, suggesting that an average (shortest) path calculated with the quiet path routing application is slightly shorter than the corresponding reference path. Despite the somewhat high standard deviations of the differences (16 % & 74.8 m), the 10<sup>th</sup> and 90<sup>th</sup> percentiles are still moderate, -58.2 m (-7.1 %) and 29 m (4.2 %), indicating that the differences are in an acceptable range for a majority of paths. In the light of these numbers, it can be concluded that the quiet path routing application performs well or at least satisfactorily in most situations.

Nevertheless, also some considerable deviations to reference paths seem to occur in some cases. The quality assessment of the paths facilitated improving the application and its street network graph by revealing problematic pathfinding results. The routing analysis was improved during the project through an iterative process of five phases: 1) revising the graph construction script, 2) revising the application logic in routing, 3) re-running the routing analysis, 4) re-assessing the quality of the paths and 5) debugging the problematic paths (if any); where higher differences in length were found, the paths were inspected in QGIS to debug possible faults in the application logic or in the street network graph. By this process, some critical, yet rare, bugs were discovered. Most of these were caused by the presence of redundant street segments (e.g. underground service roads) in the graph. Since the few unwanted segments were not highly connected to the graph, majority of paths were unaffected by them. I made three key improvements to the application via this process; functionality for filtering out service tunnels (1) and ensuring the connectivity of the graph (2) were integrated in the graph construction script and search radius and logic were extended in the function for finding and creating the origin and destination nodes (3).

**Table 12.** Differences in path length between shortest paths and reference paths (n=31228).

Difference to reference length	meters	%
Mean	-7.8	-0.21
Median	-4.2	-0.55
SD	74.8	15.9
p10	-57.6	-7.1
p90	30.5	4.5

The visual comparison of (possibly) problematic paths revealed at least three types of situations where significant differences between a path and its reference path may occur:

- 1) A path takes a detour around a private area. In HRT's route planner, also the street segments tagged as private (in OSM) are allowed at the start and at the end of a walk but forbidden as shortcuts in the middle of a walk. In the quiet path routing application, street segments tagged as private are excluded in the graph to prevent pathfinding through private residential areas (Figure 39). This is a known, yet minor, limitation of the application. These cases constitute a subset of the situations where different nearest edge was found for origin or destination;
- 2) A path starts or ends at different street segment since different nearest edge to origin or destination is found. As per the descriptive statistics in Table 13, most of the offsets of origin and destination points (compared to the reference paths) are minor. However, starting the path from a different edge, even if it is at the same distance from the origin, can lead to more or less divergent opportunities for pathfinding. Some of the differences can be traced back to the three-dimensional alignments of the edges. In the case of Pasila, for example, many sidewalks are located on top of each other; the lower lever typically features a more traditional layout of streets, sidewalks and intersections whereas the upper level features mainly exclusive walkways (raised above the cars). If the nearest edge to an origin or destination can be one of multiple overlapping candidates at the same distance, deviating paths are likely to arise depending on the first edge.
- 3) A path goes around a walkable area (i.e. detours). Some walkable OSM features consist of only polygon geometry but the graph construction script of the quiet path routing application does not include creation of "virtual street segments" across walkable areas of OSM. This is an advanced feature that is implemented in e.g. OpenTripPlanner that HRT's route planner service uses. However, pathfinding is affected by the missing walkable areas only in some

restricted areas, such as near Helsinki Central Railway Station and other major squares. In practice, for a reference path that crosses a walkable square by a virtual edge, the quiet path route planner can find only a slightly longer path as it can only utilize the sidewalks and other walkable street segments around the square (Figure 40).

**Table 13.** Statistics of offsets (i.e. distances) between the origin and destination points of the paths and the origin and destination points of the reference paths.

Offset from reference paths'	origins (m)	destinations (m)
Mean	3.0	3.9
Median	0.5	1.3
SD	9.5	12.0
p5	0.0	0.1
p10	0.1	0.2
p90	4.4	8.5
p95	24.7	15.4



**Figure 39.** Side-by-side comparison of the street network graphs of the quiet path route planner (A) and OpenTripPlanner (B) in Koskela, Helsinki. Most street segments tagged as private in OpenStreetMap are used in OpenTripPlanner but missing from the quiet path route planner. However, private streets are only usable at the beginning or end of a route in OpenTripPlanner. Map data by © OpenStreetMap contributors.



**Figure 40.** Side-by-side comparison of the street network graphs of the quiet path route planner (A) and OpenTripPlanner (B) in Kumpula campus, Helsinki. Additional ("virtual") edges are created in OpenTripPlanner to allow traversing through walkable areas in pathfinding. Map data by © OpenStreetMap contributors.

In addition to the previously described issues in pathfinding, also some minor deviations (compared to the reference paths) were identified and further investigated. In a number of cases, a path takes a shortcut by using trails or other minor pathways as opposed to the reference path that uses mainly streets and other major ways. This can be at least partly explained by the so-called “turning cost” that is used in HRT’s route planner to prevent high number of turns in pathfinding. On the other hand, the quiet path routing application finds the least cost path regardless of how many turns the path includes, by only considering the cost attributes of the edges. This may well be the most significant cause for the average path being slightly shorter (Table 12; mean = -7.8 m; -0.21 %) than the reference path.

## 5.6 Indirect assessment of pedestrians’ dynamic exposures to traffic noise can reveal unequal distribution of exposures to high noise levels

As opposed to most of the previous studies where exposure to traffic noise have been assessed in a static manner (with respect to location), a dynamic exposure assessment was carried out in this study. Pedestrians’ exposure to traffic noise was addressed indirectly by modeling commuting-related walks. The results on dynamic (i.e. journey-time) exposures to noise were aggregated at origin-level and concepts *average local walk* and *expected local walk* were introduced for interpreting the results. As per the maps representing traffic noise exposure on average walks in Helsinki (see 4.3.2), dynamic traffic noise exposure seems to vary significantly between neighborhoods. This suggests that

opportunities for walking in quiet are distributed unequally. Interestingly, many areas not directly exposed to high traffic noise levels seem to have highly exposed average walk.

One could argue that most buildings manage to protect residents from harmful levels of traffic noise. Therefore, residents' dynamic exposure to traffic noise *outside* the buildings becomes increasingly important component of their total daily noise exposure. According to the review of (static) noise-annoyance studies by Guski et al. (2017), all of the studied relationships between the share of highly annoyed (%HA) residents and sound pressure level display considerable variance in the dependent variable. Considering this finding, dynamic exposure to traffic noise may well be one prominent, but widely unstudied, explanatory variable for the unexplained differences in %HA.

Large-scale assessment of pedestrians' exposure to traffic noise could be applied in planning actions for mitigating negative health effects of noise. The highest demand for better noise control could be identified by comparing modeled utilization rates and noise levels of different street segments, as demonstrated in Appendix 6. However, more advanced analysis and data of mobility would be needed to model more probable paths of pedestrians. At least, availability and quality of alternative paths in different areas should be considered. This issue is discussed further in the next chapter (5.7).

## **5.7 The presence of alternative paths limits the accuracy of the indirect dynamic exposure assessment**

In direct assessments of dynamic exposure, real paths of pedestrians are determined by e.g. GPS tracking. In the case study of this thesis, pedestrians' dynamic exposure to traffic noise was assessed using modeled (commuting-related) walks. The assessment relies on the assumption that pedestrians use shortest paths between origins and destinations. For multimodal and particularly commuting related trips, this may be an acceptable assumption, as pedestrians often try to optimize travel-time.

However, the real taken paths are likely to deviate from the modeled shortest paths in at least two common situations: 1) a path longer than the shortest path is perceived as the shortest path and hence taken or 2) a path longer than the shortest path is known to be both longer but also *better* and hence taken. As pedestrians' can choose their route from virtually infinite number of alternatives, it is no surprise that many psychological and physical variables affect the route choice. Several studies (e.g. Cervero & Duncan, 2003; Hess, 2012; Hoogendoorn & Bovy, 2004; Verlander & Heydecker, 1997) have shed light on pedestrian route choices, or attempted to model them, and shown that they tend to vary depending on many personal (e.g. age, occupation and gender) and physical factors (e.g. traffic conditions, number of sharp turns, activity locations and presence of greenery). The route choice

problem gets increasingly complicated in multimodal routing; in addition to the alternative paths between a fixed O-D pair, pedestrian may also be able to select an alternative PT stop as destination for the walk.

Modeling route choices of pedestrians is outside the scope of this thesis. More accurate assessments of pedestrians' traffic noise exposures and opportunities for walking in quiet would require modeling pedestrians' route choices in different noise environments. How long additional distances pedestrians are willing to walk in order to avoid exposure to noise? Despite calculating alternative, quieter paths for all walks, I did not attempt to determine which of the paths is the *best*.

Undoubtedly, the reliability of the indirect dynamic exposure assessment is limited due to the unknown route choices of pedestrians in real-life. Therefore, any conclusions on the results on the average dynamic exposures to traffic noise should be made with caution. Neither do the results reveal the true spatial (in)equalities in opportunities for walking in quiet, as the availability and quality of quiet paths were not analyzed spatially. This assessment would have required compressing the spatial information of availability and quality of quiet paths to appropriate indices and inspecting the spatial variation in them.

Considering the uncertainties described in this chapter, more sophisticated assessments would be needed to validate or improve the results of the dynamic noise exposure assessment. In order to provide city planners information upon which to base actions for noise mitigation, presence and quality of quiet paths should be inspected at least for the areas with the highest dynamic noise exposures. One way to achieve this "manually" would be to use the web-based quiet path route planner.

## **5.8 Uncertainties in exposure-response relationships challenge the environmental impedance function**

Exposure-based least cost path routing has been developed as a concept only in a few studies. The implementations, including the environmental impedance functions, have been more case-specific than general (e.g. Lwin & Murayama, 2011; Quercia et al., 2014; Ribeiro & Mendes, 2011; Sharker et al., 2012; Su et al., 2010). In these studies, the focus has been rather explaining the need for such analysis and demonstrating the developed proof of concept route planners for healthier routes.

Undoubtedly, the most challenging element of this study was defining and validating an EIF for noise, as no well-established one could be found from the prior studies. Ideally, the EIF should model the

perceived annoyance from dynamic exposure to different noise levels. Thus, literature on sound pressure level – annoyance relationship was explored to guide defining the EIF. Since most of the papers where annoyance from traffic noise was assessed focus on static noise exposure, namely SPL versus annoyance by home location, the scientific basis for defining the EIF was limited.

Two alternative noise cost functions (i.e. EIFs) were defined and tested in developing the quiet path routing method: one power function and one linear function. The power function, that was selected for the quiet path routing application, is based on the Stevens (1960) power law's revision by Parmanen (2007), where sound intensity and SPL are assumed interchangeable and SPL and loudness proportional. In this study, one more assumption was appended to the previous: sound intensity in Steven's power law can be replaced with A-weighted equivalent continuous SPL. The strength of this assumption was not comprehensively assessed in the study. According to Genuit (1999), Ouis (2001) and Parmanen (2007), even just the simple A-weighted SPL may be somewhat unreliable indicator of loudness and annoyance of noise. Information of different tones and fluctuations of SPL in time, both presumably important qualities affecting the perceived loudness of traffic noise, are lost when using a heavily compressed SPL metric such as  $L_{Aeq}$ . However, since the available traffic noise data featured only A-weighted equivalent continuous sound levels, the uncertainties in  $L_{Aeq}$  – loudness relationship were not investigated more thoroughly.

It can be argued that both (power and linear) functions that are presented in the study, are likely to perform better than a non-continuous (i.e. threshold-based) cost function (e.g. Ribeiro & Mendes, 2013). The power function doubles the loudness based cost at every 10-decibel increase, and may thus be slightly better match with the highly annoyed (HA %) - SPL curves (Figure 2) than a linear function. And as mentioned in chapter 3.5.2, the power function clearly meets the most important requirement for the EIF: it assigns radically higher costs to the very highest noise levels. The selection of the noise cost function was not further justified, since it seemed to perform well in practical situations but also due to the little differences in the quiet paths between the two functions.

However, if the two noise cost functions were applied in a surface-based LCP analysis, more differences would probably arise between quiet paths, due to increased number of path alternatives. It is likely that in most cases street network graphs simply do not provide enough path alternatives between OD pairs to allow the definition of EIF to significantly affect the results of pathfinding. In the EIFs defined in this study, the sensitivity coefficient defines the relative weights of distance- and exposure-based costs in the composite cost. Therefore, considering the little differences in the quiet

path routing results between the two different EIFs, the noise sensitivity coefficient is certainly a critical component of the EIF.

## **5.9 Exposure-based routing should be developed as a concept to simultaneously consider multiple exposures**

In this study, the used traffic noise data included only vehicular traffic, leaving out noise from rail traffic, aircrafts and industrial sites. It can be argued that making separate assessments of dynamic exposure to different noise sources is important for the same reasons why separate assessments of static noise exposures are made: health effects of different kinds of noise can vary (Guski et al. 2017), and the mitigation actions for environmental noise exposure vary between different noise sources (e.g. noise barriers, speed limits, rerouting of trams or aircrafts). Also, different thresholds for sound pressure levels causing “adverse health effects” have been suggested for different noise sources (Kephhalopoulos et al., 2012).

It can be argued that the decision of assessing dynamic exposure to only vehicular traffic noise was adequate in developing a conceptual and technical framework for dynamic exposure assessment and exposure-based routing. However, this decision should be revisited when developing the quiet path routing method further. As per Guski et al. (2017: 35), one promising way to incorporate multiple noise sources in a single EIF would be to apply the concept of dominant noise source. Caution should be paid on deciding whether different weightings should be used for different noise sources based on their possibly different effects on annoyance. Yet, given the lack of explicit information of ERRs of different noise sources, a viable way of determining the dominant noise source could be to simply use the maximum SPL among different noise sources. Furthermore, using dominant noise source would match the constitution of many air quality indices (AQI); AQI is commonly determined by the maximum AQI value among its components, i.e. different pollutants (Plaia & Ruggieri, 2011).

While combining different noise sources together has its own challenges, then another level of complexity to exposure-based routing is introduced by considering exposures to several pollutants or environmental conditions. A practical, yet naive, approach for integrating multiple environmental exposures in routing analysis have been demonstrated by many web-based route planner applications: the user gets to decide a singular exposure to minimize per one pathfinding problem. However, a desirable goal would be to combine two or more environmental exposures in one least cost path problem and hence enable calculating “composite green paths”. Perhaps the greatest challenge to this arises from the need to synchronize different EIFs (of the different exposures) to allow using initially

equal weights for different exposure-based costs. For example, initial air- and noise pollution-based costs should be possible to set equally important in the composite EIF. Normalized (i.e. balanced) impedances would be needed to enable using different relative weights for different pollutants in least cost path analysis (e.g. air pollution set to half as expensive as noise). Normalizing EIFs of two completely different environmental exposures would require careful investigation of their ERRs. If it is challenging to estimate the change in environmental impedance from increasing sound pressure level by 10 dB, it would be ever more challenging to determine what change in AQI would cause an equal change. In addition, also personal differences in responses to different pollutants are likely to affect the composite environmental impedance.

Nevertheless, some practical approaches for normalizing the impedances of different exposures have been demonstrated in the previous studies. For example, Ribeiro & Mendes (2013) used the average impedances by the EIFs for air- and noise pollution in normalizing costs for composite “healthy routes”. On the other hand, Novack et al. (2018) normalized the relative weights of the different costs by dividing the costs by their maximum values observed at their test-site. This approach shares the somewhat same idea that I used in defining the normalized noise exposure index ( $EI_n$ ). Importantly, neither of these normalization techniques is based on health effects but rather equalizing the effect of the pollutants in routing.

If the ultimate goal for exposure-based routing is to minimize the net negative health effect from walking or cycling, deeper knowledge on also the positive health effects should be acquired. Also, it should be acknowledged that minimizing the net negative health effect does not necessarily mean the same as maximizing the net positive health effect, as the latter would probably mean routing considerably longer routes for increased physical activity. The tricky question remains unanswered: what is the trade-off by which the negative health effects from exposure to environmental pollutants can override the positive health effects from the physical activity of active transport modes? And vice versa, can “positive exposures” compensate the negative health effect of exposure to pollutants? When also positive exposures are incorporated in routing analysis, the goal of pathfinding is no longer “simply” least-exposure path but rather the most walkable or pleasant path. For example, greenery (e.g. Taleai & Yameqani, 2018), perceived security (e.g. Naharudin et al., 2017) and beauty (e.g. Quercia et al., 2014) have been integrated in routing analysis. As opposed to exposures to environmental pollution, it is likely that even higher level of subjectivity is associated with positive exposures. Consequently, if the number of considered exposures increases and also positive exposures are included in LCP analysis, applying basic composite EIF may become insufficient approach. Several rather complex, and often fuzzy, statistical methods have been employed in

calculating overall health or walkability scores. For example, Taleai & Yameqani (2018) demonstrated the use of analytical hierarchical process (AHP) for assigning relative weights for different criteria, whereas Sharker et al. (2012) used Bayesian belief network (BBN) in addressing the composite effect of possibly interrelated routing criteria. Despite the utilization of advanced frameworks in multi-criteria routing analysis, subjective decision-making still plays a critical role in setting up the parameters of the analysis. Therefore, to meet varying personal preferences, multiple scenarios for pathfinding should be considered despite using advanced routing criteria. One way to achieve this would be to slightly adjust the sensitivities to different criteria, and thereby route sets of alternative paths as in routing application of this study.

## VI. REFERENCES

- Agrawal, S., & Gupta, R. D. (2017). Web GIS and its architecture: A review. *Arabian Journal of Geosciences*, 10(23), 518.
- Ahuja, R. K., Mehlhorn, K., Orlin, J., & Tarjan, R. E. (1990). Faster algorithms for the shortest path problem. *Journal of the ACM (JACM)*, 37(2), 213–223. <https://doi.org/10.1145/77600.77615>
- Alam, M. S., Perugu, H., & McNabola, A. (2018). A comparison of route-choice navigation across air pollution exposure, CO<sub>2</sub> emission and traditional travel cost factors. *Transportation Research Part D: Transport and Environment*, 65, 82–100. <https://doi.org/10.1016/j.trd.2018.08.007>
- Anciaes, P., & Jones, P. (2020). Transport policy for liveability—Valuing the impacts on movement, place, and society. *Transportation Research Part A: Policy and Practice*, 132, 157–173.
- Apparicio, P., Carrier, M., Gelb, J., Séguin, A.-M., & Kingham, S. (2016). Cyclists' exposure to air pollution and road traffic noise in central city neighbourhoods of Montreal. *Journal of Transport Geography*, 57, 63–69.
- Babisch, W., Beule, B., Schust, M., Kersten, N., & Ising, H. (2005). Traffic noise and risk of myocardial infarction. *Epidemiology*, 33–40.
- Babisch, W., Houthuijs, D., Pershagen, G., Cadum, E., Katsouyanni, K., Velonakis, M., Dudley, M.-L., Marohn, H.-D., Swart, W., Breugelmans, O., Bluhm, G., Selander, J., Vigna-Taglianti, F., Pisani, S., Haralabidis, A., Dimakopoulou, K., Zachos, I., & Järup, L. (2009). Annoyance due to aircraft noise has increased over the years—Results of the HYENA study. *Environment International*, 35(8), 1169–1176. <https://doi.org/10.1016/j.envint.2009.07.012>
- Bao, S., Nitta, T., Ishikawa, K., Yanagisawa, M., & Togawa, N. (2016). A safe and comprehensive route finding method for pedestrian based on lighting and landmark. *2016 IEEE 5th Global Conference on Consumer Electronics*, 1–5.
- Bao, S., Nitta, T., Yanagisawa, M., & Togawa, N. (2017). A safe and comprehensive route finding algorithm for pedestrians based on lighting and landmark conditions. *IEICE TRANSACTIONS on Fundamentals of Electronics, Communications and Computer Sciences*, 100(11), 2439–2450.
- Beckx, C., Int Panis, L., Uljee, I., Arentze, T., Janssens, D., & Wets, G. (2009). Disaggregation of nation-wide dynamic population exposure estimates in The Netherlands: Applications of activity-based transport models. *Atmospheric Environment*, 43(34), 5454–5462. <https://doi.org/10.1016/j.atmosenv.2009.07.035>
- Boeing, G. (2017). OSMnx: New methods for acquiring, constructing, analyzing, and visualizing complex street networks. *Computers, Environment and Urban Systems*, 65, 126–139.
- Boulos, M. N. K., Warren, J., Gong, J., & Yue, P. (2010). *Web GIS in practice VIII: HTML5 and the canvas element for interactive online mapping*. Springer.
- Brandt, E., Kantele, S., & Räty, P. (2018). Liikkumistottumukset Helsingin seudulla 2018. [https://www.hsl.fi/sites/default/files/hsl\\_julkaisu\\_9\\_2019\\_netti.pdf](https://www.hsl.fi/sites/default/files/hsl_julkaisu_9_2019_netti.pdf) (accessed 10 April 2020)

- Brown, A. L., Lam, K. C., & van Kamp, I. (2015). Quantification of the exposure and effects of road traffic noise in a dense Asian city: A comparison with western cities. *Environmental Health*, 14(1), 22.
- Brown, A. L., & Van Kamp, I. (2017). WHO environmental noise guidelines for the European region: A systematic review of transport noise interventions and their impacts on health. *International Journal of Environmental Research and Public Health*, 14(8), 873.
- Buliung, R. N., Larsen, K., Faulkner, G. E., & Stone, M. R. (2013). The “path” not taken: Exploring structural differences in mapped-versus shortest-network-path school travel routes. *American Journal of Public Health*, 103(9), 1589–1596.
- Caggiani, L., Camporeale, R., & Ottomanelli, M. (2017). A real time multi-objective cyclists route choice model for a bike-sharing mobile application. 2017 5th IEEE International Conference on Models and Technologies for Intelligent Transportation Systems (MT-ITS), 645–650.
- Cervero, R., & Duncan, M. (2003). Walking, bicycling, and urban landscapes: Evidence from the San Francisco Bay Area. *American Journal of Public Health*, 93(9), 1478–1483.
- City of Helsinki. (2020). Liikennetutkimus Ja -Tilastot. <https://www.hel.fi/helsinki/fi/kartat-jaliikenne/kadut-ja-liikennesuunnittelu/tutkimus-ja-tilastot> (accessed 4 April 2020)
- Cole-Hunter, T., Morawska, L., Stewart, I., Jayaratne, R., & Solomon, C. (2012). Inhaled particle counts on bicycle commute routes of low and high proximity to motorised traffic. *Atmospheric Environment*, 61, 197–203. <https://doi.org/10.1016/j.atmosenv.2012.06.041>
- Csardi, G., & Nepusz, T. (2006). The igraph software package for complex network research. *InterJournal, Complex Systems*, 1695(5), 1–9.
- Datakustik CadnaA 2017. (n.d.). <https://www.datakustik.com/products/cadnaa/cadnaa/> (accessed 4 April 2020)
- Davies, G., & Whyatt, D. (2009). A least-cost approach to personal exposure reduction. *Transactions in GIS*, 13(2), 229–246.
- Davies, G., & Whyatt, J. D. (2014). A network-based approach for estimating pedestrian journey-time exposure to air pollution. *Science of The Total Environment*, 485–486, 62–70. <https://doi.org/10.1016/j.scitotenv.2014.03.038>
- Digitransit Routing API. <https://digitransit.fi/en/developers/apis/1-routing-api/> (accessed April 2019)
- Dijkstra, E. W. (1959a). A note on two problems in connexion with graphs. *Numerische Mathematik*, 1(1), 269–271.
- Dijkstra, E. W. (1959b). Communication with an automatic computer [PhD Thesis]. Excelsior.
- Directive 2002/49/EC of the European Parliament and of the Council of 25 June 2002 relating to the assessment and management of environmental noise—Declaration by the Commission in the Conciliation Committee on the Directive relating to the assessment and management of environmental noise. (2002, July 18). <http://data.europa.eu/eli/dir/2002/49/oj/eng>

- EEA (2019). Air quality in Europe — 2019 report. EEA Report 10/2019. European Environmental Agency. <https://www.eea.europa.eu/publications/air-quality-in-europe-2019> (accessed 2 May 2020)
- Farkas, G. (2019). Hardware-Accelerating 2D Web Maps: A Case Study. *Cartographica: The International Journal for Geographic Information and Geovisualization*, 54(4), 245–260.
- Ferreira, J. (2014). Green route planner. In *Nonlinear Maps and Their Applications* (pp. 59–68). Springer.
- Gaffuri, J. (2012). Toward web mapping with vector data. *International Conference on Geographic Information Science*, 87–101.
- Genuit, K. (1999). The use of psychoacoustic parameters combined with A-weighted SPL in noise description. *INTER-NOISE and NOISE-CON Congress and Conference Proceedings*, 1999, 1887–1892.
- GeoPandas. <https://geopandas.org/> (accessed March 2019)
- Goldberg, A. V., & Harrelson, C. (2005). Computing the shortest path: A search meets graph theory. *Proceedings of the Sixteenth Annual ACM-SIAM Symposium on Discrete Algorithms*, 156–165.
- Gulliver, J., & Briggs, D. J. (2005). Time–space modeling of journey-time exposure to traffic-related air pollution using GIS. *Environmental Research*, 97(1), 10–25. <https://doi.org/10.1016/j.envres.2004.05.002>
- Guski, R., Schreckenberg, D., & Schuemer, R. (2017). WHO environmental noise guidelines for the European region: A systematic review on environmental noise and annoyance. *International Journal of Environmental Research and Public Health*, 14(12), 1539.
- Hasenfratz, D., Arn, T., de Concini, I., Saukh, O., & Thiele, L. (2015). Health-optimal routing in urban areas. *Proceedings of the 14th International Conference on Information Processing in Sensor Networks*, 398–399.
- Hatzopoulou, M., Weichenthal, S., Barreau, G., Goldberg, M., Farrell, W., Crouse, D., & Ross, N. (2013). A web-based route planning tool to reduce cyclists' exposures to traffic pollution: A case study in Montreal, Canada. *Environmental Research*, 123, 58–61.
- Helsingin kaupungin meluselvitys 2017. (2017). <https://www.hel.fi/helsinki/fi/asuminen-jaymparisto/ymparistonsuojelu/ilmanlaatu-ja-melu/selvitys/> (accessed 30 April 2019)
- Hertel, O., Hvidberg, M., Ketzel, M., Storm, L., & Stausgaard, L. (2008). A proper choice of route significantly reduces air pollution exposure—A study on bicycle and bus trips in urban streets. *Science of the Total Environment*, 389(1), 58–70. <https://doi.org/10.1016/j.scitotenv.2007.08.058>
- Hess, D. B. (2012). Walking to the bus: Perceived versus actual walking distance to bus stops for older adults. *Transportation*, 39(2), 247–266.
- Hoogendoorn, S. P., & Bovy, P. H. (2004). Pedestrian route-choice and activity scheduling theory and models. *Transportation Research Part B: Methodological*, 38(2), 169–190.

HOPE - Urban Innovative Action – Healthy Outdoor Premises for Everyone HOPE (2020).  
<https://ilmanlaatu.eu/hanke-ja-kumppanit/> (accessed 25 April 2020)

International Standard ISO 226: 1987. (n.d.). International Organization for Standardization, Geneva, Switzerland.

Ising, H., Dienel, D., Günther, T., & Markert, B. (1980). Health effects of traffic noise. *International Archives of Occupational and Environmental Health*, 47(2), 179–190.

Jacobsen, P. L., Racioppi, F., & Rutter, H. (2009). Who owns the roads? How motorised traffic discourages walking and bicycling. *Injury Prevention*, 15(6), 369–373.

Jarno Kokkonen, Kontkanen, O., & Maijala, P. (2016). CNOSSOS-EU Noise Model Implementation in Finland. ResearchGate, 38.  
[https://www.researchgate.net/publication/307907554\\_CNOSSOS-EU\\_Noise\\_Model\\_Implementation\\_in\\_Finland](https://www.researchgate.net/publication/307907554_CNOSSOS-EU_Noise_Model_Implementation_in_Finland)

Jasika, N., Alispahic, N., Elma, A., Ilvana, K., Elma, L., & Nosovic, N. (2012). Dijkstra's shortest path algorithm serial and parallel execution performance analysis. 2012 Proceedings of the 35th International Convention MIPRO, 1811–1815.

Jonasson, H. G., & Storeheier, S. (2001). Nord 2000. New Nordic prediction method for road traffic noise.

Jäppinen, S., Toivonen, T., & Salonen, M. (2013). Modelling the potential effect of shared bicycles on public transport travel times in Greater Helsinki: An open data approach. *Applied Geography*, 43, 13–24. <https://doi.org/10.1016/j.apgeog.2013.05.010>

Kephalopoulos, S., Paviotti, M., & Anfosso-Lédée, F. (2012). Common noise assessment methods in Europe (CNOSSOS-EU).

Leaflet. (n.d.). <https://leafletjs.com/> (accessed on 23 February 2020)

Lienert, C., Jenny, B., Schnabel, O., & Hurni, L. (2012). Current trends in vector-based Internet mapping: A technical review. In *Online maps with APIs and WebServices* (pp. 23–36). Springer.

Litman, T. (2010). Quantifying the benefits of nonmotorized transportation for achieving mobility management objectives. Victoria Transport Policy Institute, 28.

Lu, X. (2005). An investigation on service-oriented architecture for constructing distributed web gis application. 2005 IEEE International Conference on Services Computing (SCC'05) Vol-1, 1, 191–197.

Lwin, K. K., & Murayama, Y. (2011). Modelling of urban green space walkability: Eco-friendly walk score calculator. *Computers, Environment and Urban Systems*, 35(5), 408–420. <https://doi.org/10.1016/j.comenvurbsys.2011.05.002>

Lwin, K. K., & Murayama, Y. (2013). Smart eco-path finder for mobile GIS users. *URISA Journal*, 25(2), 5–14.

Maghelal, P. K., & Capp, C. J. (2011). Walkability: A Review of Existing Pedestrian Indices. *Journal of the Urban & Regional Information Systems Association*, 23(2).

- Mahajan, S., Tang, Y.-S., Wu, D.-Y., Tsai, T.-C., & Chen, L.-J. (2019). CAR: The Clean Air Routing Algorithm for Path Navigation With Minimal PM2. 5 Exposure on the Move. *IEEE Access*, 7, 147373–147382.
- Mapbox GL JS. (n.d.). <https://docs.mapbox.com/mapbox-gl-js/> (accessed on 4 April 2020)
- Meeker, M., & Wu, L. (2013). Internet trends. Proc D11 Conference. Rancho Palos Verdes.
- Meeker, M., & Wu, L. (2018). Internet trends 2018. Kleiner Perkins.
- Miedema, H. M., & Oudshoorn, C. G. (2001). Annoyance from transportation noise: Relationships with exposure metrics DNL and DENL and their confidence intervals. *Environmental Health Perspectives*, 109(4), 409–416.
- Müller, S., & Voisard, A. (2015). Air quality adjusted routing for cyclists and pedestrians. Proceedings of the 1st ACM SIGSPATIAL International Workshop on the Use of GIS in Emergency Management, 1–6.
- Mölter, A., & Lindley, S. (2015). Influence of walking route choice on primary school children's exposure to air pollution—A proof of concept study using simulation. *Science of The Total Environment*, 530–531, 257–262. <https://doi.org/10.1016/j.scitotenv.2015.05.118>
- Naharudin, N., Ahmad, M., Sanusi, S., & Sadullah, A. F. M. (2017). OPTIMIZING PEDESTRIAN-FRIENDLY WALKING PATH FOR THE FIRST AND LAST MILE TRANSIT JOURNEY BY USING THE ANALYTICAL NETWORK PROCESS (ANP) DECISION MODEL AND GIS NETWORK ANALYSIS. *International Archives of the Photogrammetry, Remote Sensing & Spatial Information Sciences*, 42.
- Neis, P., & Zipf, A. (2017). OpenRouteService. Dostupné z: <Http://Www.Openrouteservice.Org>.
- Nielsen, H. L. (1997). Road traffic noise: Nordic prediction method. Nordic Council of Ministers.
- Noto, M., & Sato, H. (2000). A method for the shortest path search by extended Dijkstra algorithm. Smc 2000 Conference Proceedings. 2000 Ieee International Conference on Systems, Man and Cybernetics. “cybernetics Evolving to Systems, Humans, Organizations, and Their Complex Interactions” (Cat. No.0, 3, 2316–2320 vol.3. <https://doi.org/10.1109/ICSMC.2000.886462>)
- Novack, T., Wang, Z., & Zipf, A. (2018). A system for generating customized pleasant pedestrian routes based on OpenStreetMap data. *Sensors*, 18(11), 3794.
- OpenLayers. (n.d.). <https://openlayers.org/> (accessed on 23 February 2020)
- OpenStreetMap. <https://www.openstreetmap.org/copyright> (accessed March 2019)
- Ouis, D. (2001). ANNOYANCE FROM ROAD TRAFFIC NOISE: A REVIEW. *Journal of Environmental Psychology*, 21(1), 101–120. <https://doi.org/10.1006/jevp.2000.0187>
- Overpass API. (2019). [https://wiki.openstreetmap.org/wiki/Overpass\\_API](https://wiki.openstreetmap.org/wiki/Overpass_API) (accessed on 10 April 2019)
- Parmanen, J. (2007). A-weighted sound pressure level as a loudness/annoyance indicator for environmental sounds – Could it be improved? *Applied Acoustics*, 68(1), 58–70. <https://doi.org/10.1016/j.apacoust.2006.02.004>

- Passchier-Vermeer W, & Passchier W F. (2000). Noise exposure and public health. *Environmental Health Perspectives*, 108(suppl 1), 123–131. <https://doi.org/10.1289/ehp.00108s1123>
- Plaia, A., & Ruggieri, M. (2011). Air quality indices: A review. *Reviews in Environmental Science and Bio/Technology*, 10(2), 165–179. <https://doi.org/10.1007/s11157-010-9227-2>
- PostGIS. (n.d.). <https://postgis.net/> (accessed on 23 February 2020)
- Pucher, J., & Buehler, R. (2010). Walking and cycling for healthy cities. *Built Environment*, 36(4), 391–414.
- Pucher, J., & Dijkstra, L. (2003). Promoting safe walking and cycling to improve public health: Lessons from the Netherlands and Germany. *American Journal of Public Health*, 93(9), 1509–1516.
- Qian, J., & Eglese, R. (2016). Fuel emissions optimization in vehicle routing problems with time-varying speeds. *European Journal of Operational Research*, 248(3), 840–848. <https://doi.org/10.1016/j.ejor.2015.09.009>
- Qiu, G., & Chen, J. (2018). Web-based 3D map visualization using WebGL. *2018 13th IEEE Conference on Industrial Electronics and Applications (ICIEA)*, 759–763.
- Quercia, D. (2015). Chatty, Happy, and Smelly Maps. *Proceedings of the 24th International Conference on World Wide Web*, 741–741.
- Quercia, D., Schifanella, R., & Aiello, L. M. (2014). The shortest path to happiness: Recommending beautiful, quiet, and happy routes in the city. *Proceedings of the 25th ACM Conference on Hypertext and Social Media*, 116–125.
- Rabl, A., & de Nazelle, A. (2012). Benefits of shift from car to active transport. *Transport Policy*, 19(1), 121–131. <https://doi.org/10.1016/j.tranpol.2011.09.008>
- Recio, A., Linares, C., Banegas, J. R., & Díaz, J. (2016). Road traffic noise effects on cardiovascular, respiratory, and metabolic health: An integrative model of biological mechanisms. *Environmental Research*, 146, 359–370. <https://doi.org/10.1016/j.envres.2015.12.036>
- Reynolds, C., Winters, M., Ries, F., & Gouge, B. (2010). Active transportation in urban areas: Exploring health benefits and risks. *National Collaboration Centre for Environmental Health*, 2.
- Ribeiro, P., & Mendes, J. F. (2011). Route planning for soft modes of transport: Healthy routes. *WIT Transactions on The Built Environment*, 116, 677–688.
- Ribeiro, P., & Mendes, J. F. (2013). Healthy routes for active modes in school journeys. *International Journal of Sustainable Development and Planning*, 8(4), 591–602.
- Sharker, M. H., Karimi, H. A., & Zgibor, J. C. (2012). Health-optimal routing in pedestrian navigation services. *Proceedings of the First ACM SIGSPATIAL International Workshop on Use of GIS in Public Health*, 1–10.
- Sheng, N., & Tang, U. W. (2011). Spatial Analysis of Urban Form and Pedestrian Exposure to Traffic Noise. *International Journal of Environmental Research and Public Health*, 8(6), 1977–1990. <https://doi.org/10.3390/ijerph8061977>

- Statistics Finland. (2020). Kuntien Avainluvut. <https://www.stat.fi/tup/alue/kuntienavainluvut.html> (accessed on 4 April 2020)
- Stevens, S. S. (1960). The psychophysics of sensory function. *American Scientist*, 48(2), 226–253.
- Su, J. G., Winters, M., Nunes, M., & Brauer, M. (2010). Designing a route planner to facilitate and promote cycling in Metro Vancouver, Canada. *Transportation Research Part A: Policy and Practice*, 44(7), 495–505. <https://doi.org/10.1016/j.tra.2010.03.015>
- Tainio, M., de Nazelle, A. J., Götschi, T., Kahlmeier, S., Rojas-Rueda, D., Nieuwenhuijsen, M. J., de Sá, T. H., Kelly, P., & Woodcock, J. (2016). Can air pollution negate the health benefits of cycling and walking? *Preventive Medicine*, 87, 233–236. <https://doi.org/10.1016/j.ypmed.2016.02.002>
- Taleai, M., & Yameqani, A. S. (2018). Integration of GIS, remote sensing and Multi-Criteria Evaluation tools in the search for healthy walking paths. *KSCE Journal of Civil Engineering*, 22(1), 279–291.
- Toivonen, T., Salonen, M., Tenkanen, H., Saarsalmi, P., Jaakkola, T., & Järvi, J. (2014). Joukkoliikenteellä, autolla ja kävelien: Avoin saavutettavuusaineisto pääkaupunkiseudulta. *Terra* 126 (2014): 3.
- Torija, A. J., & Flindell, I. H. (2015). The subjective effect of low frequency content in road traffic noise. *The Journal of the Acoustical Society of America*, 137(1), 189–198. <https://doi.org/10.1121/1.4904542>
- Ueberham, M., Schlink, U., Dijst, M., & Weiland, U. (2019). Cyclists' Multiple Environmental Urban Exposures—Comparing Subjective and Objective Measurements. *Sustainability*, 11(5), 1412. <https://doi.org/10.3390/su11051412>
- Van den Hove, A., Verwaeren, J., Van den Bossche, J., Theunis, J., & De Baets, B. (2019). Development of a land use regression model for black carbon using mobile monitoring data and its application to pollution-avoiding routing. *Environmental Research*, 108619.
- Van Kempen, E., Casas, M., Pershagen, G., & Foraster, M. (2018). WHO environmental noise guidelines for the European region: A systematic review on environmental noise and cardiovascular and metabolic effects: a summary. *International Journal of Environmental Research and Public Health*, 15(2), 379.
- Veenendaal, B., Brovelli, M. A., & Li, S. (2017). Review of web mapping: Eras, trends and directions. *ISPRS International Journal of Geo-Information*, 6(10), 317.
- Verlander, N. Q., & Heydecker, B. G. (1997). Pedestrian route choice: An empirical study.
- WHO Regional Office for Europe (2011). Burden of disease from environmental noise: Quantification of healthy life years lost in Europe. [https://www.who.int/quantifying\\_ehimpacts/publications/e94888/en/](https://www.who.int/quantifying_ehimpacts/publications/e94888/en/) (accessed 22 April 2020)
- WHO (2013). Review of evidence on health aspects of air pollution – REVIHAAP Project. Technical Report. <http://www.euro.who.int/en/health-topics/environment-and-health/air->

[quality/publications/2013/review-of-evidence-on-health-aspects-of-air-pollution-revihaap-project-final-technical-report](http://www.euro.who.int/en/health-topics/health-policy/sustainable-development-goals/publications/2017/fact-sheets-on-sustainable-development-goals-health-targets/fact-sheet-on-the-sdgs-air-quality-and-health-2018) (accessed 2 May 2020)

WHO Regional Office for Europe (2018a). Fact sheet on the SDGs: Air quality and health (2018).  
<http://www.euro.who.int/en/health-topics/health-policy/sustainable-development-goals/publications/2017/fact-sheets-on-sustainable-development-goals-health-targets/fact-sheet-on-the-sdgs-air-quality-and-health-2018> (accessed 23 April 2020)

WHO Regional Office for Europe (2018b). Environmental noise guidelines for the European Region.  
[http://www.euro.who.int/\\_\\_data/assets/pdf\\_file/0008/383921/noise-guidelines-eng.pdf?ua=1](http://www.euro.who.int/__data/assets/pdf_file/0008/383921/noise-guidelines-eng.pdf?ua=1)  
(accessed 5 March 2020)

Whyatt, J. D., Pooley, C., Coulton, P., Moser, M., Bamford, W., & Davies, G. (2007). Estimating personal exposure to air pollution on the journey to and from school using GPS, GIS and mobile phone technology. 11th International Conference on Harmonisation within Atmospheric Dispersion Modelling for Regulatory Purposes, 1, 2–5.

Zielstra, D., & Hochmair, H. H. (2011). Comparative study of pedestrian accessibility to transit stations using free and proprietary network data. *Transportation Research Record*, 2217(1), 145–152.

Zielstra, D., & Hochmair, H. H. (2012). Using free and proprietary data to compare shortest-path lengths for effective pedestrian routing in street networks. *Transportation Research Record*, 2299(1), 41–47.

Zou, B., Li, S., Zheng, Z., Zhan, B. F., Yang, Z., & Wan, N. (2020). Healthier routes planning: A new method and online implementation for minimizing air pollution exposure risk. *Computers, Environment and Urban Systems*, 80, 101456.

## **ACKNOWLEDGEMENTS**

I want to thank my supervisor Tuuli Toivonen for the fruitful conversations we had when planning the thesis and for seeing the value of the quiet path routing method in developing also other exposure-based routing applications. I want to thank Age Poom for all the help and contribution in planning a green path routing application based on the quiet path routing tool. I am deeply grateful to Tuuli Toivonen and Age Poom for arranging excellent facilities for me to work on the thesis and the HOPE project, also during the time of the coronavirus crisis. I am very grateful to Henrikki Tenkanen for tips and support in setting up the server-based instance of the quiet path routing application (apparently some of the fundamentals of how internet works were still slightly unclear to me prior to this project). Also, I would like to thank Henrikki Tenkanen and all others who contributed in creating the course Automating GIS-processes – it was during that very course when I understood how great possibilities Python GIS enables.

## APPENDICES

**Appendix 1.** The packages and libraries included in the Python development environment of the thesis (i.e. environment file). Conda package manager can create the environment simply by running: [conda env create -f env-gis-flask.yml](#)

where env-gis-flask.yml is the name of the environment file.

```
name: gis-flask
channels:
  - conda-forge
  - defaults
dependencies:
  - python=3.6
  - jupyterlab
  - pylint
  - pytest
  - geopandas
  - osmnx
  - gdal
  - geoplot
  - pysal
  - flask
  - flask-cors
  - flask-testing
  - gunicorn
  - requests
  - pip
  - pip:
    - pycrs
    - polyline
```

**Appendix 2.** Noise cost coefficients for dB range 45–75 dB calculated with two different equations: linear (3) and power (4).

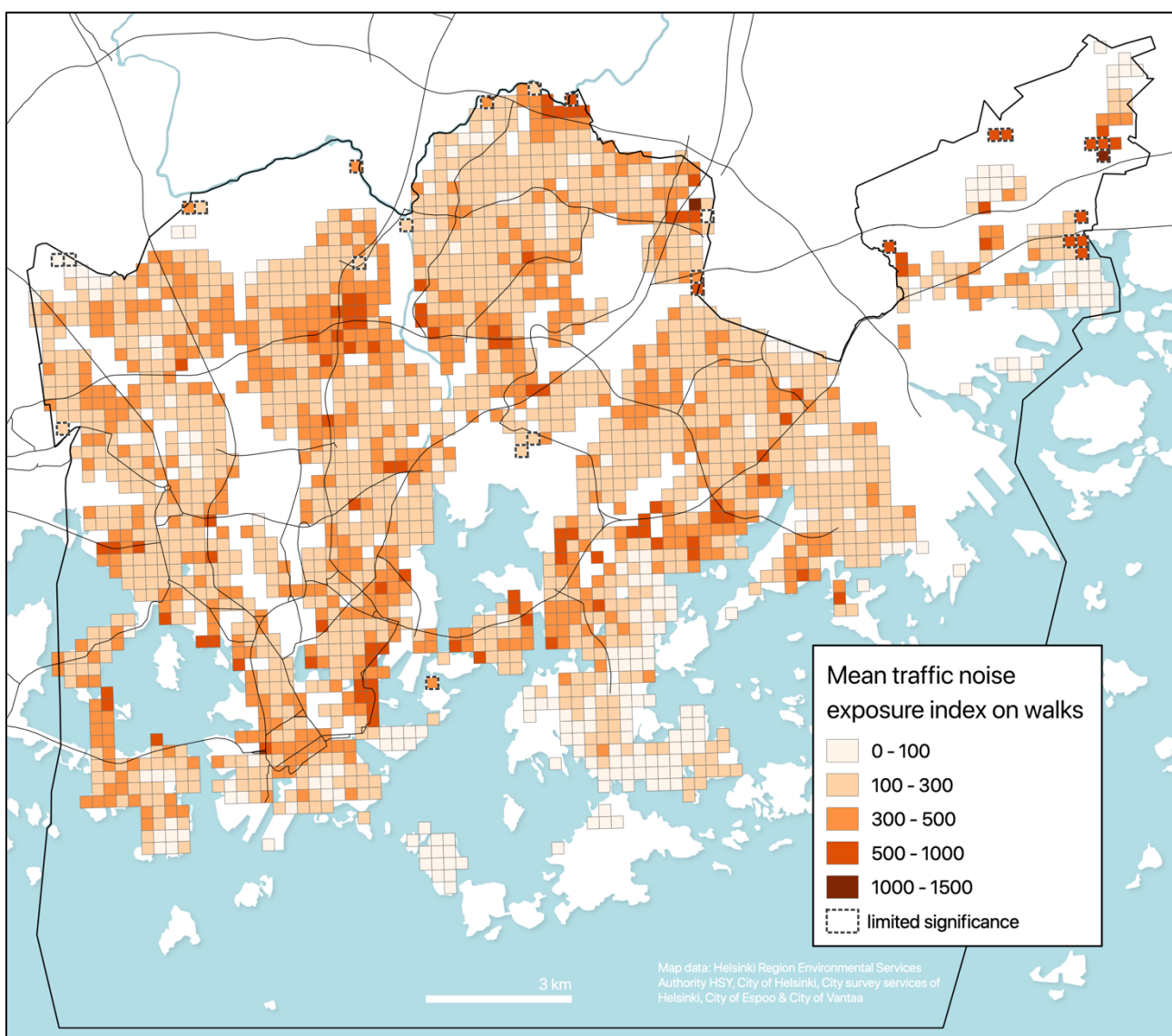
---

Noise cost coefficient ( $a_{dB_i}$ )

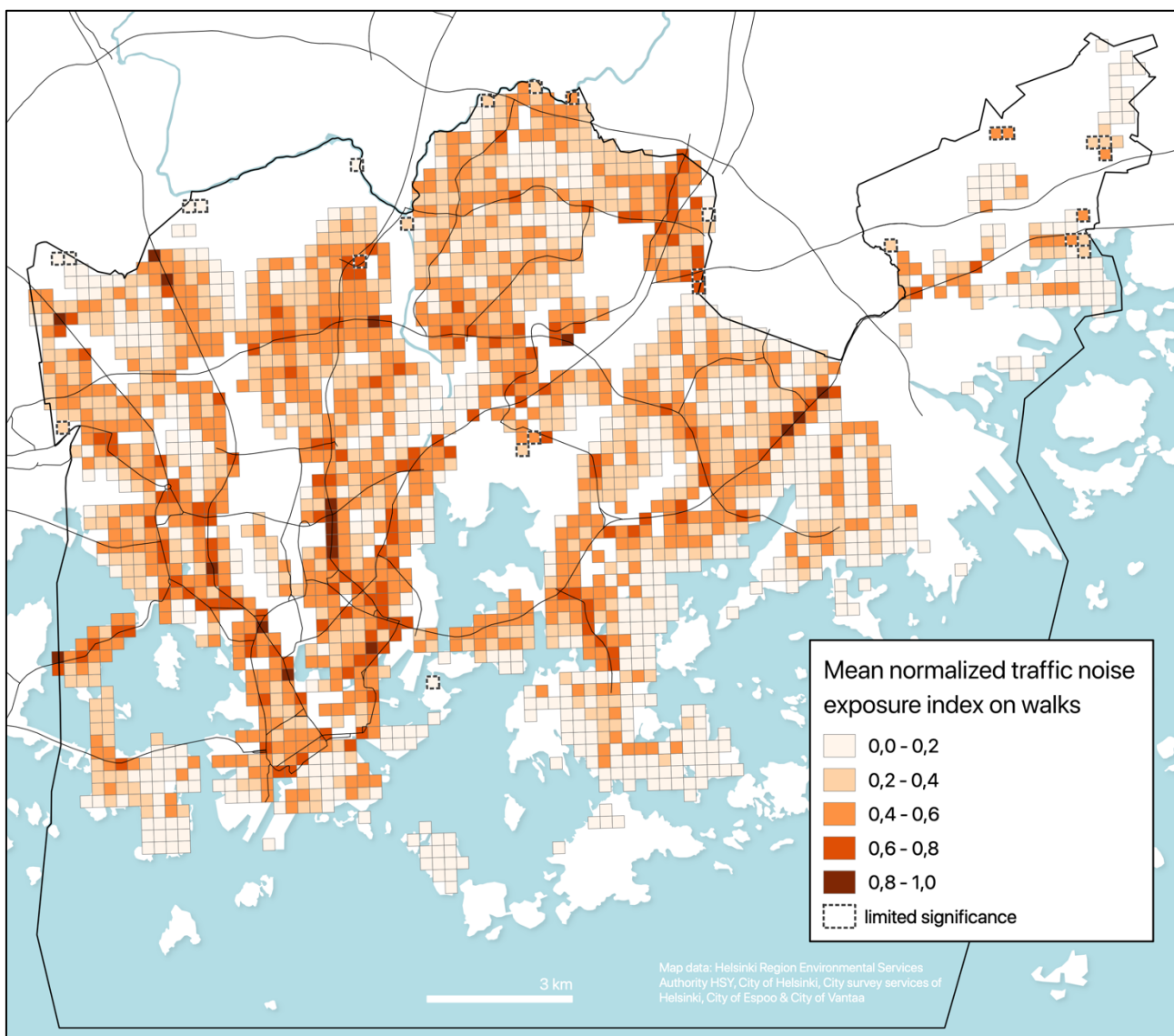
Traffic noise level (dB)	$\frac{dB_i - 40 \text{ dB}}{75 \text{ dB} - 40 \text{ dB}}$ (Eq. 3)	$10^{\frac{0.3 * dB_i}{10}} / 100$ (Eq. 4)
45–50	0.14	0.22
50–55	0.29	0.32
55–60	0.43	0.45
60–65	0.57	0.63
65–70	0.71	0.89
70–75	0.86	1.26
75–80	1.00	1.78

---

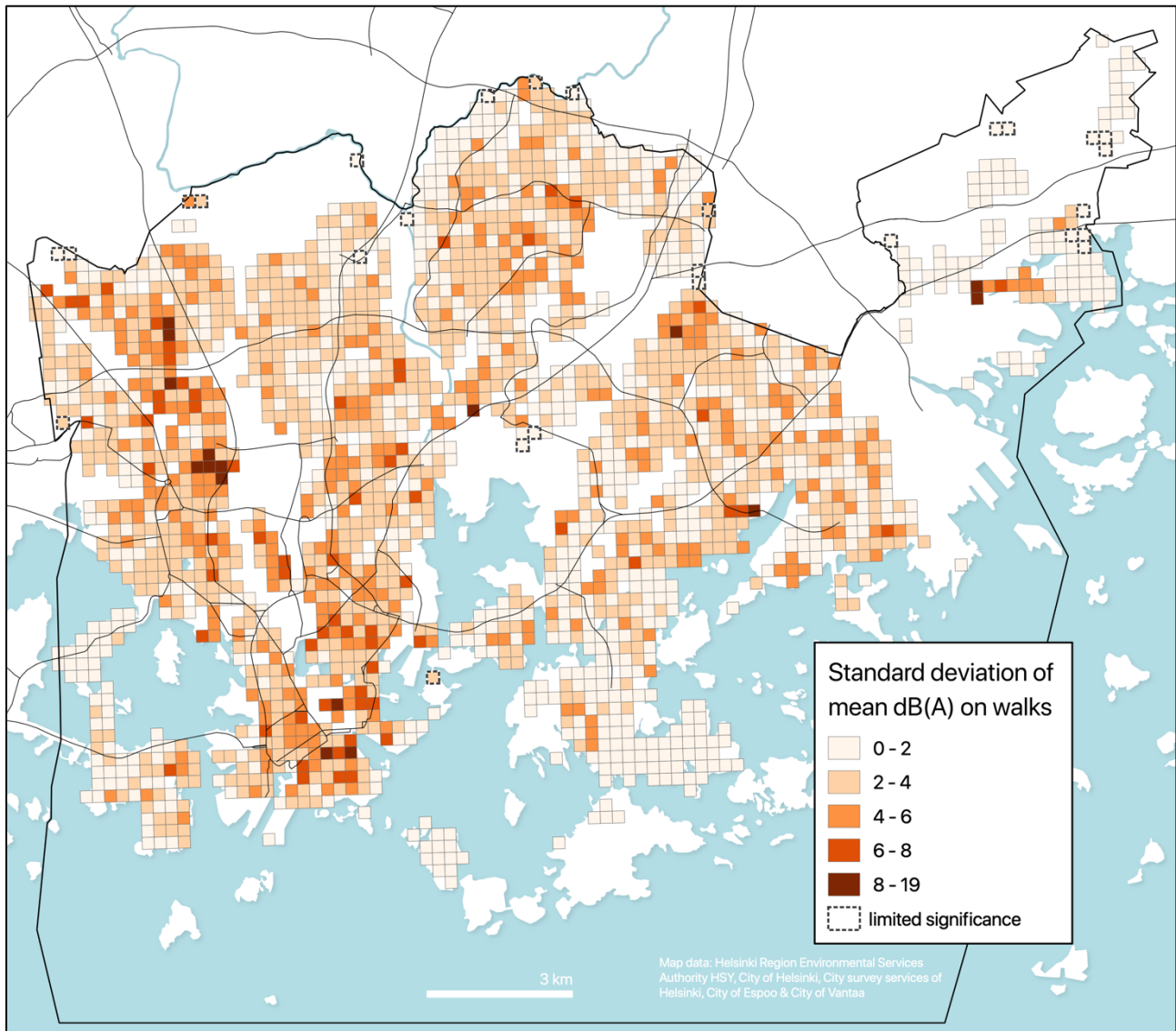
**Appendix 3.** Mean traffic noise exposure index (EI) on walks from homes to PT stops. The averages are weighted with the estimated utilization rates of the walks based on the total flow of commutes using each origin – PT stop pair.



**Appendix 4.** Mean normalized traffic noise exposure index ( $EI_n$ ) on walks from homes to PT stops. The averages are weighted with the estimated utilization rates of the walks based on the total flow of commutes using each origin – PT stop pair.



**Appendix 5.** Standard deviations of the mean traffic noise levels (dB(A)) on walks from homes to PT stops.



**Appendix 6.** Highest total modeled utilization rates and mean traffic noise levels of street segments by 80<sup>th</sup> percentile. Only street segments with modeled utilization rates higher than 0 are included in the percentiles of both variables.

